Research report

BYTEC

Tests on Prague PVB/ Glass Sandwich beams

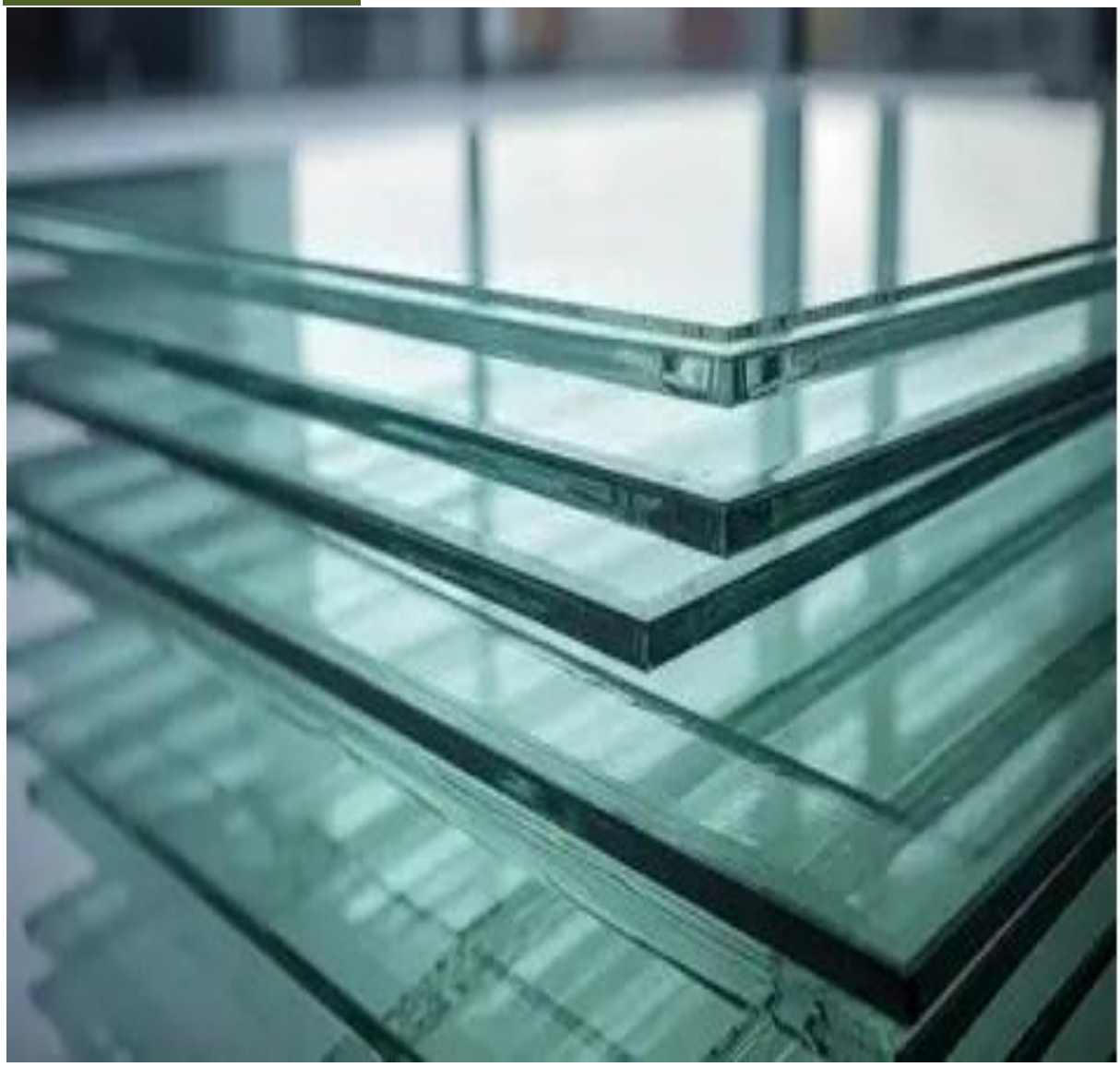

Report date: 19 May 2026 Hugo Sol

Contents

1 Introduction

In a previous Bytec report, a numerical model of a symmetrical sandwich beam was presented. The model has two degrees of freedom in each node (w and α)

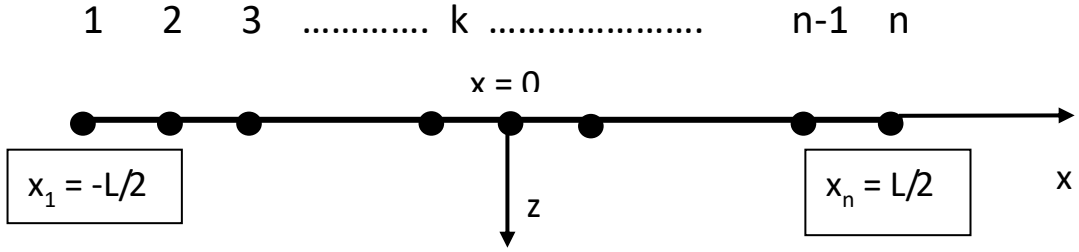

Figure 1.1. Discrete numerical model of the laminate beam

The central line of the laminated beam model is divided into a regular grid of 11 equidistant nodal points. The x-axis has its origin in the middle of the model. The basic idea is to create high polynomial shape functions and to model the beam with only one 11 node element (a macro finite element).
The model was validated with many standard finite element simulations (ANSYS and ABAQUS) and experimental measurements.

A major benefit of the model is its accuracy in combination with very small computation times. The model can dynamically compute resonance frequencies, modal shapes and damping ratios. Statically, the model can simulate deformations of 3-point and 4-point bending under static loads.

The model can also be used inversely to estimate the transverse shear modulus G of the inner layer using measured resonance frequencies.

The resonance frequencies of a glass/PVB/glass sandwich beam have strongly varying sensitivities for changes of the value of the transverse shear modulus G (see figure 1.1).

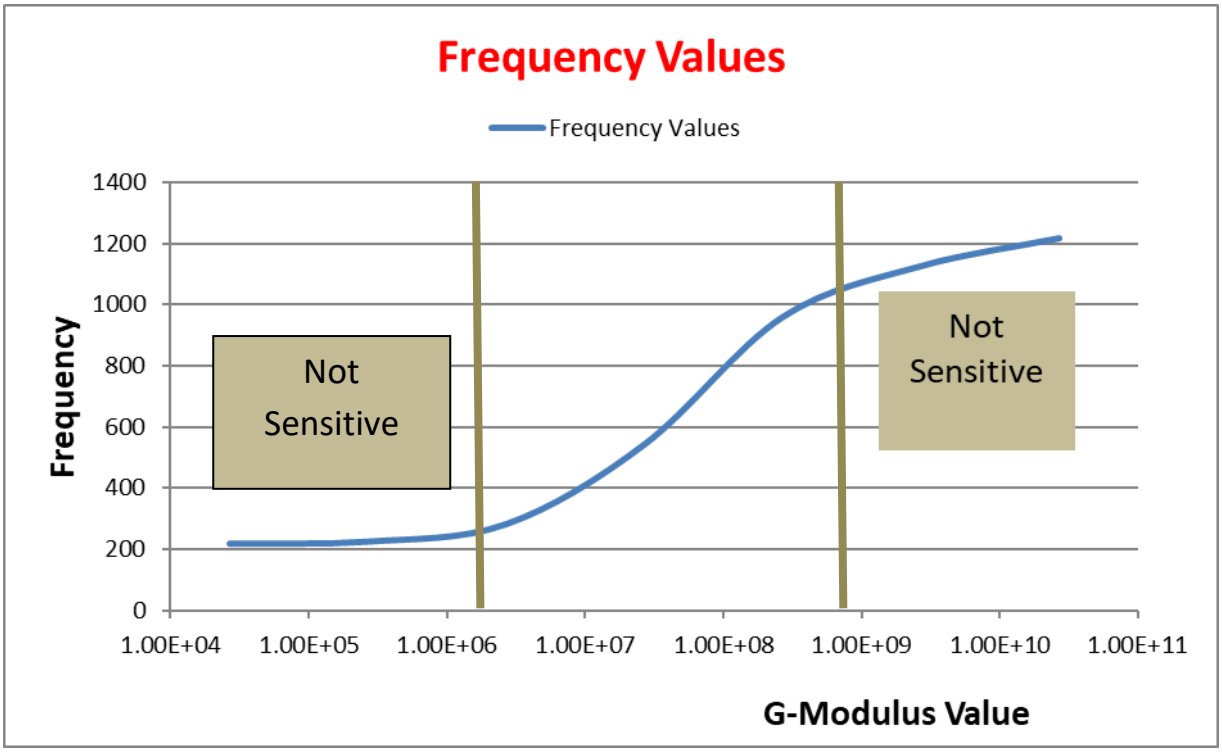

Figure 1.2 Resonance frequencies as a function of the transverse shear modulus

It was found that a glass/PVB/glass sandwich beam has two extreme modes of behavior: for big G-values, it behaves like a solid beam, for small G-values, the upper and lower glass beams deform independently. In the zones of those extreme behaviors, the sensitivity of the measured frequencies for variations of the G-value is small and hence correct identification of the G-modulus is difficult.

In October 2014, identification of the transverse shear modulus of glass sandwich beams with an inner layer of PVB material (delivered by the company Eastman – former Solutia) was identified as a function of temperature (figure 1.3). The inner PVB layer was 0.3 mm thick.

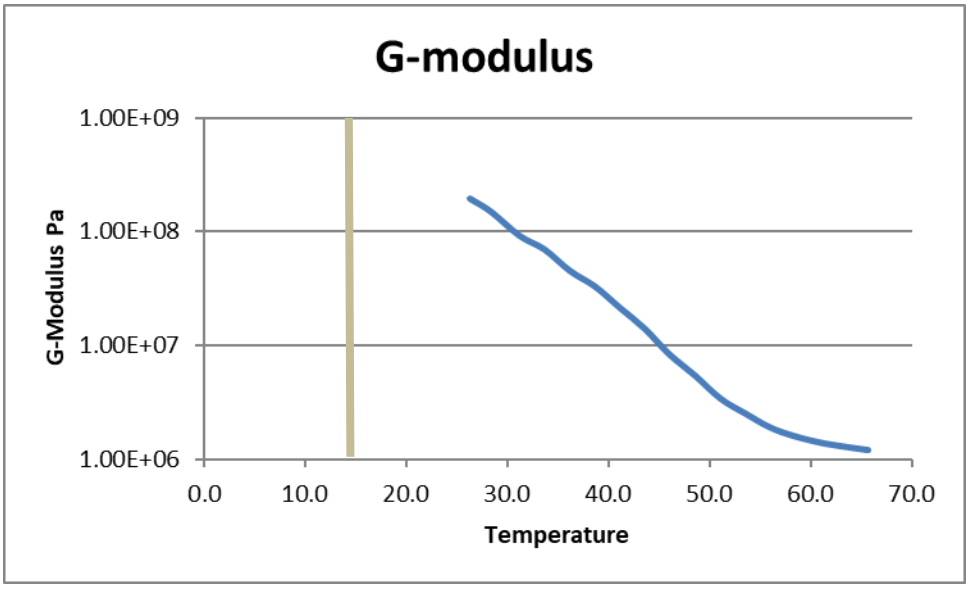

Figure 1.3 The transverse shear modulus as a function of temperature

The sensitivity of the eigenvalue lambda of the beams at lower temperatures than 25°C was too low for identification (figure 1.4). This means that the test beams only allowed identifying the G-modulus of the PVB layer for temperatures higher than 25°C.

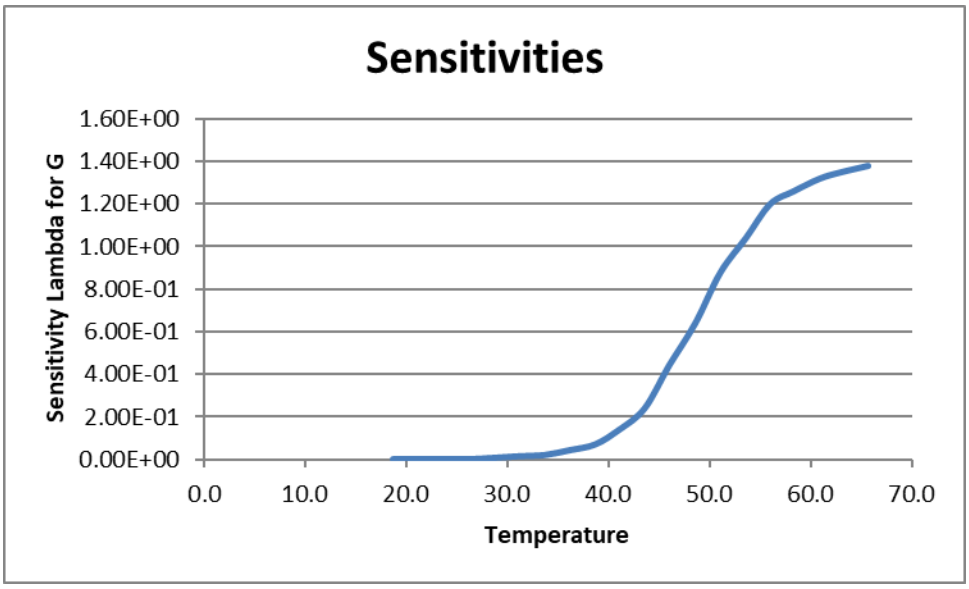

Figure 1.4 Sensitivity of the eigenvalues as a function of temperature

It was concluded that a test beam with a very thin PVB layer (0.3mm) is not suitable for identification of the G-Modulus of PVB at temperatures lower than 25°C.

In September 2024 six test beams delivered by the University of Prague were tested. The core thickness h_0 of the PVB layer varies around 1mm. The glass layer thickness h was about 4.8 mm.

Beam Nr.	Total t [m]	Width [m]	h_0 [m]	h [m]	Mass M [kg]
LGB4	0.01050	0.03012	0.0010	0.0047	0.22230
LGB5	0.01048	0.02996	0.0009	0.0048	0.22303
LGB6	0.01049	0.03048	0.0008	0.0048	0.22521
LGB7	0.01053	0.03010	0.0013	0.0046	0.22342
LGB8	0.01045	0.02998	0.0006	0.0049	0.22443
LGB9	0.01052	0.03015	0.0009	0.0048	0.22407

Table 1.1 laminated glass beams

The identification at room temperature yields following results:

Beam Nr.	Frequency [Hz]	Damping [%]	Transverse Shear Modulus [Pa]	Apparent Stiffness [m]	Max. Beam Bending Stiffness [m]
LGB4	617	2.095	1.565E8	180	204
LGB5	617	2.262	1.228E8	181	207
LGB6	617	2.262	1.474E8	181	203
LGB7	619	2.453	1.613E8	178	207
LGB8	619	2.557	1.400E8	183	201
LGB9	619	2.615	1.377E8	181	206

Table 1.2 Identified transverse shear modulus

The identified transverse shear modulus has values between 1.23E+08 and 1.61E+08.

There was also a first attempt to measure the vibration properties as a function of temperature in the climate chamber of the VUB. Figure 1.5 and figure 1.6 show the measured resonance frequencies and damping ratios in a temperature interval between -20°C and 50°C.

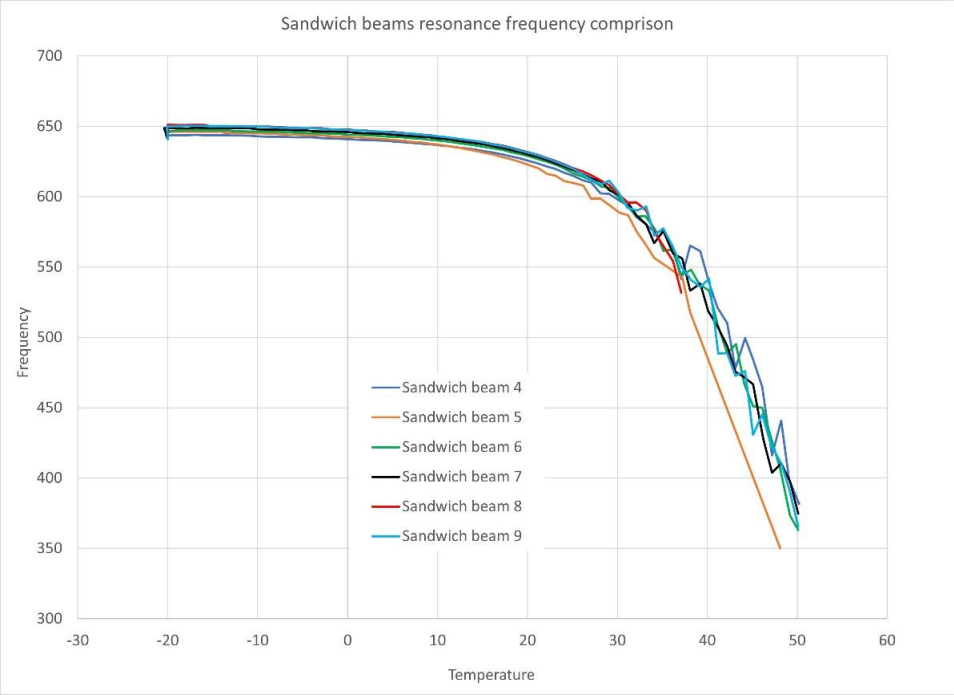

Figure 1.5 Resonance frequencies as a function of the temperature

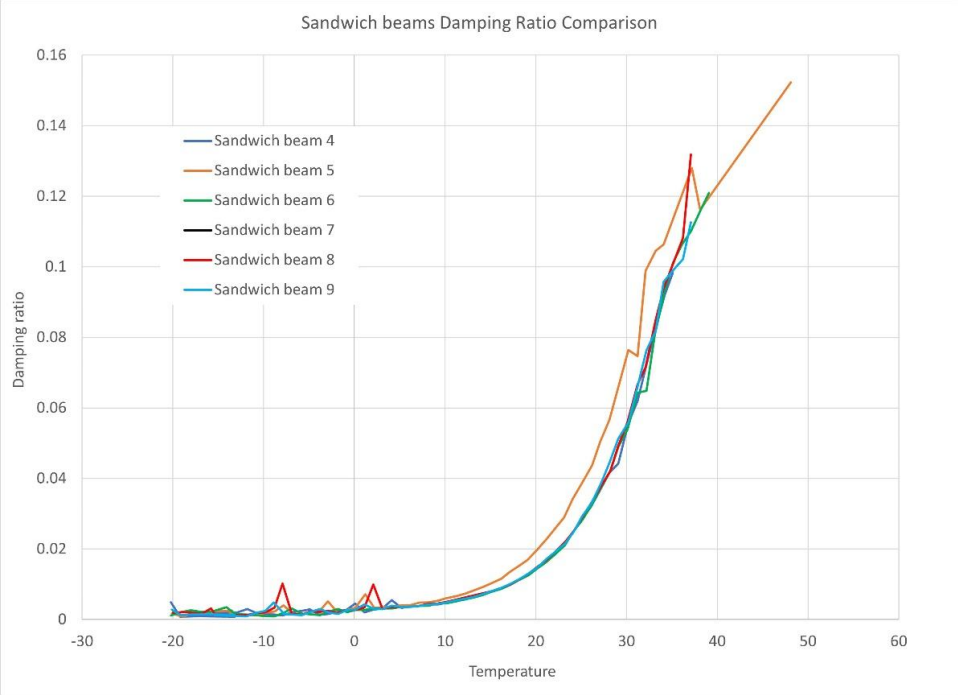

Figure 1.6 Damping ratios as a function of the temperature

It is observed that for temperatures lower than 20°C the frequencies and damping ratios are close to constant values. The test beams hence behave as solid beams with little influence from the PVB layer.

This report studies the properties of a new series of test sandwich beams, delivered by the Prague University. The laminated beams consist of 3 test series with each different PVB thickness layers, series A = 2.28 mm, series B = 1.52 mm and series C = 0.76 mm. Each of the 3 series contains 3 test samples of 4 different lengths (L1 = 30 cm, L2 = 25 cm, L3 = 20 cm and L4 = 15 cm).

As a first simulation test, to gain insight about the sensitivity of the procedure for the thickness of the PVB layer, the resonance frequencies are plotted against increasing values for the transverse shear modulus.

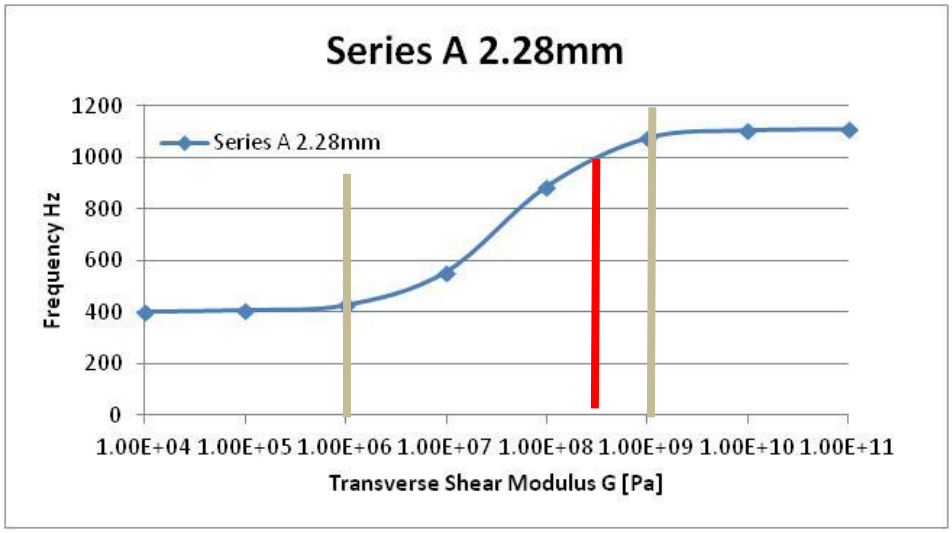

Figure 1.7 Resonance frequencies as function of the transverse shear modulus

The typical value of 1.5E+08 Pa (red color) falls into the area of easy identification (grey lines).

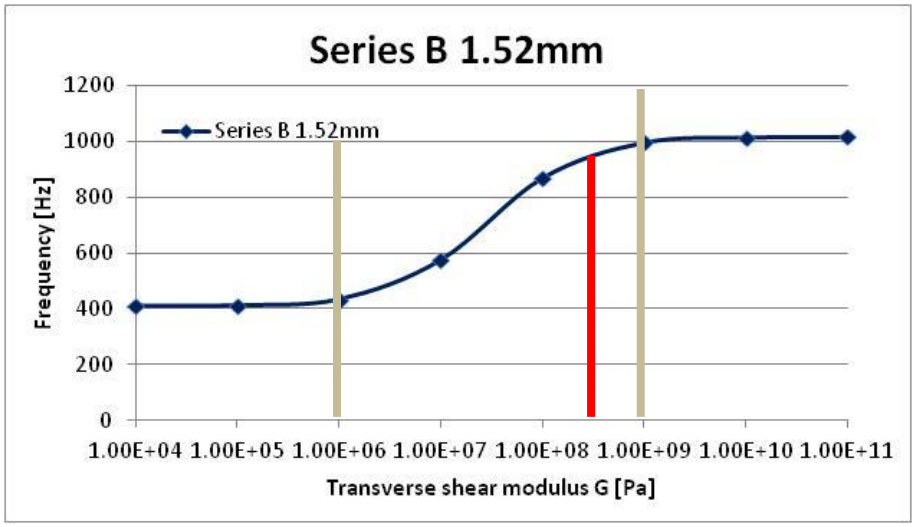

Figure 1.8 Resonance frequencies as function of the transverse shear modulus

The typical value of 1.5E+08 Pa still falls into the area of easy identification.

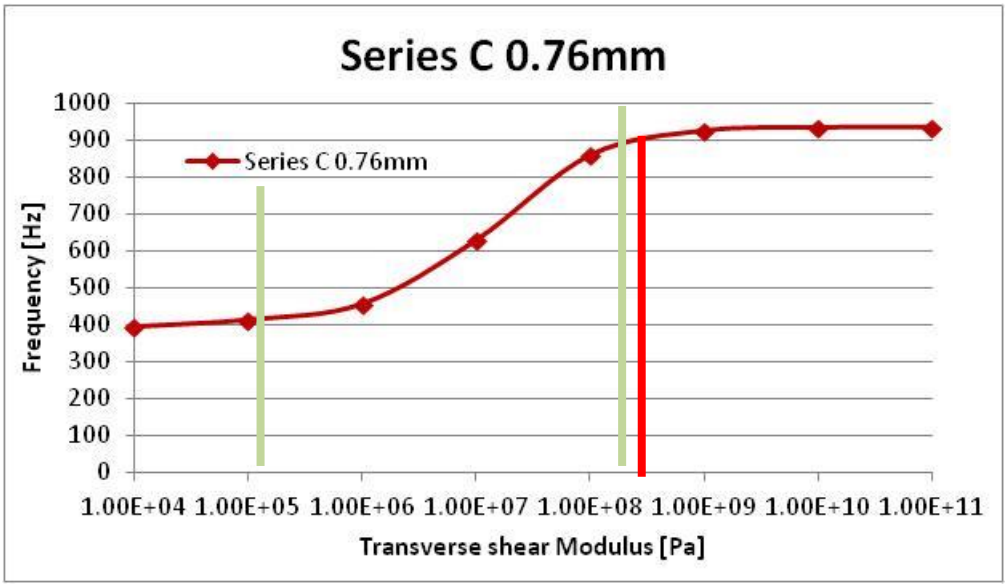

Figure 1.9 Resonance frequencies as function of the transverse shear modulus

The typical value of 1.5E+08 Pa falls now into the un-sensitive zone. It can be predicted that the identification of the transverse shear modulus will hence be more cumbersome for beams of the C-series with this thin PVB layer.

The University of Prague also delivered pure glass beams and plates. These samples will be used to establish correct values for the glass layers.

2 Test on pure glass beams and plates

2.1 Description of the geometry of the test specimens

2.1.1 Solid glass beams

Beam Nr.	Length [m]	Width [m]	Thickness [m]	Mass [kg]
GB1	0.3	0.03015	0.00490	0.10967
GB2	0.3	0.03006	0.00489	0.10904
GB3	0.3	0.03012	0.00480	0.10758

Table 2.1.1.1 Geometry solid glass beams

2.1.2 Solid glass plates

Plate Nr.	Length [m]	Width [m]	Thickness [m]	Mass [kg]
GP1	0.2995	0.2995	0.00497	1.10320
GP2	0.2995	0.2995	0.00496	1.10192
GP3	0.2995	0.2995	0.00493	1.09509

Table 2.1.2.1 Geometry solid glass plates

2.1.3 Frequency and damping tests on solid glass beams

The first resonance frequency and the associated damping ratio of the glass beams were measured with the "***Beam properties***" module of the Resonalyser software of the company BYTEC BV.

The results and the identified Young's modulus are given in the next table:

Beam Nr.	Frequency [Hz]	Damping ratio [-]	Young's modulus Real part [Pa]	Young's modulus Imaginary part [Pa]	Tangens Delta [-]
GB1	299.3	0.073	7.10E10	1.04E8	0.00147
GB2	298.8	0.067	7.15E10	9.58E7	0.00134
GB3	296.0	0.075	7.21E10	1.10E8	0.00152

Table 2.1.3.1 Results of tests on glass beams

2.1.4 Frequency and damping tests on solid glass plates

The glass plates were tested using the plate module of the Resonalyser software. The glass material was assumed to be isotropic.

The next pictures show the identification results for the 3 tested glass plates. The results include the Young's modulus E, the Poisson ratio v and the in-plane shear modulus G. The real and imaginary part of the engineering constants as well as the plate rigidities are given in figures 2.1.4.1 till 2.1.4.3

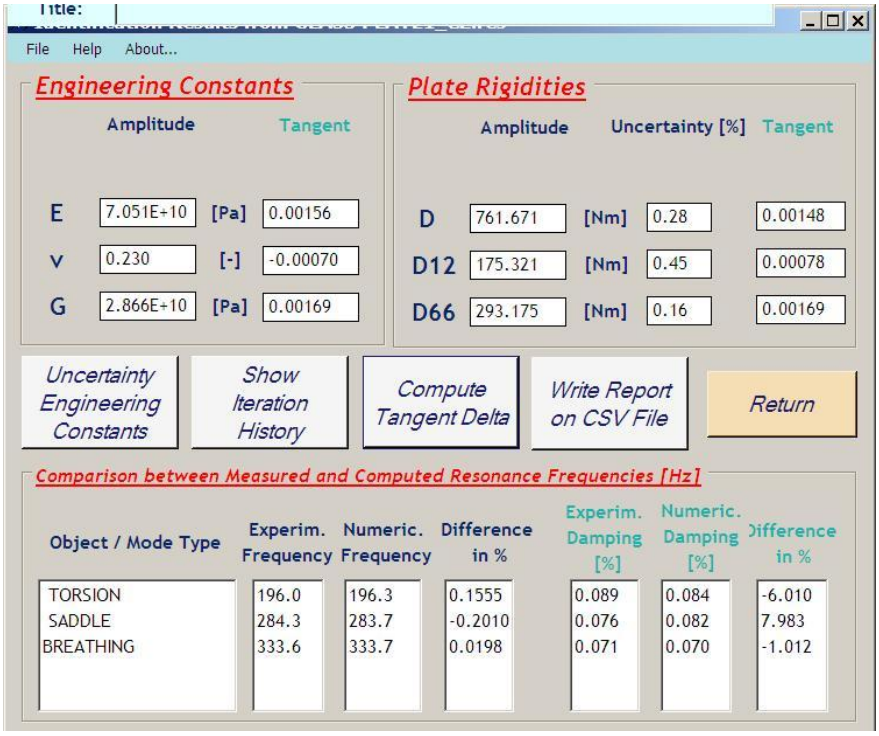

Figure 2.1.4.1 Results of glass plate 1

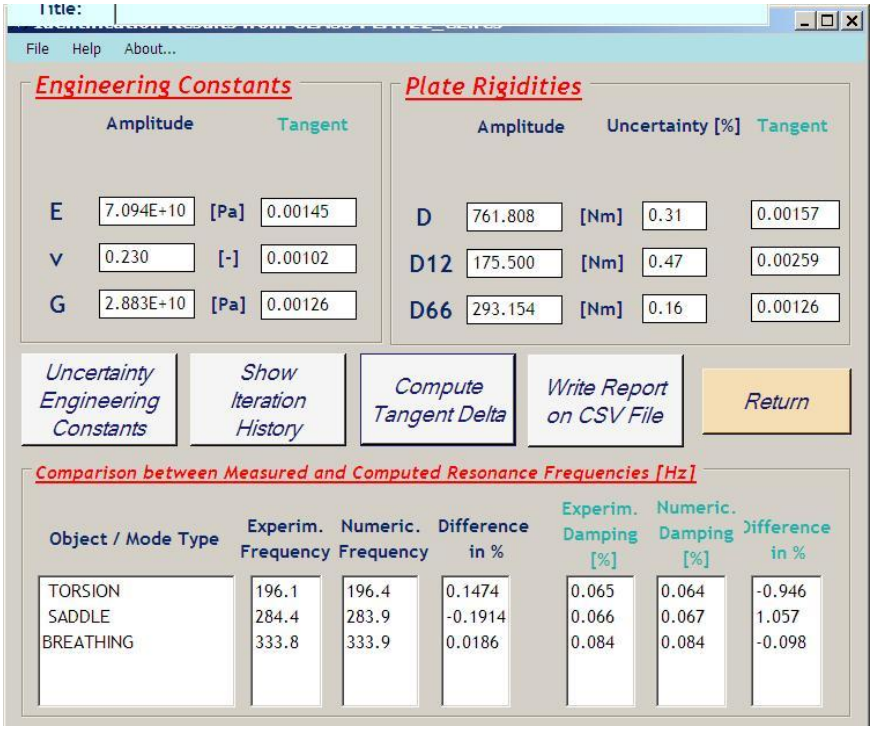

Figure 2.1.4.2 Results of glass plate 2

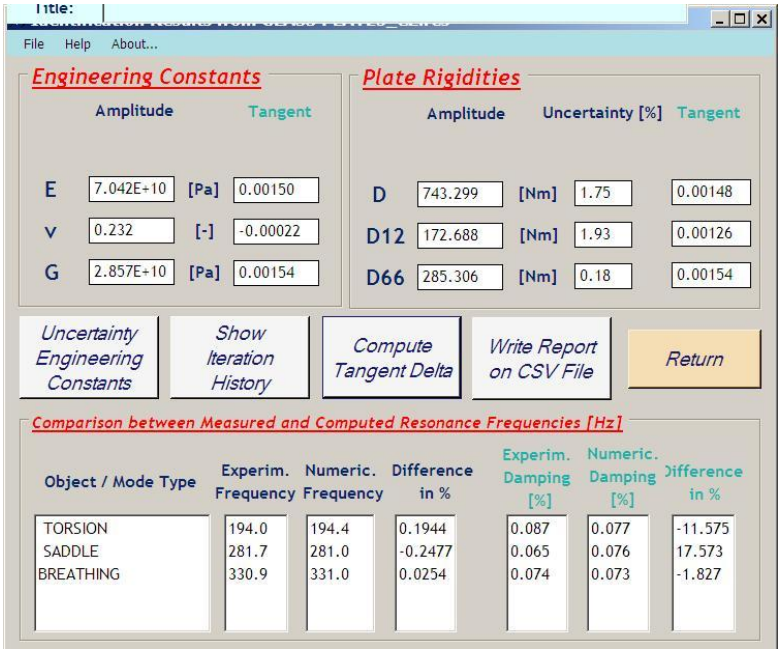

Figure 2.1.4.3 Results of glass plate 3

2.1.5 Summary of the solid glass properties

Averaging the values of the beam and plate tests, yields the following result:

Young's modulus E:	**7.09E10 + i. 1.06E08 Pa**
Tangents delta E :	**0.0015**
Poisson's ratio v:	**0.23 + i. 0**
In-plane shear modulus G:	**2.88E10 + i.4.3E07 Pa**
Tangents delta G:	**0.0015**
Glass thickness variation:	**(0.00480 m – 0.00499 m)**
Average glass thickness:	**0.00493 m**
Average glass density:	**2474 kg/m3**

These values will be used in the study of the laminated sandwich beams.

3 Laminated glass beams

The laminated beams consist of 3 test series with different PVB thickness layers, series A = 2.28 mm, series B = 1.52 mm and series C = 0.76 mm. Each of the 3 series contains 3 test samples of 4 different lengths (L1 = 30 cm, L2 = 25 cm, L3 = 20 cm and L4 = 15 cm).

The total thickness of a beam samples was never perfectly constant along the length. Typical differences between the middle section and the thickness at both the ends was 0.35 mm for the A series, 0.2 mm for the B series and 0.1 mm for the C series. Table 3.1 shows the measured laminate thicknesses of series A (PVB layer = 0.00228 m).

Beam Nr.	End-1 [m]	Middle [m]	End-2 [m]	Max Difference [m]
AL1-1	0.01181	0.01210	0.01205	0.00029
AL1-2	0.01204	0.01209	0.01209	0.00005
AL1-3	0.01206	0.01197	0.01191	0.00017
AL2-1	0.01207	0.01203	0.01210	0.00007
AL2-2	0.01205	0.01199	0.01196	0.00009
AL2-3	0.01182	0.01212	0.01207	0.00030
AL3-1	0.01211	0.01206	0.01177	0.00034
AL3-2	0.01180	0.01207	0.01212	0.00032
AL3-3	0.01184	0.01197	0.01215	0.00031
AL4-1	0.01178	0.01191	0.01207	0.00029
AL4-2	0.01209	0.01199	0.01193	0.00016
AL4-3	0.01168	0.01183	0.01202	0.00035

Table 3.1. Variation of the total thickness of laminate beams series A

The thickness distribution of AL4-1 was also investigated with an optical microscope Levenhuk DTX (accuracy 0.01 mm)

Beam A-1L	End-1 [mm]	Middle [mm]	End-2 [mm]	Max Difference [m]
PVB	1.94	2.03	2.13	0.00016
Upper glass	4.93	4.79	4.79	0.00014
Lower glass	4.80	4.78	4.88	0.00008
Total	11.67	11.60	11.80	0.00020

Table 3.2. Variation the layer thicknesses of laminate beam AL4-1.

The thicknesses measured with the optical microscope reveal that the actual thickness of the PVB layer in the A-series can be lower than 2.28 mm at several positions. There is clearly an uncertainty about the thicknesses of the glass and the thicknesses of the PVB layers. The measured thickness in the middle of the beams will be taken as the logical reference. There are two possible approaches:

1. The thickness of the PVB layer is assumed to be constant. The thickness of the glass layers is adapted in order to reach the measured thickness in the middle of the beams

2. The thickness of the glass layers is assumed to be constant. The thickness of the PVB layers is adapted in order to reach the measured thickness in the middle of the beams

The next chapter 3.1 will report the results conform to the first approach (constant assumed thickness of the PVB layers)

The input values for the experiments were determined as follows:

- The glass density was assumed constant as rho = 2474 kg/m3
- The PVB density was assumed constant as rho = 1065 kg/m3
- In this first approach, the thicknesses of the PVB layers were assumed constant: for series A = 2.28 mm, for series B = 1.52 mm, for series C = 0.76 mm.
- The assumed constant laminate thickness was measured in the middle of the beams with a caliper (0.01 mm accuracy)
- In the first approach, the glass layer thicknesses were computed as total thickness minus the PVB layer thickness. Both glass layers were assumed to have the same thickness
- The width of the beams was adapted in such a way that the total mass was equal to the measured mass value (+ 0.00045 kg correction for the 5 mm suspension holes). The total mass was measured with an accuracy of 0.00001 kg.
- The resonance frequencies were measured with an accuracy of 0.1%
- The damping ratios were measured with an accuracy of 5%
- The test room was air-conditioned at 22°C with a variation of 0.5°C.

3.1 Assumption of constant PVB layer thickness

3.1.1 Geometry and mass of series A (2.28 mm)

Based on the value of the density of glass (ρ = 2474 kg/m3) and the density of PVB (ρ_0 = 1065 kg/m3), the total laminate thickness t, the length L, the total measured mass M, the average thickness of the glass h, the thickness of the PVB layer h_0, the average width W can be computed:

$$M = L.W(2h\rho + h_0\rho_0)$$
$$W = \frac{M}{L.(2h\rho + h_0\rho_0)} \quad (3.1)$$

Beam Nr.	Length L [m]	Width W [m]	Laminate Thickness t [m]	Thickness PVB Layer h_0 [m]	Thickness Glass Layer h [m]	Mass M [kg]
AL1-1	0.30	0.0302	0.01210	0.00228	0.00491	0.24205
AL1-2	0.30	0.0301	0.01209	0.00228	0.00491	0.24077
AL1-3	0.30	0.0302	0.01197	0.00228	0.00485	0.24086
AL2-1	0.25	0.0302	0.01203	0.00228	0.00488	0.20078
AL2-2	0.25	0.0307	0.01199	0.00228	0.00486	0.20255
AL2-3	0.25	0.0304	0.01212	0.00228	0.00492	0.20069
AL3-1	0.20	0.0302	0.01206	0.00228	0.00489	0.16041
AL3-2	0.20	0.0303	0.01207	0.00228	0.00490	0.16001
AL3-3	0.20	0.0304	0.01197	0.00228	0.00485	0.16030
AL4-1	0.15	0.0308	0.01191	0.00228	0.00482	0.12123
AL4-2	0.15	0.0306	0.01199	0.00228	0.00486	0.12113
AL4-3	0.15	0.0307	0.01183	0.00228	0.00478	0.12023

Table 3.1.1.1 laminated glass beams geometry series A (2.28mm)

The values for the laminate thickness were measured in the middle of the beam sample with a digital caliper (0.01 mm accuracy).

3.1.2 Geometry and mass of series B (1.52 mm)

Beam Nr.	Length L [m]	Width W [m]	Laminate Thickness t [m]	Thickness PVB Layer h_0 [m]	Thickness Glass Layer h [m]	Mass M [kg]
BL1-1	0.30	0.0305	0.01114	0.00152	0.00481	0.23229
BL1-2	0.30	0.0306	0.01115	0.00152	0.00482	0.23311
BL1-3	0.30	0.0305	0.01115	0.00152	0.00482	0.23263
BL2-1	0.25	0.0304	0.01115	0.00152	0.00482	0.19334
BL2-2	0.25	0.0302	0.01116	0.00152	0.00482	0.19200
BL2-3	0.25	0.0301	0.01115	0.00152	0.00482	0.19143
BL3-1	0.20	0.0304	0.01114	0.00152	0.00481	0.15386
BL3-2	0.20	0.0305	0.01111	0.00152	0.00480	0.15428
BL3-3	0.20	0.0303	0.01117	0.00152	0.00483	0.15413
BL4-1	0.15	0.0301	0.01113	0.00152	0.00481	0.11444
BL4-2	0.15	0.0308	0.01113	0.00152	0.00481	0.11715
BL4-3	0.15	0.0303	0.01111	0.00152	0.00480	0.11474

Table 3.1.2.1 Geometry laminated glass beams series B (1.52mm)

3.1.3 Geometry and mass of series C (0.76 mm)

Beam Nr.	Length L [m]	Width W [m]	Laminate Thickness t [m]	Thickness PVB Layer h_0 [m]	Thickness Glass Layer h [m]	Mass M [kg]
CL1-1	0.30	0.0301	0.01042	0.00076	0.00483	0.22286
CL1-2	0.30	0.0302	0.01044	0.00076	0.00484	0.22376
CL1-3	0.30	0.0298	0.01040	0.00076	0.00482	0.21977
CL2-1	0.25	0.0305	0.01042	0.00076	0.00483	0.18792
CL2-2	0.25	0.0301	0.01043	0.00076	0.00484	0.18614
CL2-3	0.25	0.0303	0.01040	0.00076	0.00482	0.18614
CL3-1	0.20	0.0296	0.01039	0.00076	0.00481	0.14500
CL3-2	0.20	0.0298	0.01041	0.00076	0.00483	0.14686
CL3-3	0.20	0.0300	0.01041	0.00076	0.00483	0.14781
CL4-1	0.15	0.0299	0.01042	0.00076	0.00483	0.11049
CL4-2	0.15	0.0302	0.01042	0.00076	0.00483	0.11155
CL4-3	0.15	0.0306	0.01040	0.00076	0.00482	0.11280

Table 3.1.3.1 Geometry laminated glass beams series C (0.76mm)

3.1.4 Identification of the transverse shear modulus of the laminate beams at room temperature (21-22°C)

The transverse shear storage modulus was identified using the glass properties, the beam geometry and the measured resonance frequency.

The tangents delta of the transverse shear modulus of the PVB was computed using the measured damping ratio and the ratio of the potential energy (PE) of the PVB layer and the total potential energy (PE) of the beam vibrating at the first resonance frequency with a bending modal shape.

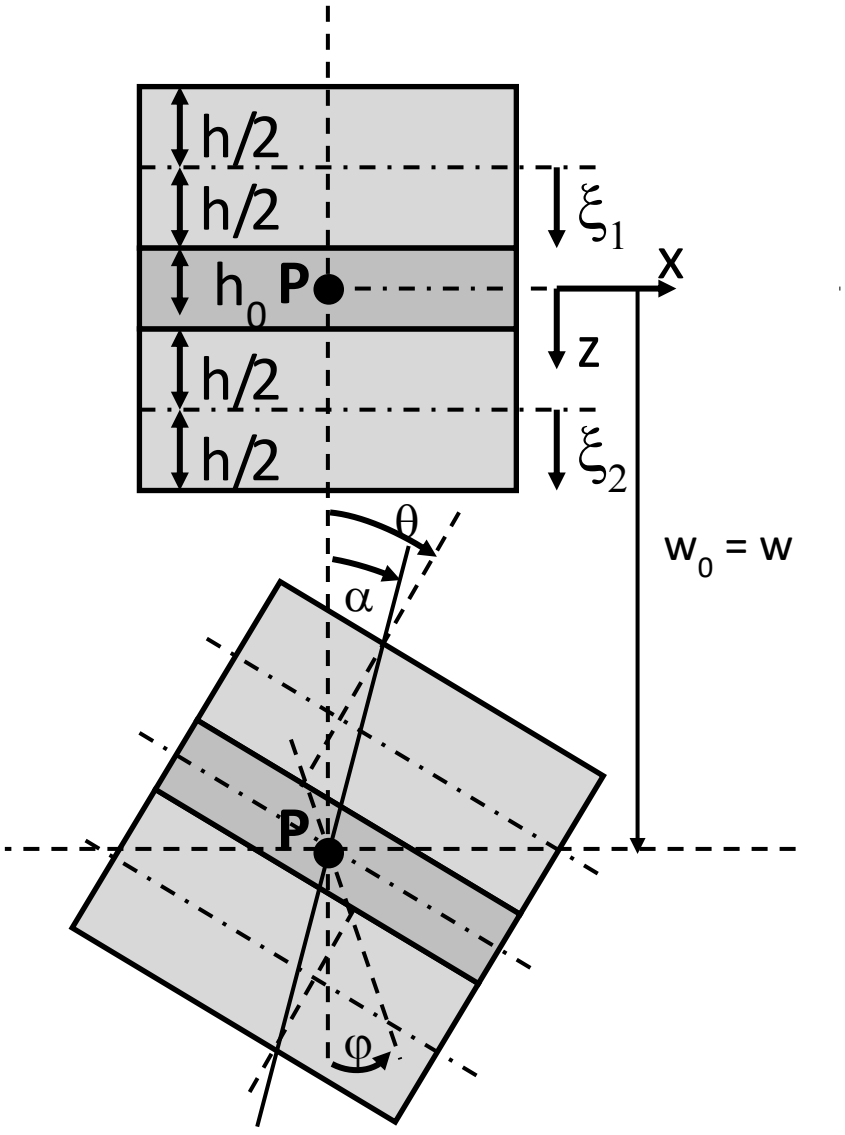

Figure 3.1.4.1. Deformation of a triplex glass beam

The expression for the potential energy PE and kinetic energy KE can be expressed as a function of the selected global degrees of freedom w and α.

$$Total\,PE = \int_{-L/2}^{L/2} E\frac{bh^3}{12}\left(\frac{\partial^2 w}{\partial x^2}\right)^2 dx + \int_{-L/2}^{L/2} Ebh\left(\frac{(2h+h_0)}{2} + \frac{h}{2}\frac{\partial^2 w}{\partial x^2}\right)^2 dx +$$
$$\frac{1}{2}\int_{-L/2}^{L/2} h_0 bG_0\left(\frac{\alpha(2h+h_0)}{h_0} + \frac{\partial w}{\partial x}\frac{(2h+h_0)}{h_0}\right)^2 dx + \frac{1}{2}\int_{-L/2}^{L/2} E_0\frac{bh_0^3}{12}\left(\frac{\partial^2 w}{\partial x^2}\right)^2 dx \quad (3.2)$$

$$(PE)_{PVB} = \frac{1}{2}\int_{-L/2}^{L/2} h_0 bG_0\left(\frac{\alpha(2h+h_0)}{h_0} + \frac{\partial w}{\partial x}\frac{(2h+h_0)}{h_0}\right)^2 dx \quad (3.3)$$

The total potential energy (3.2) has contributions from the glass and PVB layers. It is logically assumed that all the dissipated energy originates from the shearing behavior of the PVB layer, expression (3.4).

$$(\tan\delta)_{PVB} = \frac{Dissipated\ Energy}{2\pi(PE)_{PVB}} = \frac{2\xi_{Measured}}{(PE)_{PVB}/TotalPE} \quad (3.4)$$

The kinetic energy KE can be computed with (3.5):

$$KE = \frac{1}{2}\int_{-L/2}^{L/2}(\rho A + \rho_0 A_0)\left(\frac{\partial w}{\partial t}\right)^2 dx + \frac{1}{2}\int_{-L/2}^{L/2}(\rho I + \rho_0 I_0)\left(\frac{\partial \alpha}{\partial t}\right)^2 dx \quad (3.5)$$

The potential and kinetic energy contributions can be computed with the numerical model of the laminated sandwich beam. To validate the correct value of expressions (3.2) and (3.5), the potential and also kinetic energy is computed with the numerical model on the following example:

Length Beam	:	.25000 m
Width Beam	:	3.01000E-02 m
Thick Skin layer	:	4.84000E-03 m
Thick Poly layer	:	7.60000E-04 m
Specific Mass Skin:		2475.0 kg/m3
Specific Mass Poly :		1065.0 kg/m3
Beam Mass	:	.18637 kg
E-modulus Skin	:	7.09000E+10 Pa
E-modulus Poly	:	4.23100E+08 Pa
G-modulus Poly	:	1.00000E+11 Pa

The result is:

COMPUTED SANDWICH FREQUENCY:	934.89 Hz
TOTAL POTENTIAL ENERGY:	1.72526E+07 Nm
CONTRIBUTION BENDING MOMENT:	3.44013E+06 Nm
CONTRIBUTION NORMAL FORCE:	1.38089E+07 Nm
CONTRIBUTION SHEAR FORCE:	3505.1 Nm
CONTRIBUTION BENDING CORE:	39.742 Nm
TOTAL KINETIC ENERGY:	1.72526E+07 Nm
CONTRIBUTION MASS:	1.71242E+07 Nm
CONTRIBUTION INERTIA:	1.28441E+05 Nm

It can be observed that the total potential energy is exactly equal to the total kinetic energy (this is Rayleigh's principle). This supports the correctness of the numerical model.

Figures 3.4.1.2 and 3.4.1.3 illustrate the measurement of the resonance frequency using the Resonalyser instrument and the identification of the damping ratio.

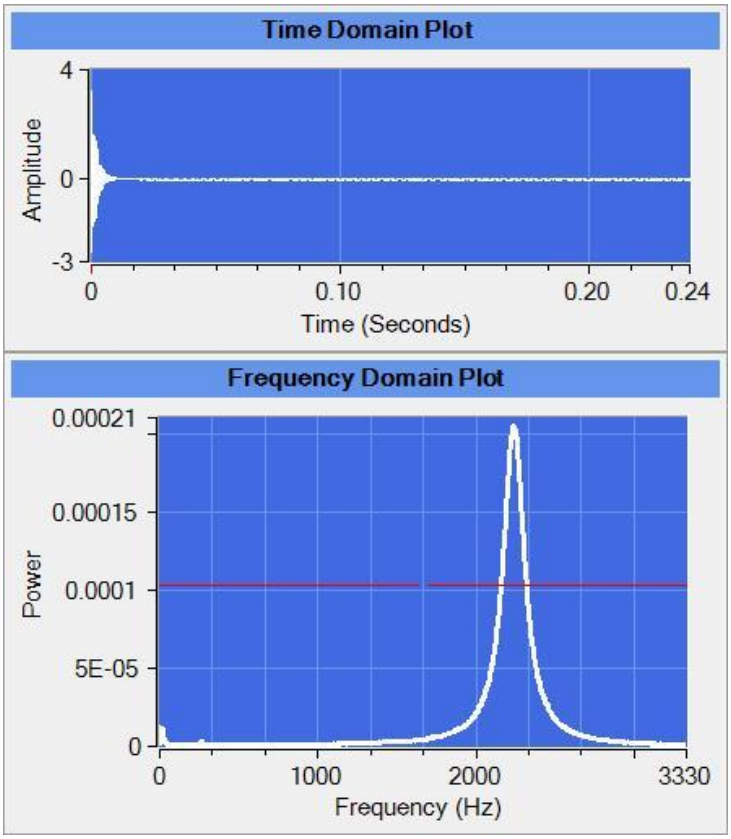

Figure 3.4.1.2. Measurement of the resonance frequency with impulse excitation

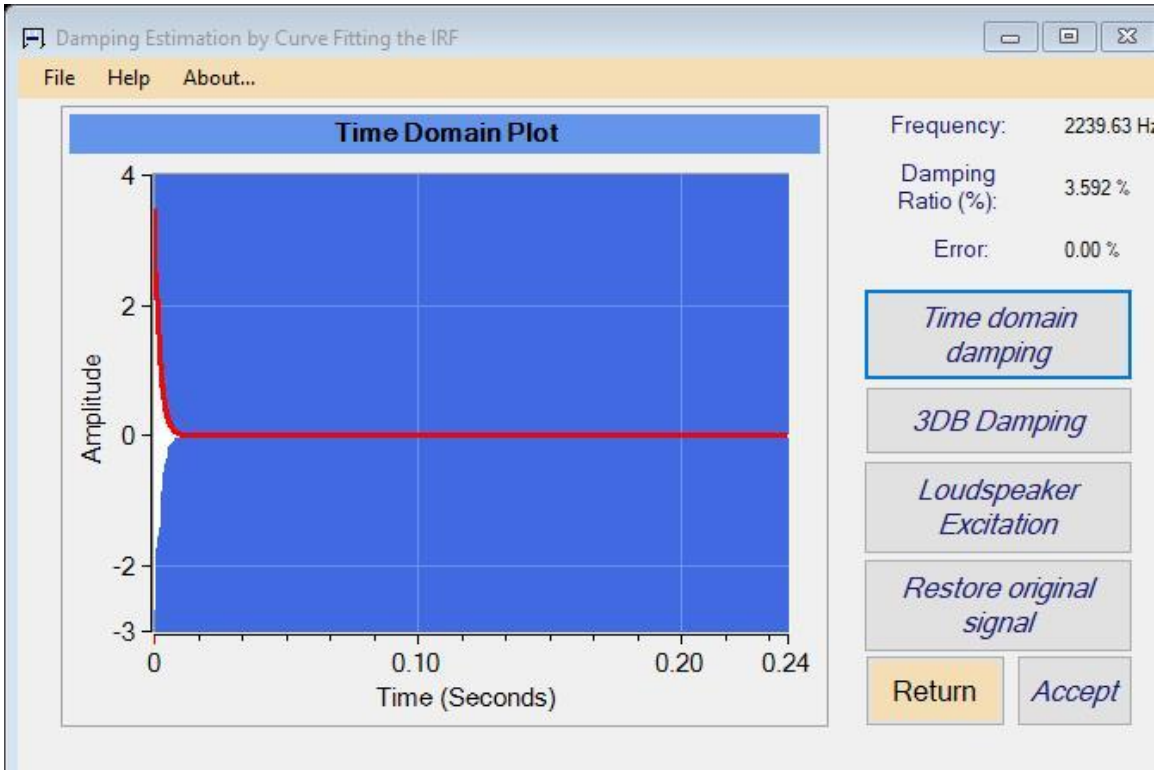

Figure 3.4.1.3. Identification of the damping ratio by curve fitting in the time domain.

Figure 3.4.1.4 shows an example of an identification result using the numerical model with the Resonalyser software.

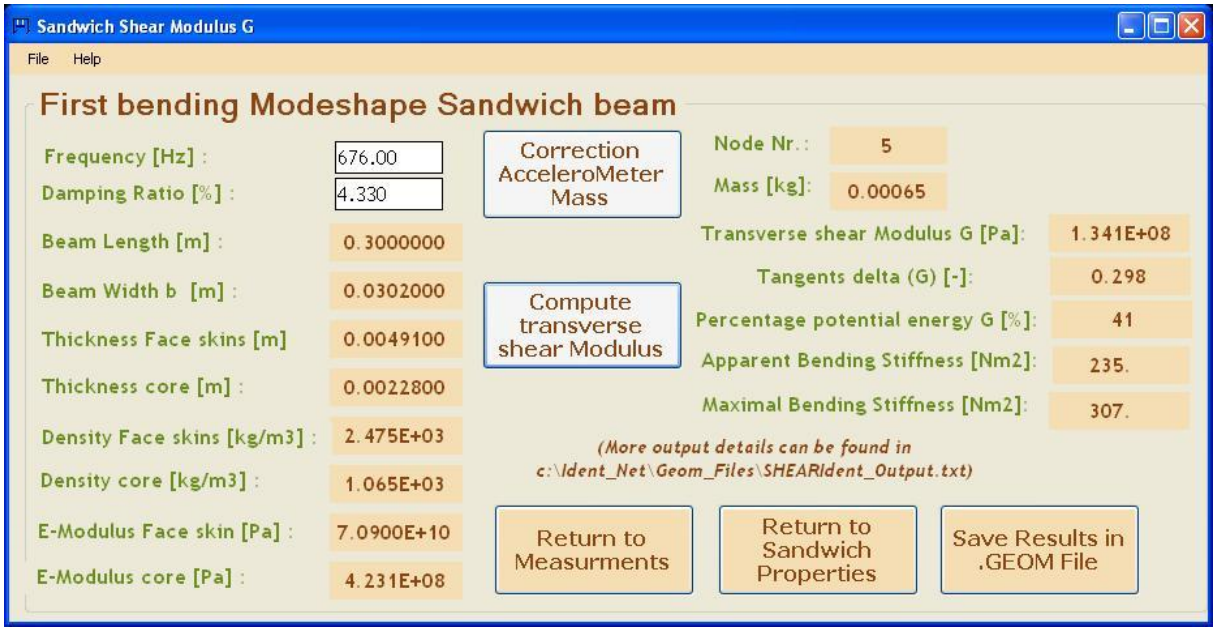

Figure 3.4.1.4. Print screen (Resonalyser software) of a transverse shear identification.

The following paragraphs summarize the results for the 3 test series.

3.1.5 Identification of the transverse shear modulus of series A (2.28 mm)

Beam Nr.	Measured Frequency [Hz]	Measured Damping ratio [%]	Transverse Shear Modulus [Pa]	Potential Energy Ratio PVB/Total	Tangents Delta Shear Modulus
AL1-1	676	4.330	1.317E8	22.0	0.394
AL1-2	677	4.530	1.335E8	21.9	0.414
AL1-3	674	4.177	1.384E8	21.2	0.394
AL2-1	936	4.941	1.432E8	25.9	0.382
AL2-2	934	4.911	1.438E8	25.8	0.381
AL2-3	939	5.012	1.409E8	26.3	0.381
AL3-1	1366	6.521	1.413E8	32.7	0.400
AL3-2	1385	6.103	1.528E8	31.5	0.387
AL3-3	1366	6.227	1.459E8	32.0	0.389
AL4-1	2197	6.731	1.502E8	39.0	0.330
AL4-2	2209	6.598	1.545E8	38.7	0.341
AL4-3	2180	6.716	1.521E8	38.8	0.348

Table 3.1.5.1. Identified transverse shear modulus properties series A (2.28 mm)

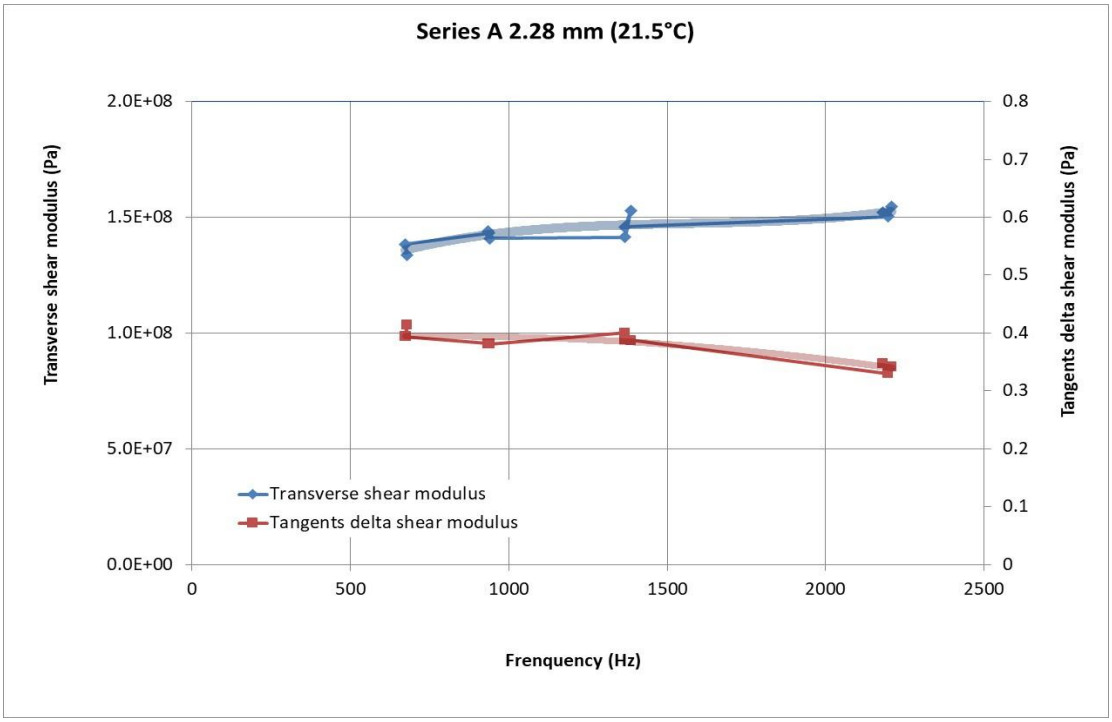

Figure 3.1.5.2. Identified transverse shear modulus properties series A (2.28 mm)

The average value of the storage part of the G-modulus at the lowest frequencies equals to 1.32 E8 Pa, at the highest frequency 1.52 E8 Pa.

The tangents delta value decreases from 0.39 towards 0.55 and seems to be more frequency dependent.

3.1.6 Identification of the transverse shear modulus of series B (1.52 mm)

Beam Nr.	Measured Frequency [Hz]	Measured Damping ratio [%]	Transverse Shear Modulus [Pa]	Potential Energy Ratio PVB/Total	Tangents Delta Shear Modulus
BL1-1	644	3.948	1.356E8	15.5	0.509
BL1-2	642	3.888	1.294E8	16.0	0.486
BL1-3	642	3.853	1.294E8	16.0	0.482
BL2-1	898	4.498	1.366E8	19.7	0.457
BL2-2	893	4.473	1.293E8	20.4	0.439
BL2-3	890	4.536	1.237E8	21.0	0.432
BL3-1	1329	5.413	1.350E8	25.7	0.421
BL3-2	1325	5.283	1.334E8	25.9	0.408
BL3-3	1318	5.515	1.239E8	26.9	0.410
BL4-1	2176	5.944	1.402E8	32.7	0.364
BL4-2	2167	6.088	1.366E8	33.0	0.369
BL4-3	2172	6.182	1.415E8	32.6	0.379

Table 3.1.6.1. Identified transverse shear modulus properties series B

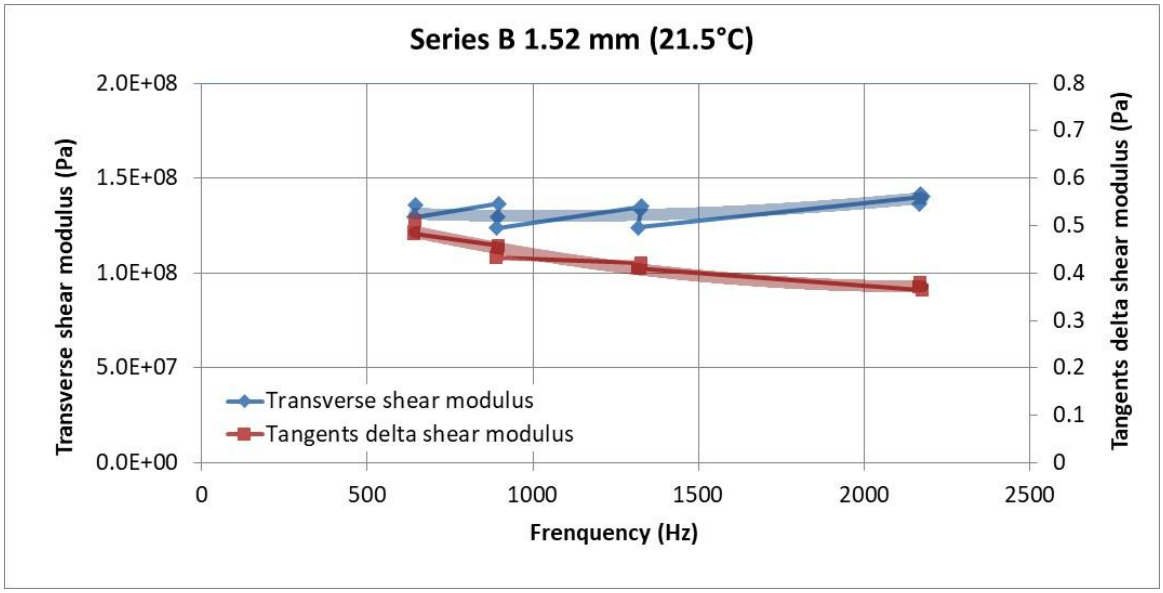

Figure 3.1.6.2. Identified transverse shear modulus properties series B

The average value of the storage part of the G-modulus at the lowest frequencies equals to 1.36 E8 Pa, at the highest frequency 1.41 E8 Pa.

The tangents delta value decreases from 0.50 towards 0.38 and seems to be more frequency dependent.

3.1.7 Identification of the transverse shear modulus of series C (0.76 mm)

Beam Nr.	Measured Frequency [Hz]	Measured Damping ratio [%]	Transverse Shear Modulus [Pa]	Potential Energy Ratio PVB/Total	Tangents Delta Shear Modulus
CL1-1	621	1.994	1.504E8	7.809	0.511
CL1-2	621	1.965	1.504E8	7.81	0.503
CL1-3	620	1.949	1.504E8	7.81	0.499
CL2-1	877	2.275	1.490E8	10.6	0.429
CL2-2	876	2.313	1.382E8	11.2	0.413
CL2-3	876	2.293	1.474E8	10.6	0.433
CL3-1	1337	2.816	1.663E8	13.5	0.417
CL3-2	1332	2.848	1.501E8	14.6	0.390
CL3-3	1316	2.849	1.283E8	16.3	0.350
CL4-1	2238	3.282	1.479E8	21.2	0.310
CL4-2	2243	3.443	1.510E8	21.0	0.328
CL4-3	2236	3.591	1.489E8	21.1	0.340

Table 3.1.7.1. Identified transverse shear modulus properties series C (0.72 mm)

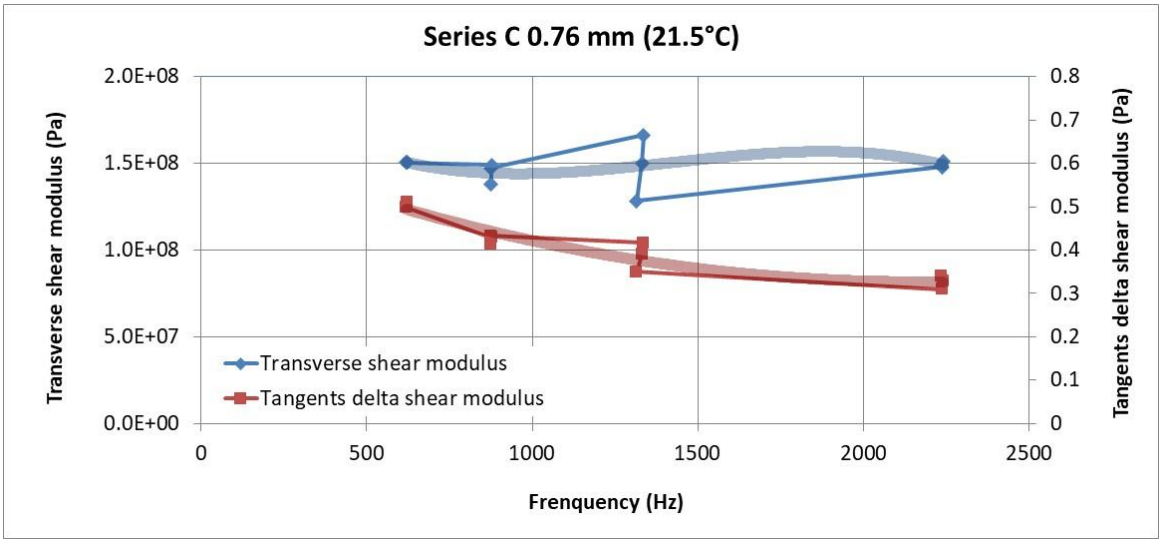

Figure 3.1.7.2. Identified transverse shear modulus properties series C (0.72 mm)

The average value of the storage part of the G-modulus at the lowest frequencies equals to 1.50 E8 Pa and are equal at the highest frequency

The tangents delta value increases from 0.511 towards 0.34 and seems to be more frequency dependent.

3.1.8 Comparison of the results

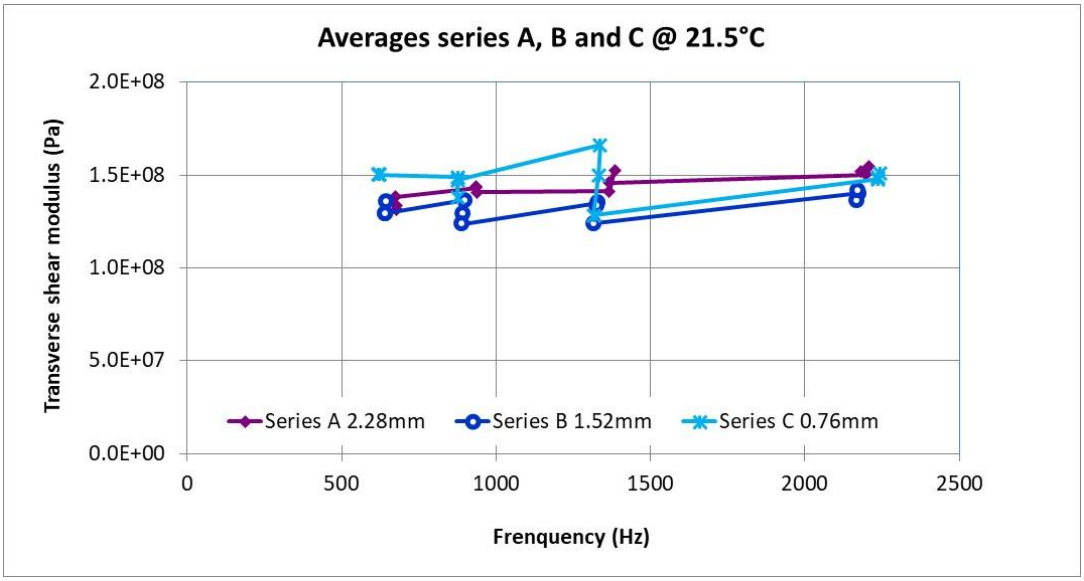

Figure 3.1.8.1. Identified transverse shear storage modulus

The value of the storage shear modulus for all series increases a little bit as a function of frequency. The thinnest PVB layer (series C) gives slightly higher values for the storage modulus.

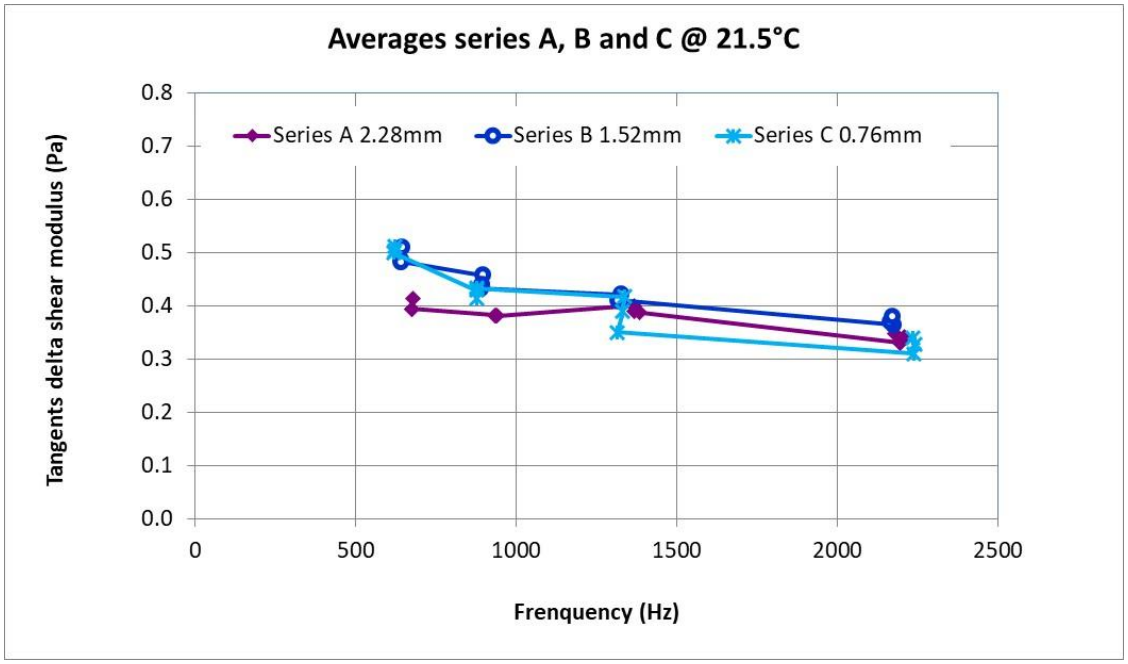

Figure 3.1.8.2. Identified transverse shear loss modulus (tangents delta)

All the tangents delta values decrease with increasing frequency. The thinnest PVB layer (series C) gives lower values for the loss modulus.

Since storage and loss modulus are material properties, it could be expected that the 3 series would provide the same values for storage and loss modulus.

The samples with the thinnest PVB layer seem to have little deviating properties. It should be examined with DMA tests if the in-plane Young's modulus E_0 also shows deviating properties for the thinnest PVB layer samples.

3.1.9 Sensitivity for input values

The input values for the experiments were determined as follows:

- The glass density was assumed constant as rho = 2474 kg/m3
- The PVB density was assumed constant as rho = 1065 kg/m3
- The thickness of the PVB layers were assumed constant: for series A = 2.28 mm, for series B = 1.52 mm, for series C = 0.76 mm.
- The total laminate thickness was measured in the middle of the beams with a caliper (0.01 mm accuracy)
- The glass layer thicknesses were found as total thickness minus the PVB layer thickness. Both glass layers were assumed to have the same thickness
- The width of the beams was adapted in such a way that the total mass was equal to the measured mass value (+ 0.00045 kg correction for the 5mm suspension holes). The total mass was measured with an accuracy of 0.00001 kg.
- The resonance frequencies were measured with an accuracy of 0.1%
- The damping ratios were measured with an accuracy of 5%
- The test room was air-conditioned at 22°C with a variation of 0.5°C.

The obtained results for the storage modulus values in section 3.1 show variation for each of the 3 beams at more or less the same frequency. A sensitivity analysis is conducted to examine the origin of these variations.

3.1.10 Influence of PVB thickness variations

It can be checked how much influence a reduction of about 0.30 mm of the PVB layer has on the identified transverse shear modulus.

As an example the PVB layer of beam AL4-1 is observed:

- The PVB layer is reduced from 2.28 mm to 2.00 mm (-12%).
- The resonance frequency reduces from 2197 Hz to 2071 Hz
- The identified transverse shear modulus reduces from 1.548E+08 Pa to 1.397E+08 Pa. This is a variation = 0.151E+08 Pa (-10%).

The assumption that the PVB layer is constant over the length of the beams is not completely valid. In reality the PVB layer seems to vary from point to point along the length of the beams. This is probably the main source of scatter in the obtained results for the identified transverse shear modulus.

3.2 Assumption of constant glass layer thickness

The measured glass thickness in the beams and plates in chapter 1 was varying between the values 0.0480 m and 0.0499 m with an average value of 0.0493 m. If it is now assumed that in the series A, B and C the glass thickness is constant, the consequence will be that the inner PVB layer thickness h_0 is not constant. In this chapter, the thickness of the glass layers is assumed to be constant.

3.2.1 Geometry and mass of series A (2.28 mm)

Based on the value of the density of glass (ρ = 2474 kg/m3) and the density of PVB (ρ_0 = 1065 kg/m3), the total laminate thickness t measured in the middle of the beams, the length L, the total measured mass M, the assumed constant average thickness of the glass h = 0.0493, the computed thickness of the PVB layer h_0 = total thickness t minus 2 times h), the average width W can be estimated:

$$M = L.W(2h\rho + h_0\rho_0)$$
$$W = \frac{M}{L.(2h\rho + h_0\rho_0)} \qquad (3.6)$$

Beam Nr.	Length L [m]	Width W [m]	Laminate Thickness t [m]	Thickness PVB Layer h_0 [m]	Thickness Glass Layer h [m]	Mass M [kg]
AL1-1	0.30	0.0302	0.01210	0.00224	0.00493	0.24205
AL1-2	0.30	0.0300	0.01209	0.00223	0.00493	0.24077
AL1-3	0.30	0.0302	0.01197	0.00211	0.00493	0.24086
AL2-1	0.25	0.0301	0.01203	0.00217	0.00493	0.20078
AL2-2	0.25	0.0305	0.01199	0.00213	0.00493	0.20255
AL2-3	0.25	0.0300	0.01212	0.00226	0.00493	0.20069
AL3-1	0.20	0.0301	0.01206	0.00220	0.00493	0.16041
AL3-2	0.20	0.0300	0.01207	0.00221	0.00493	0.16001
AL3-3	0.20	0.0302	0.01197	0.00211	0.00493	0.16030
AL4-1	0.15	0.0305	0.01191	0.00205	0.00493	0.12123
AL4-2	0.15	0.0304	0.01199	0.00213	0.00493	0.12113
AL4-3	0.15	0.0304	0.01183	0.00197	0.00493	0.12023

Table 3.2.1 laminated glass beams geometry series A (2.28 mm)

The values for the total laminate thickness were measured in the middle of the beam sample with a digital caliper (0.01 mm accuracy).

3.2.2 Geometry and mass of series B (1.52 mm)

Beam Nr.	Length L [m]	Width W [m]	Laminate Thickness t [m]	Thickness PVB Layer h_0 [m]	Thickness Glass Layer h [m]	Mass M [kg]
BL1-1	0.30	0.0301	0.01114	0.00128	0.00493	0.23229
BL1-2	0.30	0.0302	0.01115	0.00129	0.00493	0.23311
BL1-3	0.30	0.0302	0.01115	0.00129	0.00493	0.23263
BL2-1	0.25	0.0301	0.01115	0.00129	0.00493	0.19334
BL2-2	0.25	0.0299	0.01116	0.00130	0.00493	0.19200
BL2-3	0.25	0.0298	0.01115	0.00129	0.00493	0.19143
BL3-1	0.20	0.0300	0.01114	0.00128	0.00493	0.15386
BL3-2	0.20	0.0301	0.01111	0.00125	0.00493	0.15428
BL3-3	0.20	0.0300	0.01117	0.00131	0.00493	0.15413
BL4-1	0.15	0.0297	0.01113	0.00127	0.00493	0.11444
BL4-2	0.15	0.0305	0.01113	0.00127	0.00493	0.11715
BL4-3	0.15	0.0298	0.01111	0.00128	0.00493	0.11474

Table 3.2.2.1 Geometry laminated glass beams series B (1.52mm)

3.2.3 Geometry and mass of series C (0.76 mm)

Beam Nr.	Length L [m]	Width W [m]	Laminate Thickness t [m]	Thickness PVB Layer h_0 [m]	Thickness Glass Layer h [m]	Mass M [kg]
CL1-1	0.30	0.0298	0.01042	0.00056	0.00493	0.22286
CL1-2	0.30	0.0299	0.01044	0.00058	0.00493	0.22376
CL1-3	0.30	0.0294	0.01040	0.00054	0.00493	0.21977
CL2-1	0.25	0.0302	0.01042	0.00056	0.00493	0.18792
CL2-2	0.25	0.0299	0.01043	0.00057	0.00493	0.18614
CL2-3	0.25	0.0299	0.01040	0.00054	0.00493	0.18614
CL3-1	0.20	0.0291	0.01039	0.00053	0.00493	0.14500
CL3-2	0.20	0.0295	0.01041	0.00055	0.00493	0.14686
CL3-3	0.20	0.0297	0.01041	0.00055	0.00493	0.14781
CL4-1	0.15	0.0296	0.01042	0.00056	0.00493	0.11049
CL4-2	0.15	0.0299	0.01042	0.00056	0.00493	0.11155
CL4-3	0.15	0.0302	0.01040	0.00054	0.00493	0.11280

Table 3.2.3.1 Geometry laminated glass beams series C (0.76mm)

3.2.4 Identification of the transverse shear modulus of series A (2.28 mm)

Beam Nr.	Measured Frequency [Hz]	Measured Damping ratio [%]	Transverse Shear Modulus [Pa]	Potential Energy Ratio PVB/Total	Tangents Delta Shear Modulus
AL1-1	676	4.330	1.274E8	22.3	0.388
AL1-2	677	4.530	1.296E8	22.0	0.412
AL1-3	674	4.177	1.306E8	20.9	0.400
AL2-1	936	4.941	1.367E8	25.8	0.383
AL2-2	934	4.911	1.358E8	25.6	0.384
AL2-3	939	5.012	1.371E8	26.5	0.378
AL3-1	1366	6.521	1.352E8	32.6	0.400
AL3-2	1385	6.103	1.472E8	31.5	0.387
AL3-3	1366	6.227	1.351E8	32.7	0.381
AL4-1	2197	6.731	1.394E8	38.1	0.353
AL4-2	2209	6.598	1.441E8	38.4	0.344
AL4-3	2180	6.716	1.331E8	37.9	0.354

Table 3.2.4.1. Identified transverse shear modulus properties series A (2.28 mm)

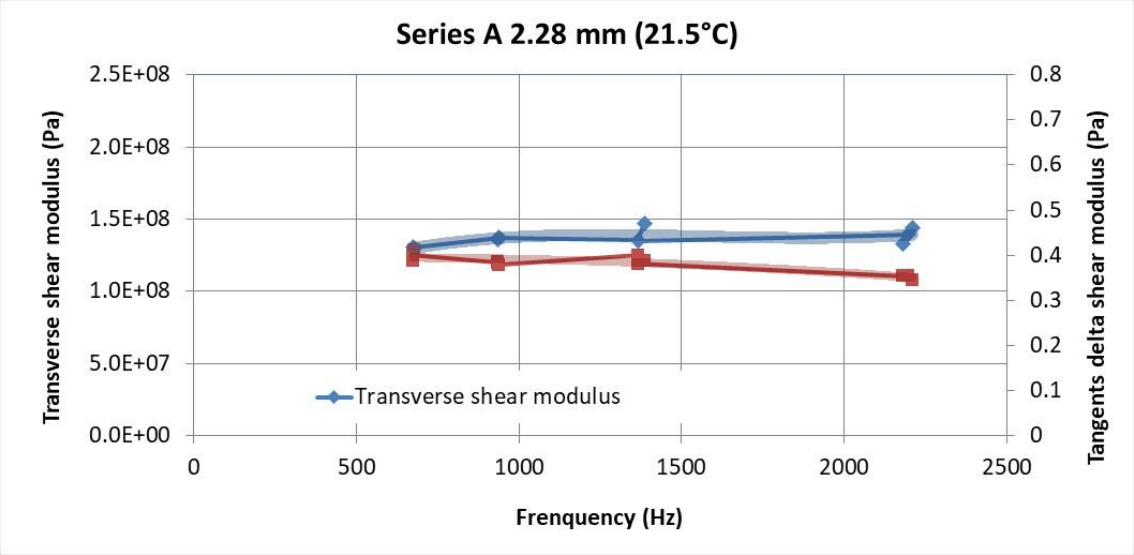

Figure 3.2.4.2. Identified transverse shear modulus properties series A (2.28 mm)

The average value of the storage part of the G-modulus at the lowest frequencies equals to 1.27 E8 Pa, at the highest frequency 1.33 E8 Pa.

The tangents delta value decreases from 0.39 towards 0.55 and seems to be more frequency dependent.

3.2.5 Identification of the transverse shear modulus of series B (1.52 mm)

Beam Nr.	Measured Frequency [Hz]	Measured Damping ratio [%]	Transverse Shear Modulus [Pa]	Potential Energy Ratio PVB/Total	Tangents Delta Shear Modulus
BL1-1	644	3.948	1.208E8	14.8	0.534
BL1-2	642	3.888	1.159E8	15.3	0.508
BL1-3	642	3.853	1.159E8	15.3	0.504
BL2-1	898	4.498	1.201E8	19.2	0.469
BL2-2	893	4.473	1.132E8	20.0	0.447
BL2-3	890	4.536	1.097E8	20.3	0.447
BL3-1	1329	5.413	1.171E8	25.1	0.431
BL3-2	1325	5.283	1.171E8	24.7	0.438
BL3-3	1318	5.515	1.098E8	26.3	0.419
BL4-1	2176	5.944	1.198E8	31.9	0.373
BL4-2	2167	6.088	1.167E8	32.2	0.378
BL4-3	2172	6.182	1.187E8	32.2	0.384

Table 3.2.5.1. Identified transverse shear modulus properties series B

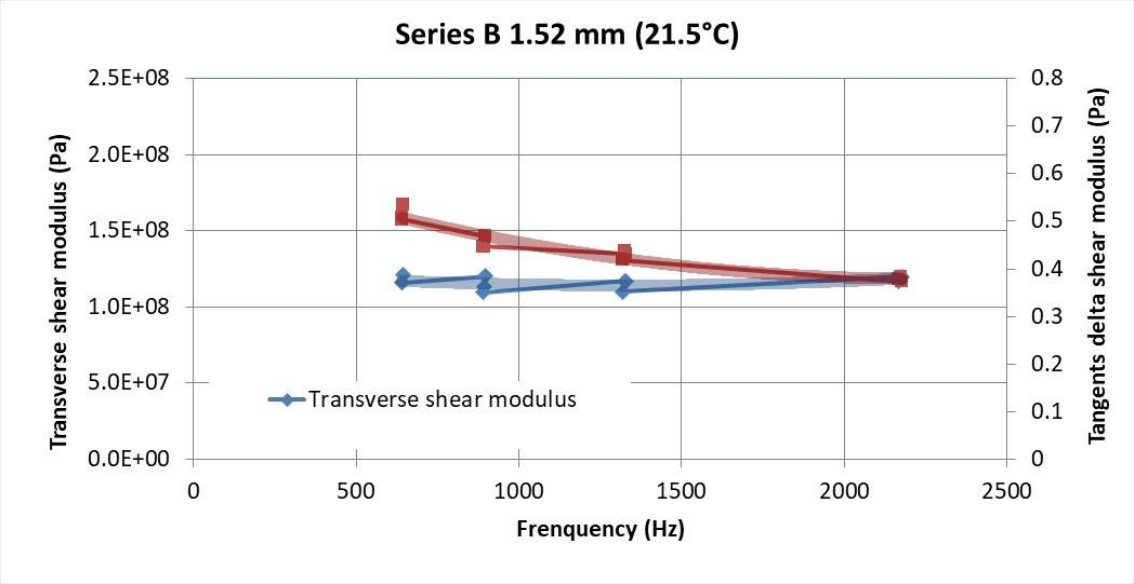

Figure 3.2.5.2. Identified transverse shear modulus properties series B

The average value of the storage part of the G-modulus seem to be more or less constant with an average value of 1.15 E8 Pa.

The tangents delta value decreases from 0.53 towards 0.38 and seems to be more frequency dependent.

3.2.6 Identification of the transverse shear modulus of series C (0.76 mm)

Beam Nr.	Measured Frequency [Hz]	Measured Damping ratio [%]	Transverse Shear Modulus [Pa]	Potential Energy Ratio PVB/Glass	Tangents Delta Shear Modulus
CL1-1	621	1.994	1.207E8	7.267	0.549
CL1-2	621	1.965	1.173E8	7.677	0.512
CL1-3	620	1.949	1.189E8	7.123	0.547
CL2-1	877	2.275	1.141E8	10.2	0.466
CL2-2	876	2.313	1.111E8	10.6	0.436
CL2-3	876	2.293	1.126E8	10.0	0.459
CL3-1	1337	2.816	1.214E8	13.0	0.433
CL3-2	1332	2.848	1.152E8	13.9	0.410
CL3-3	1316	2.849	9.777E7	15.6	0.365
CL4-1	2238	3.282	1.118E8	20.7	0.317
CL4-2	2243	3.443	1.142E8	20.5	0.336
CL4-3	2236	3.591	1.090E8	20.5	0.350

Table 3.2.6.1. Identified transverse shear modulus properties series C (0.72 mm)

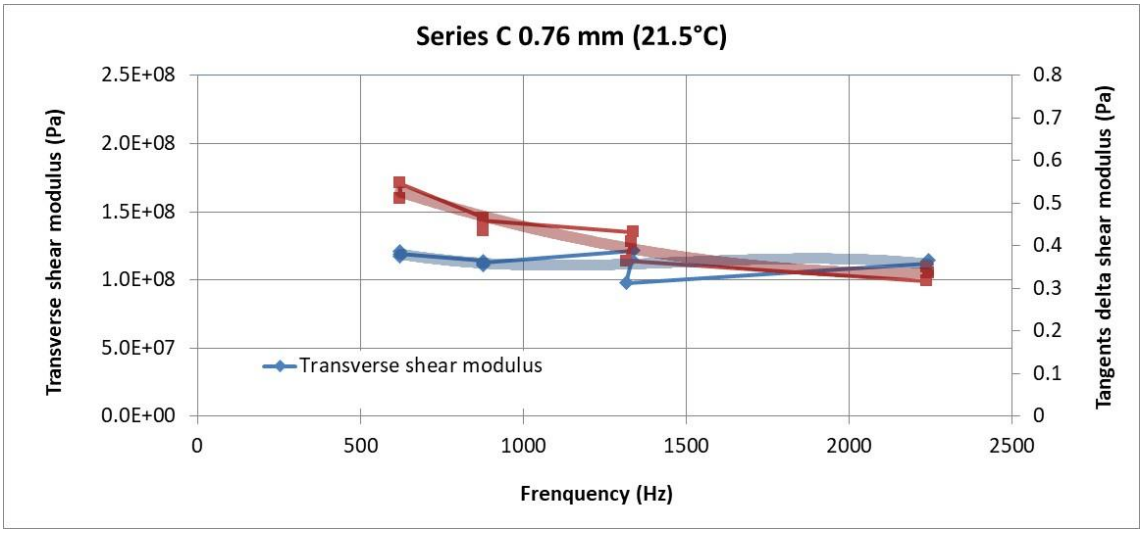

Figure 3.2.6.2. Identified transverse shear modulus properties series C (0.72 mm)

The average value of the storage part of the G-modulus seem to be more or less constant with an average value of 1.15 E8 Pa.

The tangents delta value increases from 0.55 towards 0.35 and seems to be more frequency dependent.

3.2.7 Comparison of the results

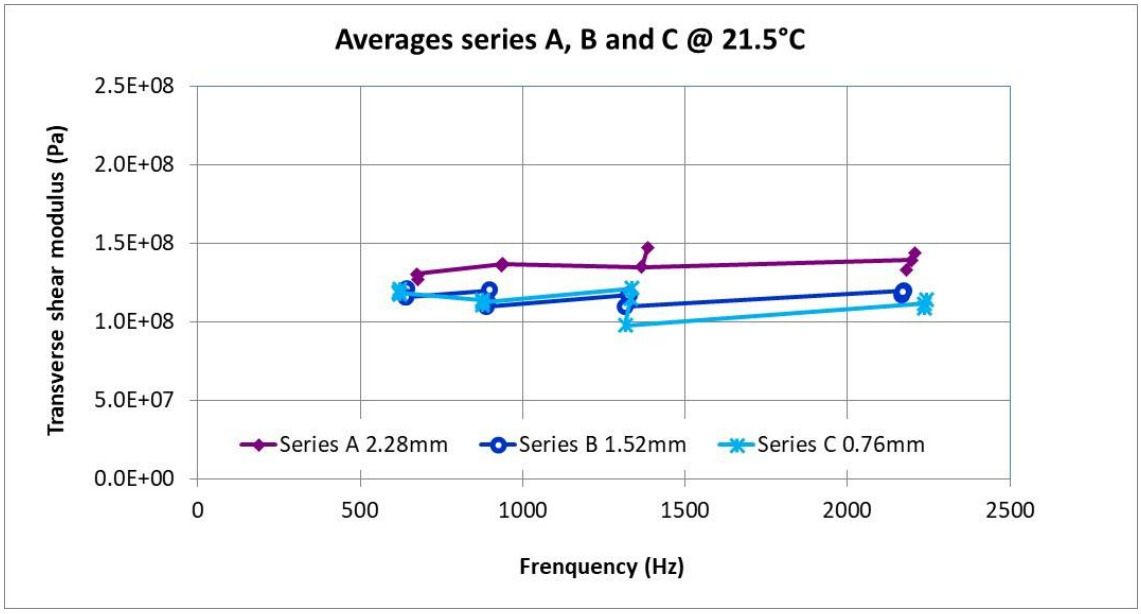

Figure 3.2.7.1. Identified transverse shear storage modulus

The average value of the storage shear modulus for all series seems to be nearly constant.

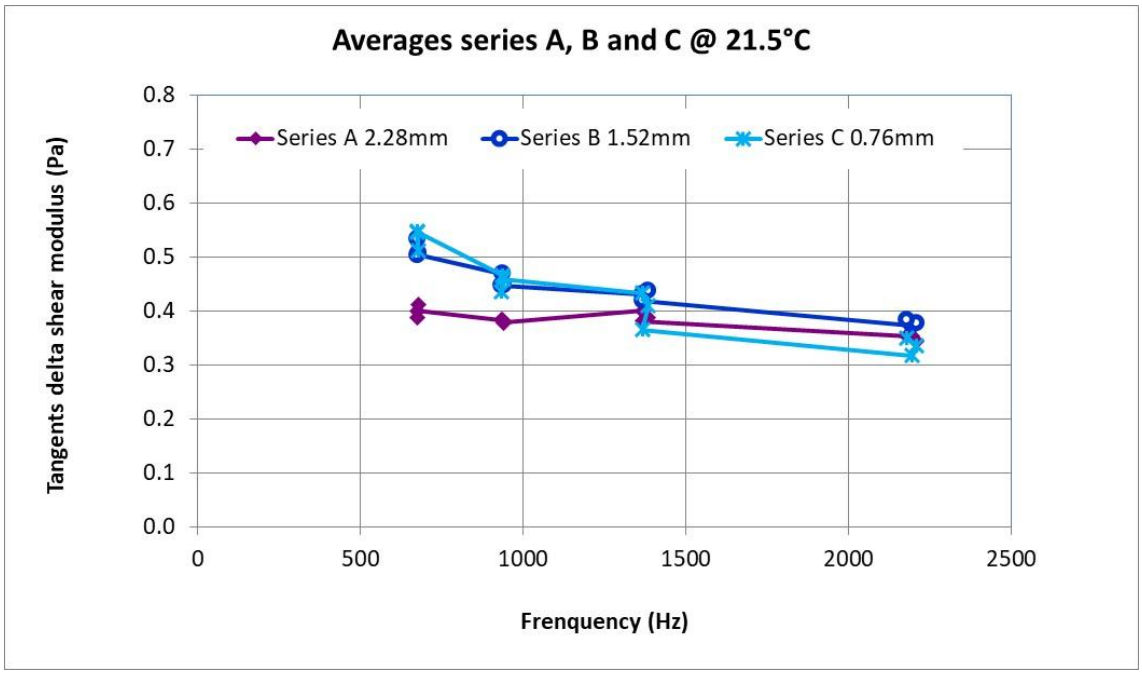

Figure 3.2.7.2. Identified transverse shear loss modulus (tangents delta)

All the tangents delta values decrease with increasing frequency.

4 Comparison constant PVB versus constant glass thickness

4.1 Series A (2.28mm)

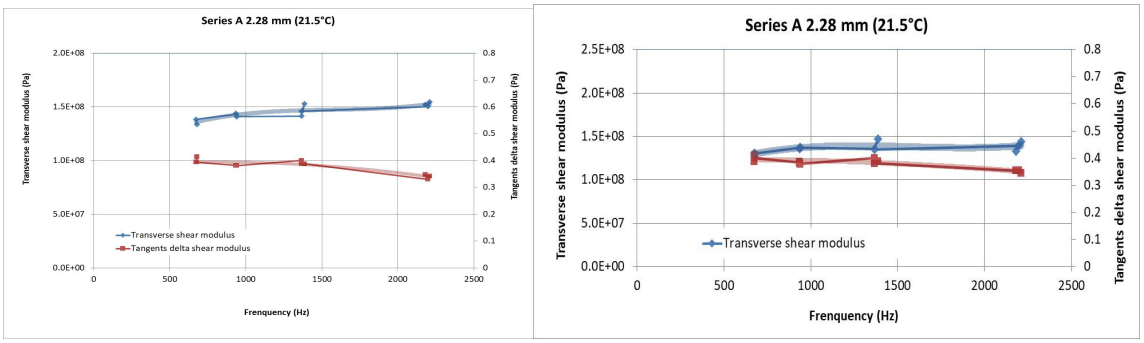

(a) Constant PVB thickness **(b) Constant Glass thickness**

Figure 4.1.1. Identified transverse shear modulus series 2.28mm

4.2 Series B (1.52mm)

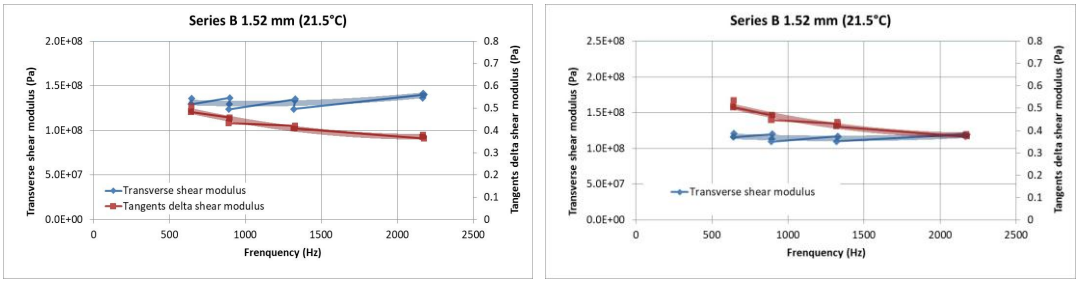

(a) Constant PVB thickness **(b) Constant Glass thickness**

Figure 4.1.2. Identified transverse shear modulus series 1.52mm

4.3 Series C (0.76mm)

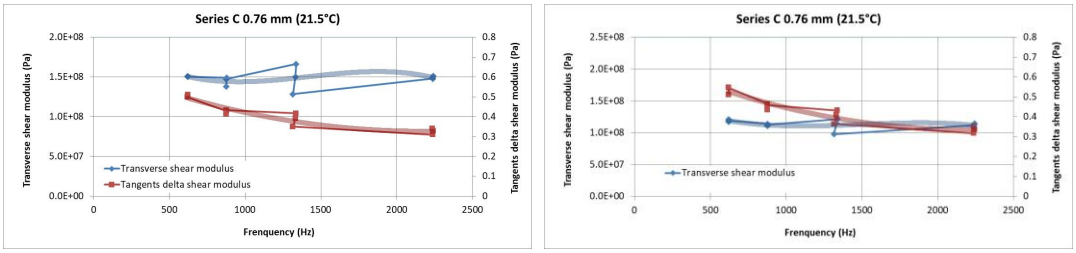

(a) Constant PVB thickness **(b) Constant Glass thickness**

Figure 4.1.3. Identified transverse shear modulus series 0.76mm

The storage modulus values of the constant glass thickness series are lower.

5 Variable thickness of PVB layer

The previous chapter has shown that the thickness of the PVB layer and the thickness of the glass layers are important for the final identified value of the transverse shear modulus of the PVB material. The measured glass thickness in the beams and plates in chapter 1 was varying between the values 0.0480 m and 0.0497 m with an average value of 0.0493 m. It was decided to investigate more in detail the thickness of the PVB layer and the glass layers. Therefore the thicknesses are measured with a digital electronic outside micrometer (type Filetta of the company Schut) with 0.001 precision and measurement pressure control (see Figure 5.1)

Figure 5.1. Giletta electronic micrometer (Shut)

It was found that the two glass layers of the beams systematically didn't have the same thickness. One layer had a thickness varying between 4.95 and 4.99 with an average value of 4.992 mm; the other layer had a thickness varying between 4.80 and 4.92 with an average thickness of 4.894 mm. Since the mathematical model is symmetric, it was decided to take a constant value of 4.943 mm for both glass layers.

It is now assumed that in the series A, B and C the glass thickness is constant. The consequence will be that the inner PVB layer thickness h_0 is not constant. To take the variation of the thickness of the PVB layer into account, a new numerical model with variable PVB thickness was developed. The model can have a different thickness in every one of the 11 nodal points.

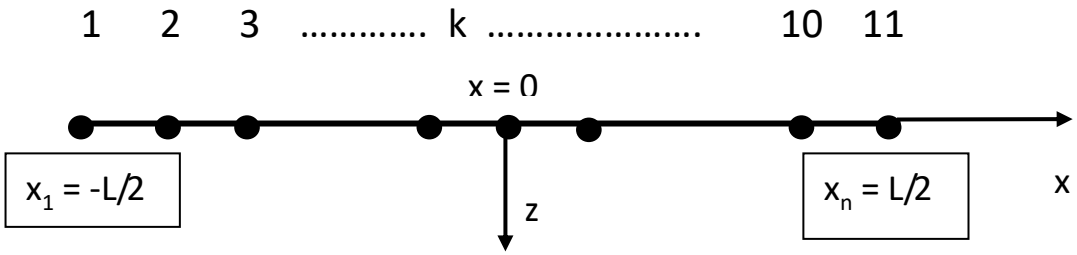

Figure 5.2. Discrete numerical model of the laminate beam with 11 nodes

The temperature is 21.5°C, the relative humidity is 40%. Just like the previous tests, the samples were carefully preconditioned for a long time.

5.1 Geometry and mass of series A (2.28 mm)

The next table gives the geometry, based on the value of the density of glass (ρ = 2474 kg/m3) and the density of PVB (ρ_0 = 1065 kg/m3), the length L, the total measured mass M, and the width (taken the same as in the previous paragraph)

Beam Nr.	Length L [m]	Width W [m]	Thickness Glass Layer h [m]	Mass M [kg]
AL1-1	0.30	0.0302	0.004943	0.24205
AL1-2	0.30	0.0300	0.004943	0.24077
AL1-3	0.30	0.0302	0.004943	0.24086
AL2-1	0.25	0.0301	0.004943	0.20078
AL2-2	0.25	0.0305	0.004943	0.20255
AL2-3	0.25	0.0300	0.004943	0.20069
AL3-1	0.20	0.0301	0.004943	0.16041
AL3-2	0.20	0.0300	0.004943	0.16001
AL3-3	0.20	0.0302	0.004943	0.16030
AL4-1	0.15	0.0305	0.004943	0.12123
AL4-2	0.15	0.0304	0.004943	0.12113
AL4-3	0.15	0.0304	0.004943	0.12023

Table 5.1.1 laminated glass beams geometry series A (2.28 mm)

The values for the total laminate thickness were measured in the 11 nodal points of the beam sample with the digital micrometer (0.001 mm accuracy). The thickness of the PVB layer in each point is calculated as the total thickness minus two times the thickness of the glass (= 9.886 mm).

Beam Nr.	Node 1 [mm]	Node 2 [mm]	Node 3 [mm]	Node 4 [mm]	Node 5 [mm]	Node 6 [mm]	Node 7 [mm]	Node 8 [mm]	Node 9 [mm]	Node 10 [mm]	Node 11 [mm]
AL1-1	12.065 2.179	12.077 2.191	12.092 2.206	12.107 2.221	12.119 2.233	12.123 2.236	12.077 2.191	12.052 2.166	11.951 2.065	11.853 1.967	11.770 1.884
AL1-2	12.081 2.195	12.094 2.208	12.096 2.210	12.083 2.197	12.065 2.179	12.052 2.166	12.046 2.160	12.036 2.150	12.038 2.152	12.038 2.152	12.045 2.159
AL1-3	11.914 2.028	11.923 2.037	11.939 2.053	11.959 2.073	11.973 2.087	11.992 2.106	12.016 2.130	12.039 2.153	12.059 2.173	12.065 2.179	12.066 2.180
AL2-1	12.120 2.234	12.114 2.228	12.110 2.224	12.092 2.206	12.079 2.193	12.069 2.183	12.064 2.178	12.057 2.171	12.054 2.168	12.056 2.170	12.057 2.171
AL2-2	11.973 2.087	11.988 2.102	11.994 2.108	11.991 2.105	11.998 2.112	12.009 2.123	12.021 2.135	12.034 2.148	12.053 2.167	12.066 2.180	12.081 2.195
AL2-3	12.078 2.192	12.115 2.229	12.154 2.268	12.171 2.285	12.176 2.290	12.167 2.281	12.115 2.229	12.056 2.170	11.978 2.092	11.865 1.979	11.847 1.961
AL3-1	11.694 1.808	11.769 1.883	11.850 1.964	11.932 2.046	12.004 2.118	12.067 2.181	12.131 2.245	12.140 2.254	12.141 2.255	12.136 2.250	12.127 2.241
AL3-2	11.720 1.834	11.792 1.906	11.870 1.984	11.951 2.065	12.018 2.132	12.078 2.192	12.121 2.235	12.138 2.252	12.151 2.265	12.152 2.266	12.137 2.251
AL3-3	12.124 2.238	12.110 2.224	12.087 2.201	12.058 2.172	12.030 2.144	12.010 2.124	11.974 2.088	11.939 2.053	11.903 2.017	11.877 1.991	11.851 1.965
AL4-1	12.077 2.191	12.048 2.162	12.032 2.146	12.010 2.124	11.977 2.091	11.950 2.064	11.940 2.054	11.913 2.027	11.858 1.972	11.828 1.942	11.780 1.894
AL4-2	11.974 2.088	11.987 2.101	12.002 2.116	12.010 2.124	12.025 2.139	12.037 2.151	12.052 2.166	12.064 2.178	12.073 2.187	12.088 2.202	12.093 2.207
AL4-3	12.066 2.180	12.035 2.149	12.002 2.116	11.966 2.080	11.931 2.045	11.905 2.019	11.854 1.968	11.806 1.920	11.759 1.873	11.718 1.832	11.673 1.787

Table 5.1.2 laminated glass beams geometry series A (2.28 mm)

5.2 Geometry and mass of series B (1.52 mm)

Beam Nr.	Length L [m]	Width W [m]	Thickness Glass Layer h [m]	Mass M [kg]
BL1-1	0.30	0.0301	0.004943	0.23229
BL1-2	0.30	0.0302	0.004943	0.23311
BL1-3	0.30	0.0302	0.004943	0.23263
BL2-1	0.25	0.0301	0.004943	0.19334
BL2-2	0.25	0.0299	0.004943	0.19200
BL2-3	0.25	0.0298	0.004943	0.19143
BL3-1	0.20	0.0300	0.004943	0.15386
BL3-2	0.20	0.0301	0.004943	0.15428
BL3-3	0.20	0.0300	0.004943	0.15413
BL4-1	0.15	0.0297	0.004943	0.11444
BL4-2	0.15	0.0305	0.004943	0.11715
BL4-3	0.15	0.0298	0.004943	0.11474

Table 5.2.1 Geometry laminated glass beams series B (1.52mm)

Beam Nr.	Node 1 [mm]	Node 2 [mm]	Node 3 [mm]	Node 4 [mm]	Node 5 [mm]	Node 6 [mm]	Node 7 [mm]	Node 8 [mm]	Node 9 [mm]	Node 10 [mm]	Node 11 [mm]
BL1-1	11.041 1.155	11.093 1.207	11.186 1.300	11.184 1.298	11.210 1.324	11.215 1.329	11.215 1.329	11.198 1.312	11.189 1.303	11.147 1.261	11.125 1.239
BL1-2	11.173 1.287	11.181 1.295	11.190 1.304	11.188 1.302	11.194 1.308	11.202 1.316	11.204 1.318	11.173 1.287	11.108 1.222	11.074 1.188	10.965 1.079
BL1-3	11.203 1.317	11.223 1.337	11.223 1.337	11.214 1.328	11.201 1.315	11.184 1.298	11.150 1.264	11.081 1.195	10.987 1.101	10.921 1.035	10.787 0.901
BL2-1	11.154 1.268	11.167 1.281	11.176 1.290	11.193 1.307	11.202 1.316	11.225 1.339	11.210 1.324	11.204 1.318	11.184 1.298	11.164 1.278	11.141 1.255
BL2-2	11.227 1.341	11.207 1.321	11.206 1.320	11.196 1.310	11.191 1.305	11.175 1.289	11.144 1.258	11.103 1.217	11.065 1.179	10.972 1.086	10.902 1.016
BL2-3	11.208 1.322	11.208 1.322	11.208 1.322	11.188 1.302	11.184 1.298	11.184 1.298	11.184 1.298	11.179 1.293	11.152 1.266	11.135 1.249	11.125 1.239
BL3-1	11.166 1.280	11.165 1.279	11.161 1.275	11.159 1.273	11.157 1.271	11.155 1.269	11.147 1.261	11.143 1.257	11.143 1.257	11.121 1.235	11.112 1.226
BL3-2	11.015 1.129	11.034 1.148	11.078 1.192	11.080 1.194	11.099 1.213	11.129 1.243	11.139 1.253	11.152 1.266	11.153 1.267	11.160 1.274	11.161 1.275
BL3-3	11.164 1.278	11.176 1.290	11.193 1.307	11.201 1.315	11.201 1.315	11.201 1.315	11.201 1.315	11.195 1.309	11.165 1.279	11.147 1.261	11.133 1.247
BL4-1	10.980 1.094	11.003 1.117	11.030 1.144	11.079 1.193	11.113 1.227	11.143 1.257	11.176 1.290	11.190 1.304	11.203 1.317	11.202 1.316	11.202 1.316
BL4-2	10.996 1.110	11.025 1.139	11.061 1.175	11.095 1.209	11.130 1.244	11.157 1.271	11.170 1.284	11.186 1.300	11.204 1.318	11.208 1.322	11.208 1.322
BL4-3	11.062 1.176	11.068 1.182	11.079 1.193	11.095 1.209	11.107 1.221	11.118 1.232	11.130 1.244	11.138 1.252	11.142 1.256	11.144 1.258	11.144 1.258

Table 5.2.2 Thickness of laminate (Black) and PVB layer (Red) of Beam B (1.52 mm)

5.3 Geometry and mass of series C (0.76 mm)

Beam Nr.	Length L [m]	Width W [m]	Thickness Glass Layer h [m]	Mass M [kg]
CL1-1	0.30	0.0298	0.004943	0.22286
CL1-2	0.30	0.0299	0.004943	0.22376
CL1-3	0.30	0.0294	0.004943	0.21977
CL2-1	0.25	0.0302	0.004943	0.18792
CL2-2	0.25	0.0299	0.004943	0.18614
CL2-3	0.25	0.0299	0.004943	0.18614
CL3-1	0.20	0.0291	0.004943	0.14500
CL3-2	0.20	0.0295	0.004943	0.14686
CL3-3	0.20	0.0297	0.004943	0.14781
CL4-1	0.15	0.0296	0.004943	0.11049
CL4-2	0.15	0.0299	0.004943	0.11155
CL4-3	0.15	0.0302	0.004943	0.11280

Table 5.3.1 Geometry laminated glass beams series C (0.76mm)

Beam Nr.	Node 1 [mm]	Node 2 [mm]	Node 3 [mm]	Node 4 [mm]	Node 5 [mm]	Node 6 [mm]	Node 7 [mm]	Node 8 [mm]	Node 9 [mm]	Node 10 [mm]	Node 11 [mm]
CL1-1	10.404 0.518	10.411 0.525	10.415 0.529	10.422 0.536	10.417 0.531	10.413 0.527	10.413 0.527	10.421 0.535	10.418 0.532	10.419 0.533	10.412 0.526
CL1-2	10.393 0.507	10.390 0.504	10.392 0.506	10.394 0.508	10.404 0.518	10.404 0.518	10.409 0.523	10.410 0.524	10.416 0.530	10.418 0.532	10.404 0.518
CL1-3	10.396 0.510	10.390 0.504	10.386 0.500	10.383 0.497	10.387 0.501	10.396 0.510	10.407 0.521	10.413 0.527	10.415 0.527	10.399 0.513	10.385 0.499
CL2-1	10.400 0.514	10.410 0.524	10.410 0.524	10.413 0.527	10.411 0.525	10.413 0.527	10.401 0.515	10.399 0.513	10.397 0.511	10.396 0.510	10391 0.505
CL2-2	10.401 0.515	10.408 0.522	10.410 0.524	10.408 0.522	10.403 0.517	10.399 0.513	10.396 0.510	10.396 0.510	10.394 0.508	10.389 0.503	10.387 0.501
CL2-3	10.370 0.484	10.376 0.490	10.387 0.501	10.390 0.504	10.395 0.509	10.396 0.510	10.398 0.512	10.399 0.513	10.398 0.512	10.392 0.506	10.392 0.506
CL3-1	10.409 0.523	10.408 0.522	10.409 0.523	10.410 0.524	10.403 0.517	10.392 0.506	10.381 0.495	10.366 0.480	10.358 0.472	10.351 0.465	10.326 0.440
CL3-2	10.364 0.478	10.366 0.480	10.379 0.493	10.378 0.492	10.381 0.495	10.385 0.499	10.390 0.504	10.394 0.508	10.396 0.510	10.389 0.503	10.389 0.503
CL3-3	10.350 0.464	10.366 0.480	10.388 0.502	10.393 0.507	10.401 0.515	10.405 0.519	10.399 0.513	10.396 0.510	10.392 0.506	10.391 0.505	10.394 0.508
CL4-1	10.371 0.485	10.376 0.490	10.382 0.496	10.388 0.502	10.387 0.501	10.385 0.499	10.386 0.500	10.387 0.501	10.388 0.502	10.390 0.504	10.388 0.502
CL4-2	10.388 0.502	10.391 0.505	10.397 0.511	10.400 0.514	10.408 0.522	10.406 0.520	10.408 0.522	10.403 0.517	10.405 0.519	10.394 0.508	10.389 0.503
CL4-3	10.393 0.507	10.393 0.507	10.395 0.509	10.397 0.511	10.397 0.511	10.393 0.507	10.393 0.507	10.394 0.508	10.382 0.496	10.380 0.494	10.370 0.484

Table 5.3.2 laminated glass beams geometry series C (0.76 mm)

The measured frequency and damping ratio were taken the same as for the previous series of tests

5.4 Identification of the transverse shear modulus of series A (2.28 mm)

Beam Nr.	Measured Frequency [Hz]	Measured Damping ratio [%]	Transverse Shear Modulus [Pa]	Tangents Delta Transverse Shear	Relative Sensitivity λ/G [-]	Uncertainty 0.1% Frequency [%]
AL1-1	676	4.330	1.255E+8	0.394	0.220	9.1
AL1-2	677	4.530	1.332E+8	0.427	0.210	9.4
AL1-3	674	4.177	1.308E+8	0.400	0.209	9.6
AL2-1	936	4.941	1.370E+8	0.380	0.260	7.7
AL2-2	934	4.911	1.369E+8	0.385	0.255	7.8
AL2-3	939	5.012	1.333E+8	0.378	0.265	7.6
AL3-1	1366	6.521	1.320E+8	0.405	0.322	6.2
AL3-2	1385	6.103	1.446E+8	0.392	0.311	6.4
AL3-3	1366	6.227	1.364E+8	0.393	0.306	6.5
AL4-1	2197	6.731	1.390E+8	0.352	0.382	5.2
AL4-2	2209	6.598	1.442E+8	0.343	0.385	5.2
AL4-3	2180	6.716	1.329E+8	0.352	0.382	5.2

Table 5.4.1. Identified transverse shear modulus properties series A (2.28 mm)

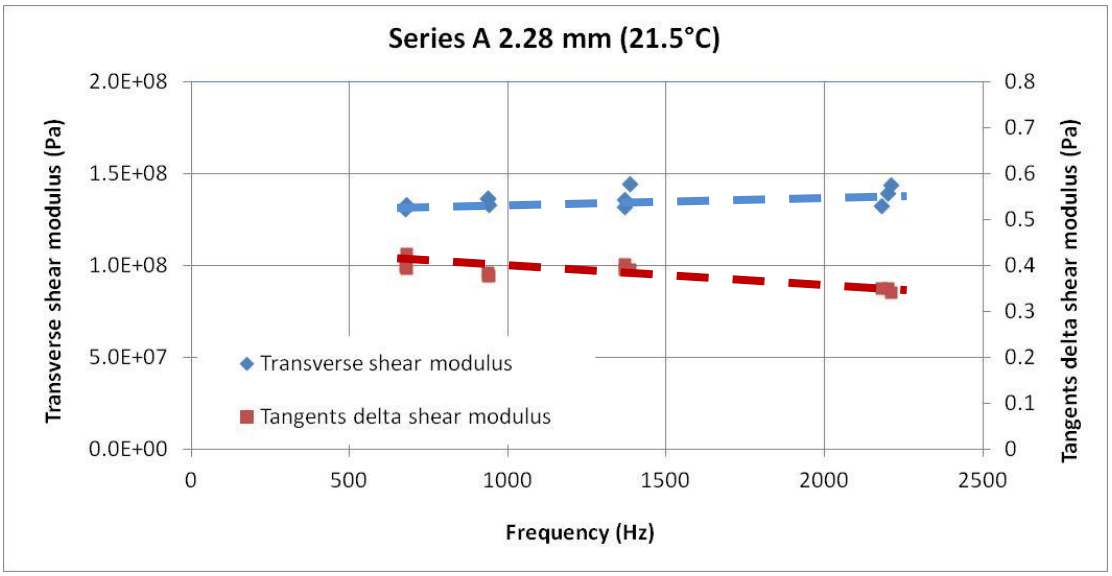

Figure 5.4.2. Identified transverse shear modulus properties series A (2.28 mm)

The storage modulus was slightly increasing with the frequency and could be curve fitted with a linear line. An average value of 1.35 E+8 was identified. The tangent delta was decreasing with increasing frequency and could be curve fitted with a linear line. An average value of 0.39 was identified.

5.5 Identification of the transverse shear modulus of series B (1.52 mm)

Beam Nr.	Measured Frequency [Hz]	Measured Damping ratio [%]	Transverse Shear Modulus [Pa]	Tangents Delta Transverse Shear	Relative Sensitivity λ/G [-]	Uncertainty 0.1% Frequency [%]
BL1-1	644	3.948	1.141E+8	0.509	0.155	12.9
BL1-2	642	3.888	1.108E+8	0.495	0.157	12.7
BL1-3	642	3.853	1.108E+8	0.504	0.153	13.0
BL2-1	898	4.498	1.174E+8	0.454	0.197	10.2
BL2-2	893	4.473	1.106E+8	0.436	0.197	10.2
BL2-3	890	4.536	1.091E+8	0.445	0.204	9.8
BL3-1	1329	5.413	1.168E+8	0.435	0.249	8.0
BL3-2	1325	5.283	1.134E+8	0.426	0.248	8.1
BL3-3	1318	5.515	1.084E+8	0.419	0.263	7.6
BL4-1	2176	5.944	1.172E+8	0.375	0.317	6.3
BL4-2	2167	6.088	1.149E+8	0.379	0.321	6.2
BL4-3	2172	6.182	1.168E+8	0.390	0.317	6.3

Table 5.5.1. Identified transverse shear modulus properties series B

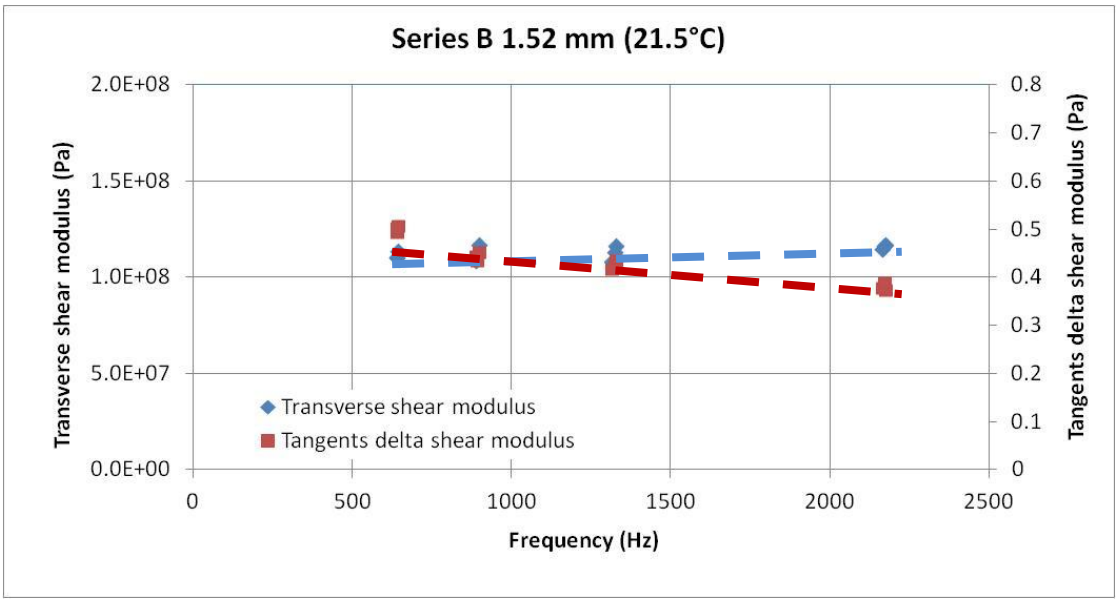

Figure 5.5.1. Identified transverse shear modulus properties series B

Again like for the A-series, the storage modulus was slightly increasing with the frequency and could be curve fitted with a linear line. An average value of 1.13 E+8 was identified. The tangent delta was decreasing with increasing frequency and could be curve fitted with a linear line. An average value of 0.43 was identified.

5.6 Identification of the transverse shear modulus of series C (0.76 mm)

Beam Nr.	Measured Frequency [Hz]	Measured Damping ratio [%]	Transverse Shear Modulus [Pa]	Tangents Delta Transverse Shear	Relative Sensitivity λ/G [-]	Uncertainty 0.1% Frequency [%]
CL1-1	621	1.994	1.269E+8	0.600	0.067	30.1
CL1-2	621	1.965	1.285E+8	0.614	0.064	31.2
CL1-3	620	1.949	1.244E+8	0.598	0.065	30.7
CL2-1	877	2.275	1.158E+8	0.479	0.095	21.1
CL2-2	876	2.313	1.142E+8	0.486	0.095	21.0
CL2-3	876	2.293	1.132E+8	0.487	0.094	21.2
CL3-1	1337	2.816	1.193E+8	0.447	0.126	15.9
CL3-2	1332	2.848	1.135E+8	0.438	0.130	15.4
CL3-3	1316	2.849	9.441E+7	0.380	0.150	13.3
CL4-1	2238	3.282	1.061E+8	0.332	0.198	10.1
CL4-2	2243	3.443	1.086E+8	0.348	0.198	10.1
CL4-3	2236	3.591	1.054E+8	0.357	0.201	10.0

Table 5.6.1. Identified transverse shear modulus properties series C (0.72 mm)

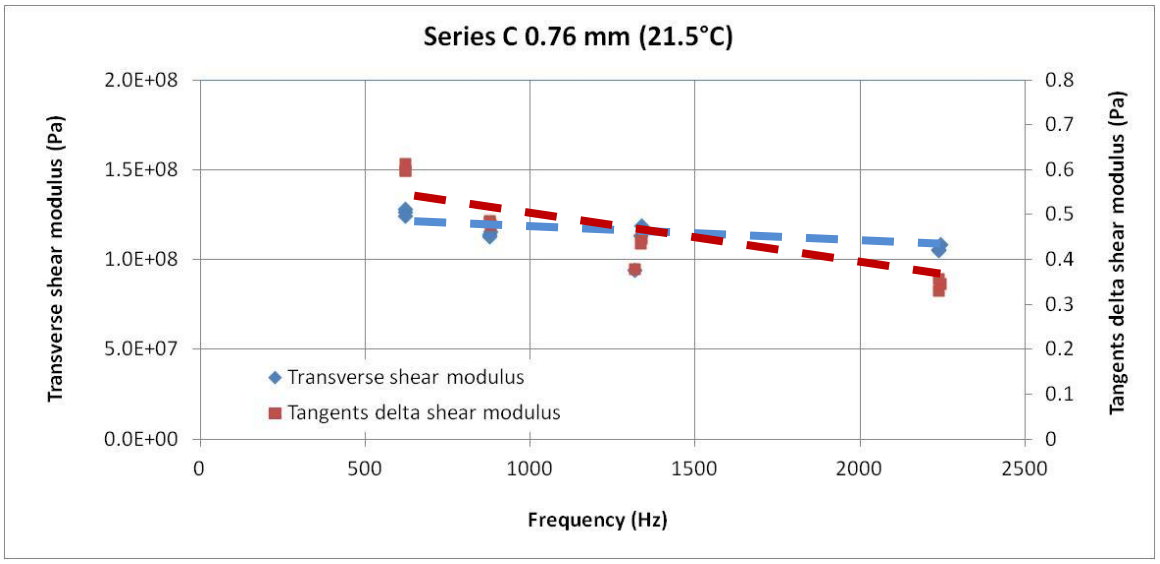

Figure 5.6.2. Identified transverse shear modulus properties series C (0.72 mm)

Contrary to the A and B-series, the storage modulus was slightly decreasing with the frequency. An average value of 1.15 E+8 was identified. The tangent delta was decreasing with increasing frequency and could be curve fitted with a linear line. An average value of 0.46 was identified.

There is much more scatter for the C series as for the series A and B

5.7 Comparison of the results

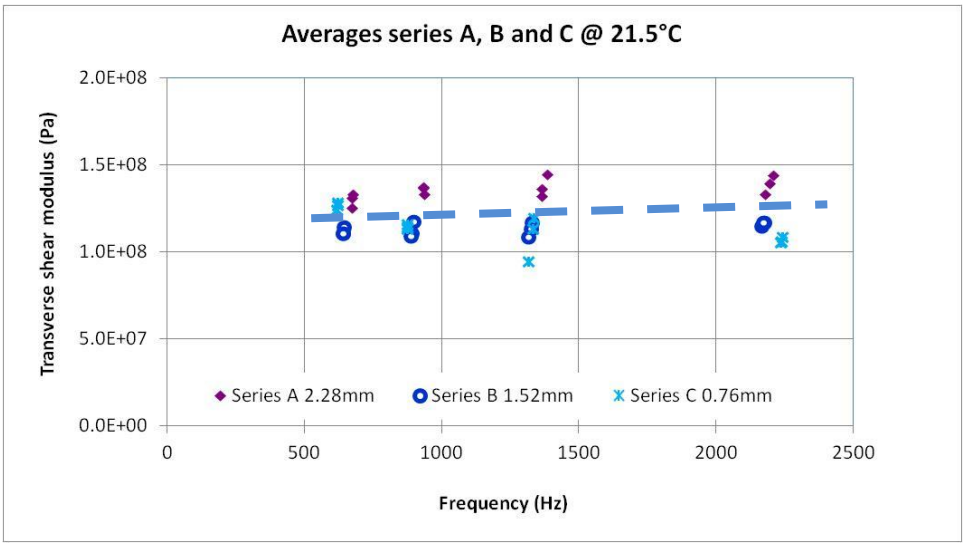

Figure 5.7.1. Identified transverse shear storage modulus

The average value of the storage shear modulus for all series seems to be nearly constant and equal to 1.25E+8

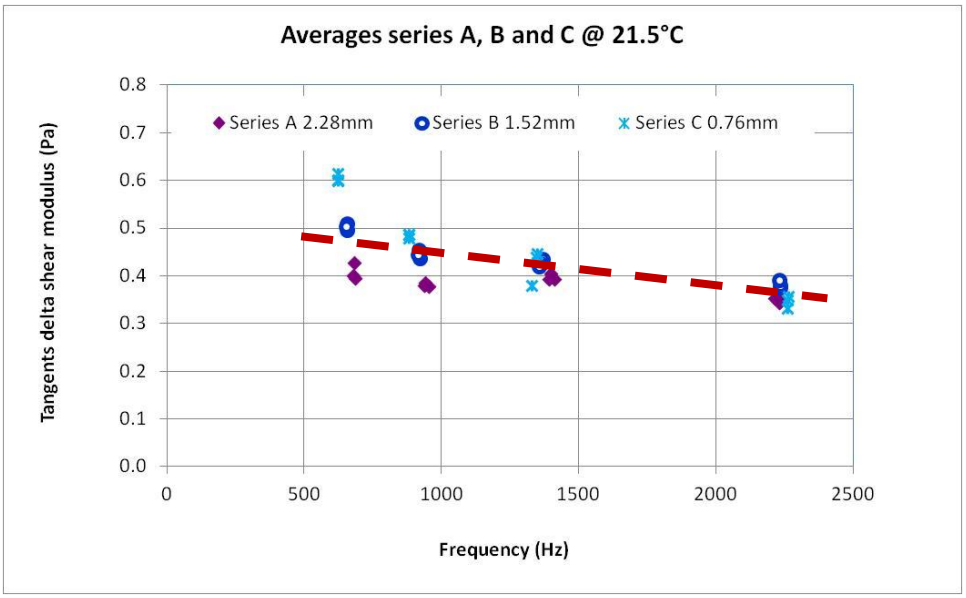

Figure 5.7.2. Identified transverse shear loss modulus (tangents delta)

All the tangents delta values decrease with increasing frequency. If the first values of the 0.76 mm beams are considered as outliers, then the tangents delta varies from about 0.45 towards 0.35

6 Temperature dependant properties

6.1 Introduction to temperature control

Since the mechanical properties of PVB are highly dependent on the temperature, additional identification tests are carried out in a climate chamber. The impulse excitation technique is used to measure the vibration properties.
A considerable advantage of the impulse excitation technique is its simplicity, but some actions need good consideration. Applying an impact using a lateral stick driven by pneumatic or electromechanical force may seem straightforward. However, delivering a controlled impulse to a freely suspended sample is challenging due to rigid body oscillations of the suspended samples. These oscillations are inevitable in a climate chamber or temperature cavity, as air fans distribute air to achieve a uniform temperature. Consequently, the exact position of the sample is uncertain, leading to impacts that may occur too early or too late, with excessive or insufficient force. As a result of the impulse, the suspended sample oscillates considerably. To prevent multiple impacts, the lateral stick must be retracted swiftly immediately after the impulse, which is cumbersome to realize practically.

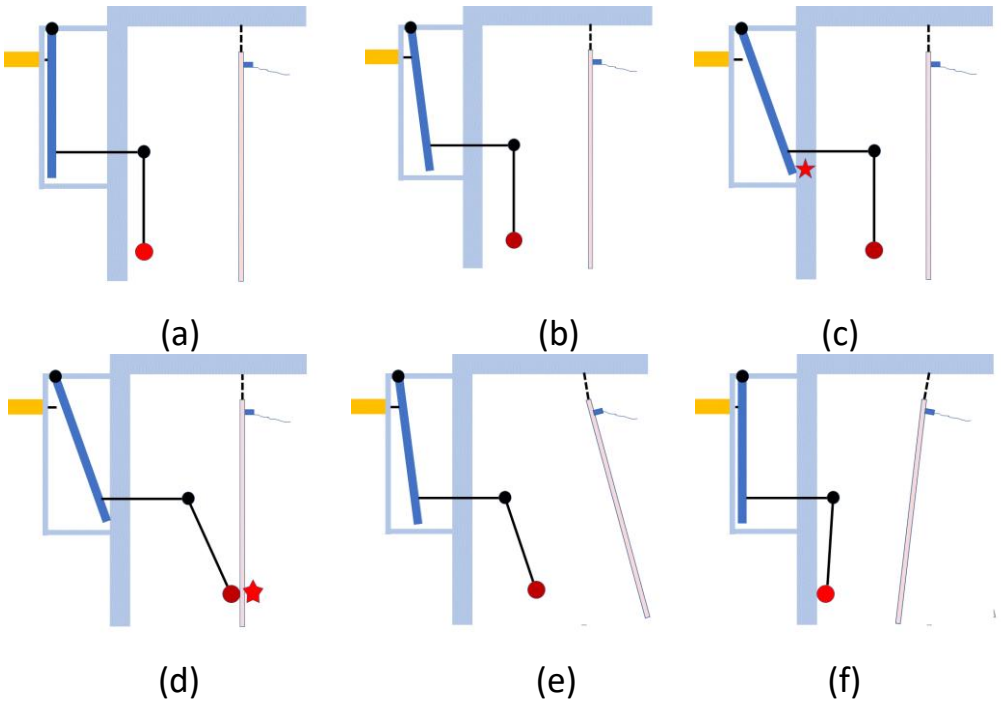

Figure 6.1. Different stages of pendulum impactpendulum mechanism externally mounted on the chamber wall. The pendulum is connected through a small aperture through the chamber wall.

The pendulum mechanism is actuated by a solenoid (yellow in Figure 6.1.a). Upon activation by a voltage, the solenoid propels a lever (dark blue in Figure 6.1.b), which strikes the wall of the climate chamber (light blue in figure 6.1.c). Due to inertia, the pendulum is set in motion until it impacts the sample (Figure 6.1.d). The sample receives an impulse and oscillates away, while the pendulum mass rebounds. Gravity pulls the lever back to the initial position (figure 6.1.e). All components of the pendulum mechanism return to their starting positions, while the sample continues to oscillate (figure 6.1.f). There is only a single impulse, with no multiple impacts.

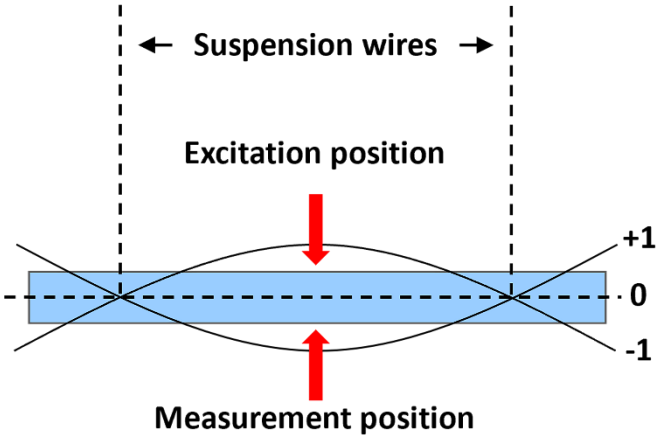

Figure 6.2. Position for suspension wires and excitation position for the flexural vibration of a beam

The voltage on the solenoid can be adjusted to tune the launching force. The size of the ball on the pendulum can be chosen to ensure it rebounds after impact. The material of the ball can be chosen to achieve the desired spectrum of excited frequencies (hard materials excite higher frequencies while soft materials transfer more energy in lower frequencies). The length of the pendulum can be adapted to ensure the impulse occurs at the correct location.
The identification of the complex transverse shear modulus can be performed using the measured resonance frequencies and damping ratios. To accurately measure the damping ratio, the suspension must not add external influences. Therefore, the beams are suspended at the location of their nodal lines (figure 6.2). The excitation and measurement position for the beams is at their center.

The objective of the IET on sandwich beams is to automatically measure the IRF at specified temperatures and programmed time intervals. It is essential that the temperature distribution within the sample remains homogeneous across all temperature steps. A challenge arises in transitioning the isothermal temperature distribution of a freely suspended sample from one value to

another, as this process requires time. The transient heat conduction in a beam is influenced by the convection occurring at the surfaces. The temperature profile varies over time at different internal positions, with the surface temperature changing relatively quickly, while the temperature at the sample's mid-plane changes more slowly. Key control parameters include the convection heat transfer coefficient h, the thermal conductivity k, the specific heat capacity Cp and the density rho of the materials of the sample. The practical question is estimating the duration required to transition from an isothermal state at an initial temperature (Ti) to an isothermal state at another temperature (T).

The time evolution of the temperature T at the center of a sample exposed to a surface temperature TS is described by formula (7):

$$T = T_S + (T_i - T_S)Ae^{-\frac{4\alpha\lambda^2}{D^2}t} \tag{6.1}$$

In (6.1), T represents the temperature at the center of the sample, t is time, D is the sample's thickness, TS is the surface temperature and α is the thermal diffusivity. Coefficients A and λ are functions of the Biot number Bi:

$$B_i = \frac{hD}{2k} \tag{6.2}$$

$$\alpha = \frac{k}{\rho C_p} \tag{6.3}$$

The coefficients A and λ for specific Biot number values can be found in tables or computed using numerical finite element models. The Resonalyser software incorporates such thermal numerical models. When the value of center temperature T approaches TS, the sample can be considered isothermal. For sandwich beams the formula (6.1) must be applied twice: first the temperature must reach the interface glass/PVB, next that temperature is the surface value for the PVB layer.

The resonance frequencies and damping ratios of the beams can be measured by IET at the subsequent isothermal states. After measuring and identifying the transverse shear value at this state, a new temperature step can be set. Before setting the temperature steps and timing values for the automated procedure, the delay time (see Figure 6.3) required to reach an isothermal state at different steps must be computed based on the assumed known thermal parameters of the sample. For given thermal properties of the test samples, the temperature in the climate chamber at different temperature steps and the time durations can be set by the automated control program. Figure 6.3 illustrates a simple temperature and time stepping program starting at an

isothermal state with temperature TA and progressing towards temperature TB.

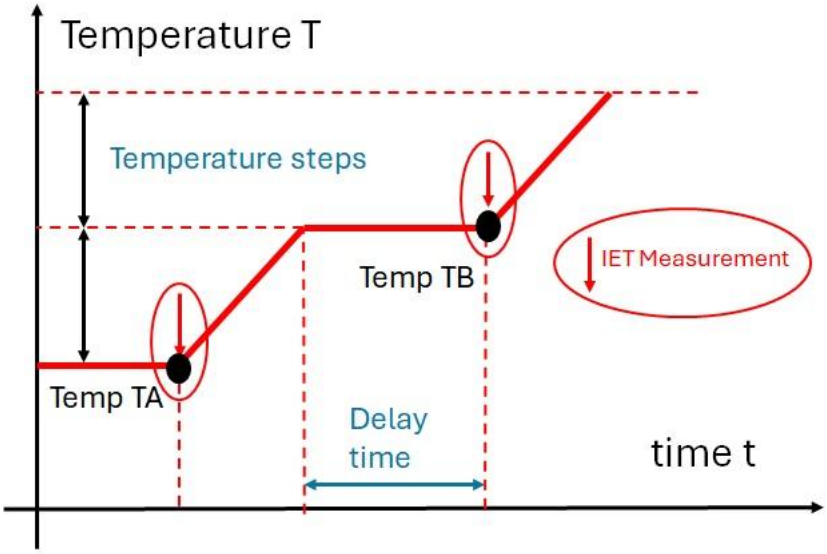

Figure 6.3. A simple temperature and time stepping program starting at an isothermal state with temperature TA towards temperature TB

Theoretically, it takes an infinite amount of time to reach the new isothermal state. Therefore, a more elaborate approach with an overshoot temperature step is convenient (see Figure 6.4).

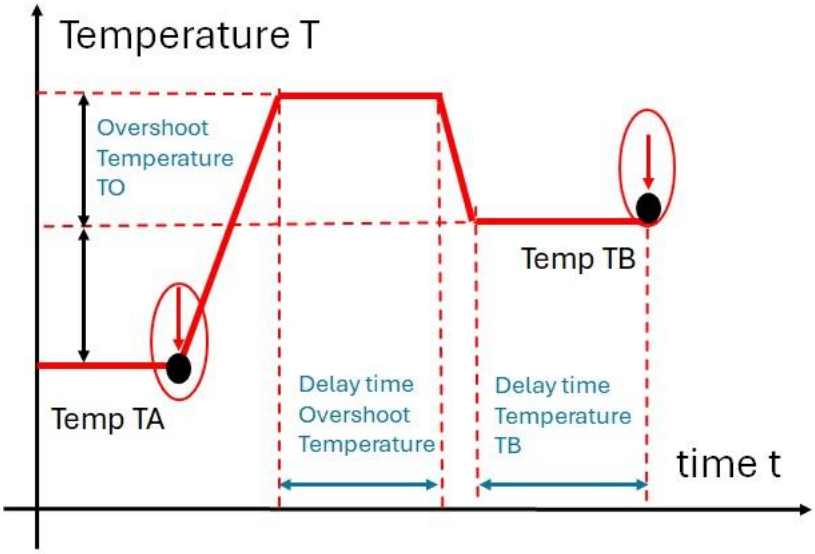

Figure 6.4. A temperature and time stepping program with an overshoot temperature.

With an overshoot temperature (TO) at the sample surfaces, the temperature at the center T will reach more quickly or even surpass the desired temperature TB. Subsequently, with the desired temperature TB at the surface, the samples will evolve faster to an isothermal state at TB. The delay times for the overshoot and temperature TB together with the value of the temperature steps must be set before starting the automated measurement procedure.

A climate chamber is outfitted with four pendulum excitation units corresponding to four measurement channels. Four sandwich beams with different length are freely suspended within the climate chamber cavity. Each test sample is equipped with a 0.19-gram solid DJB company Micro Miniature Piezo-Tronic IEPE Accelerometer - A/128/V.
Pendulum unit 1 excites the suspended largest sandwich beam on channel 1, while pendulum units 2, 3 and 4 excite sandwich beams of shorter lengths on channels 2, 3 and 4, respectively.

Figure 6.5. Climate chamber with pendulum units on channels 1 and 2

Figure 6.5 illustrates the left side of the climate chamber with pendulum units 1 and 2 attached. The frequency and damping ratio of Beam 1 are derived from the measured Impulse Response Function (IRF) of the sample on channel 1. Similarly, the frequencies and damping ratios of Beams 2, 3 and 4 are derived

from the IRFs measured on channels 2, 3 and 4. The measurement interval, including the initial and final temperatures, is set along with the required temperature steps and delay times. Following the measurement of the IRFs on the four channels, the identification of the transverse shear moduli of all tested beams is performed using the Resonalyser software. The frequencies and damping ratios at each temperature step, along with the four identified transverse shear values, can be monitored in real-time on graphs displayed on a computer screen.

6.2 Test on sandwich beams with 2.28mm PVB layer

6.2.1 Cycling temperature tests

For the test on the 2.28 mm samples, a temperature step of 1° per half hour was selected with an overshoot regime. The temperature was cycling from room temperature (20°C) towards -10°C and back.

Figures (6.2.1 - 6.2.4) show the measurement and identification results.

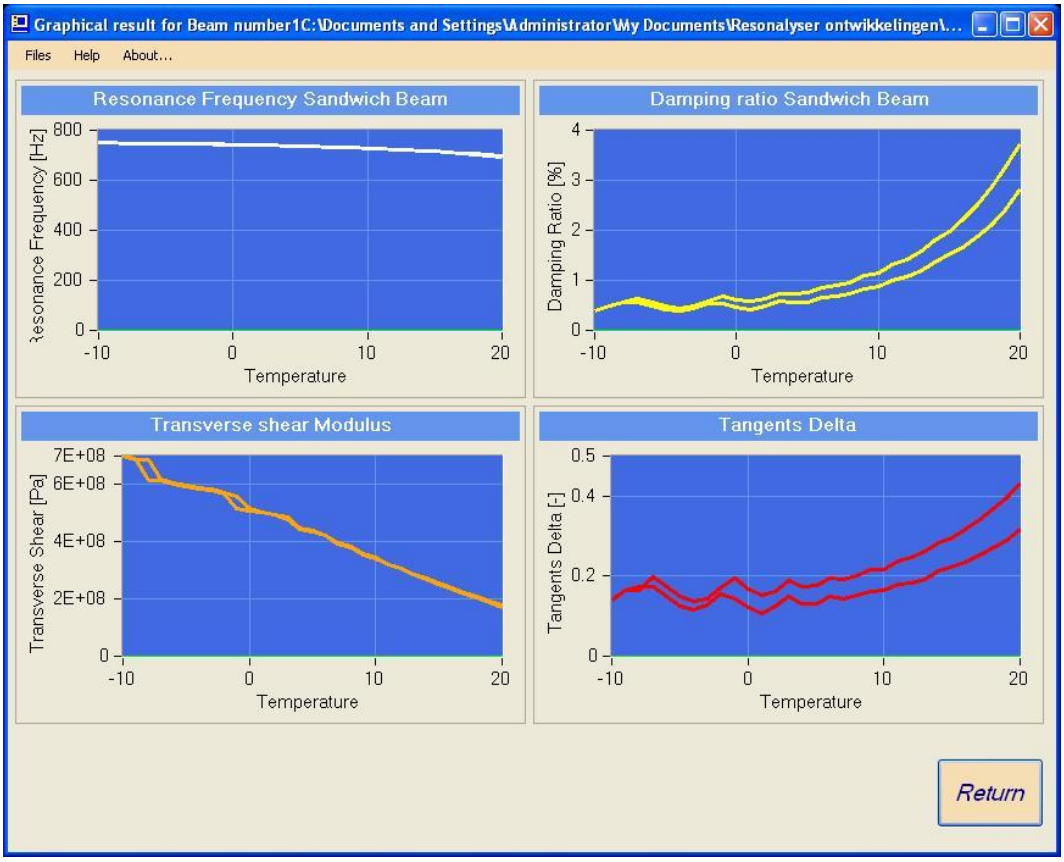

Figure 6.2.1. Resonance frequencies (up-left), damping ratio (up-right), transverse shear storage modulus (down-left) and tangents delta (down-right) of an AL beam 300 mm in a temperature interval from room temperature 20°C towards -10°C and back.

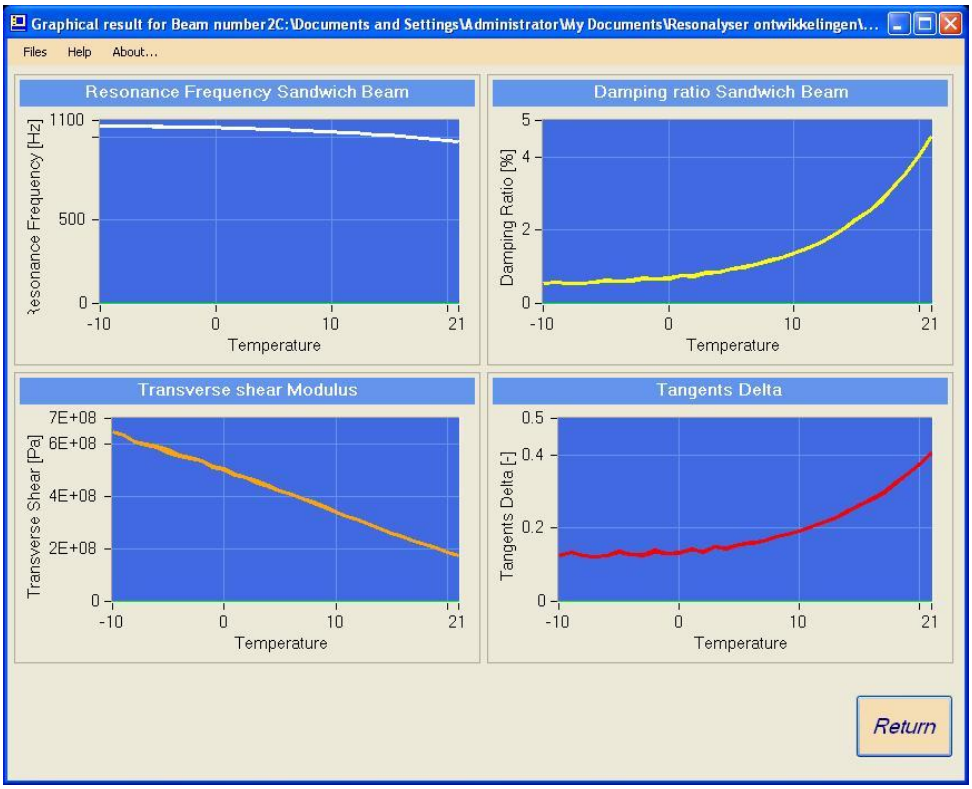

Figure 6.2.2. Resonance frequencies (up-left), damping ratio (up-right), transverse shear storage modulus (down-left) and tangents delta down-right of an AL beam 250 mm in a temperature interval from room temperature 20°C towards -10°C and back

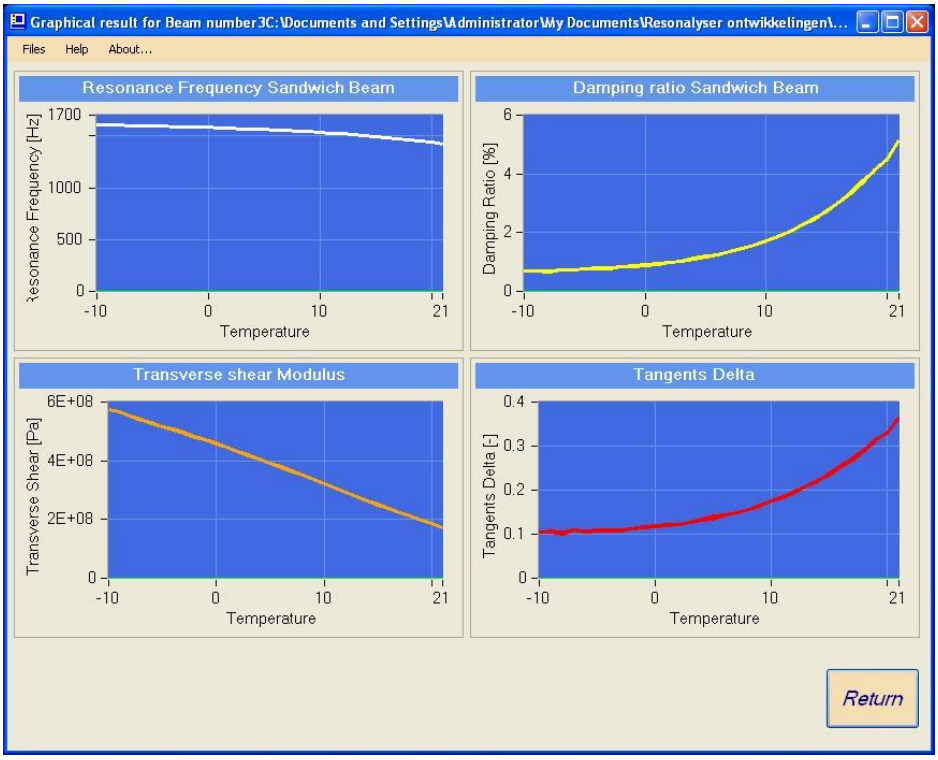

Figure 6.2.3. Resonance frequencies (up-left), damping ratio (up-right), transverse shear storage modulus (down-left) and tangents delta down-right of an AL beam 200 mm in a temperature interval from room temperature 20°C towards -10°C and back

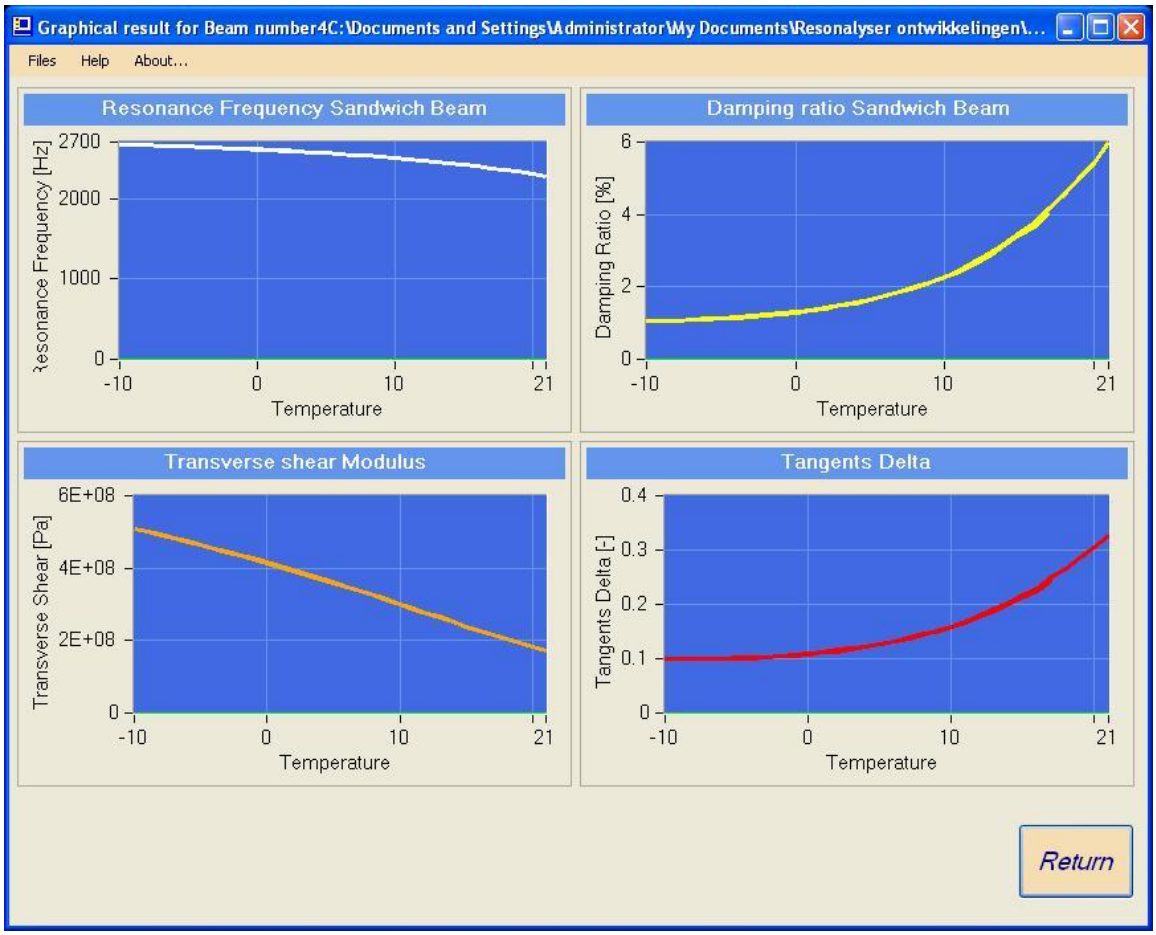

Figure 6.2.1. Resonance frequencies (up-left), damping ratio (up-right), transverse shear storage modulus (down-left) and tangents delta down-right of an AL beam 150 mm in a temperature interval from room temperature 20°C towards -10°C and back

The figures show that the go and return curves in the temperature interval are good. Only the damping curve of the 300mm specimen shows some hysteresis, but remains within the 5% tolerance for damping measurements.

The following paragraphs show results for measurements in a temperature interval ranging from -10°C till 40°C.

6.2.2 Test curves of 2.28 mm sandwich beams (-10°C – 40°C)

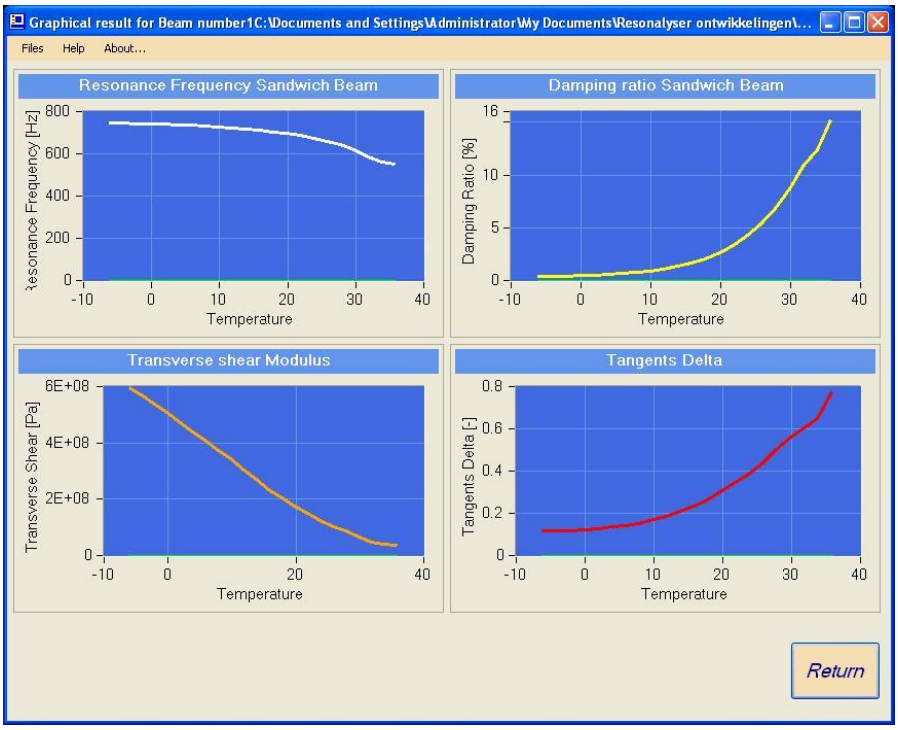

Figure 6.2.2.1. Resonance frequencies (up-left), damping ratio (up-right), transverse shear storage modulus (down-left) and tangents delta down-right of an AL beam 300 mm in a temperature interval from room temperature -10°C towards 40°C.

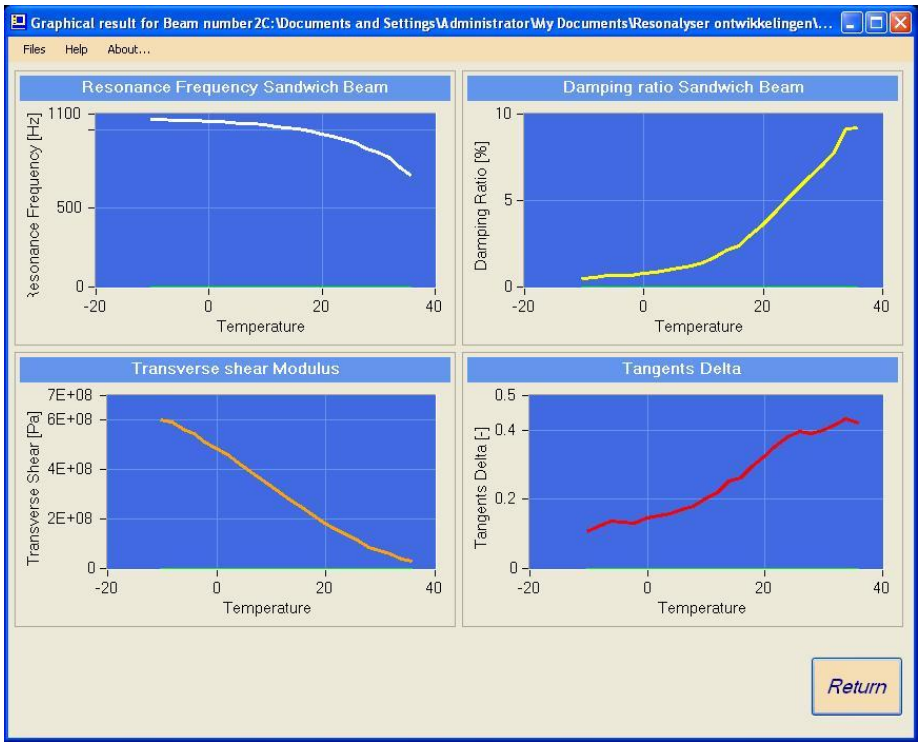

Figure 6.2.2.2. Resonance frequencies (up-left), damping ratio (up-right), transverse shear storage modulus (down-left) and tangents delta down-right of an AL beam 250 mm in a temperature interval from room temperature -10°C towards 40°C.

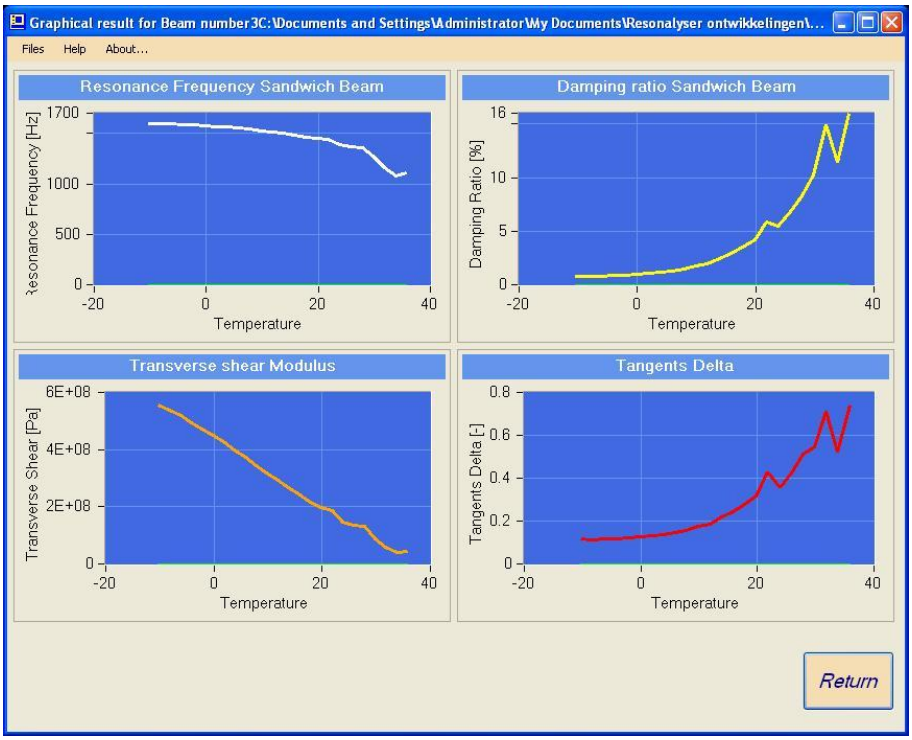

Figure 6.2.2.3. Resonance frequencies (up-left), damping ratio (up-right), transverse shear storage modulus (down-left) and tangents delta down-right of an AL beam 200 mm in a temperature interval from room temperature -10°C towards 40°C.

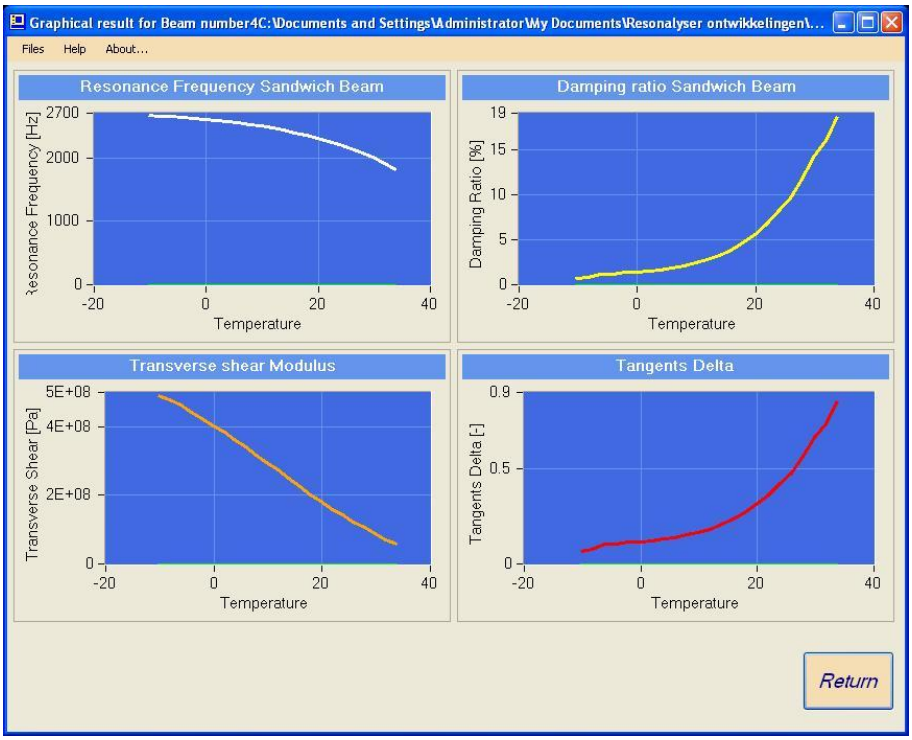

Figure 6.2.2.4. Resonance frequencies (up-left), damping ratio (up-right), transverse shear storage modulus (down-left) and tangents delta down-right of an AL beam 150 mm in a temperature interval from room temperature -10°C towards 40°C.

The results can be summarized in temperature and frequency plots (Figures 6.2.2.5 - 6.2.2.8)

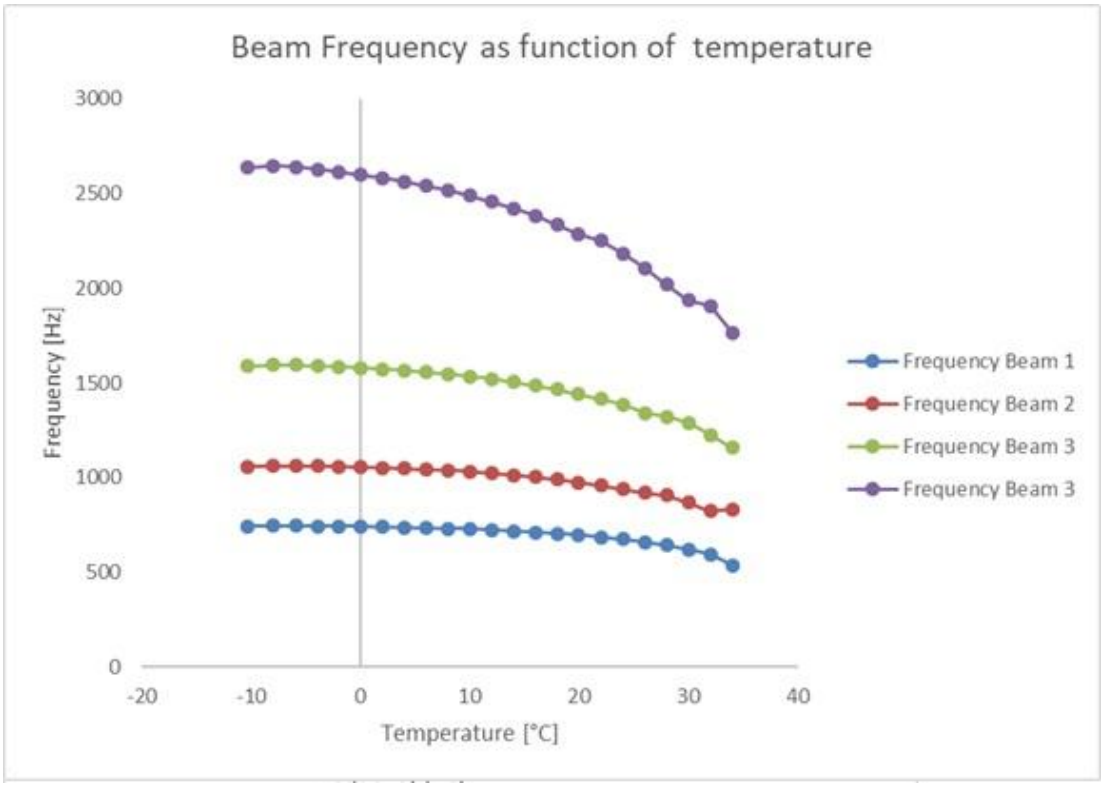

Figure 6.2.2.5. Resonance frequencies AL 2.28mm as function of temperature

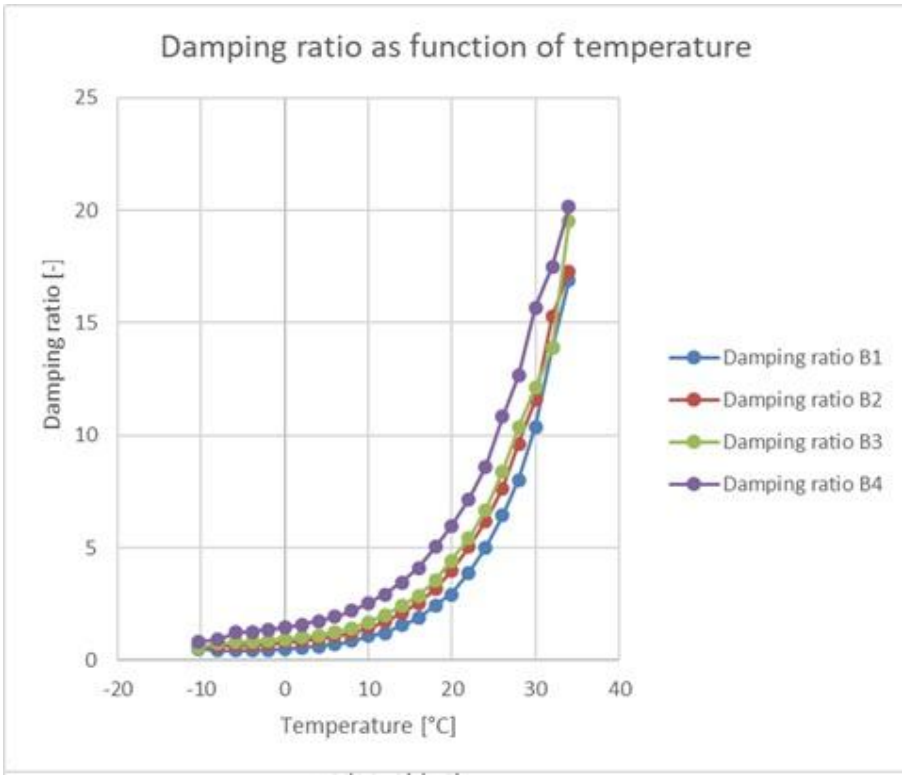

Figure 6.2.2.6. Damping ratios AL 2.28mm as function of temperature

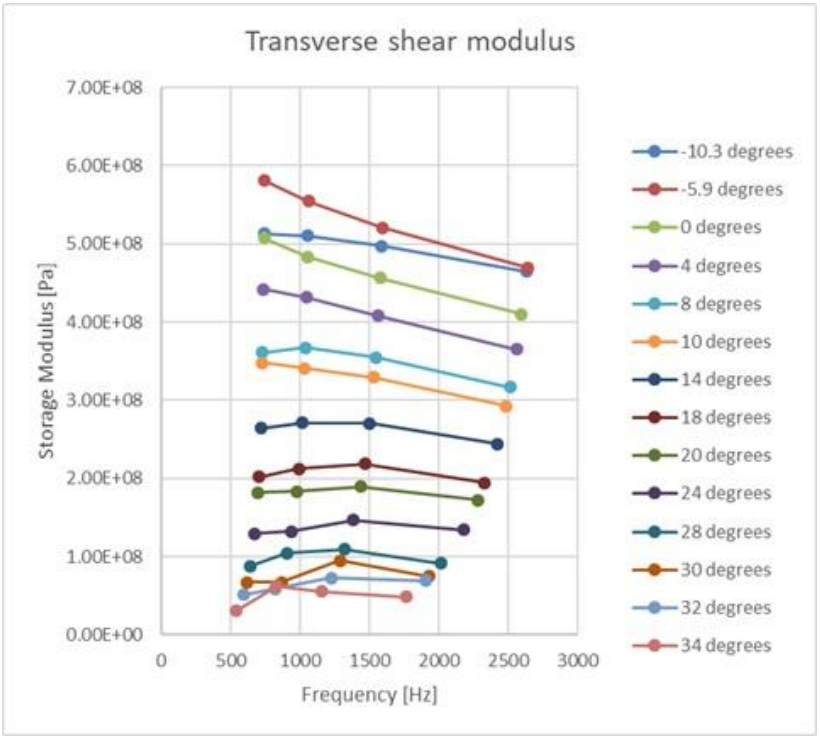

Figure 6.2.2.7. Storage transverse shear modulus AL 2.28mm as function of frequency

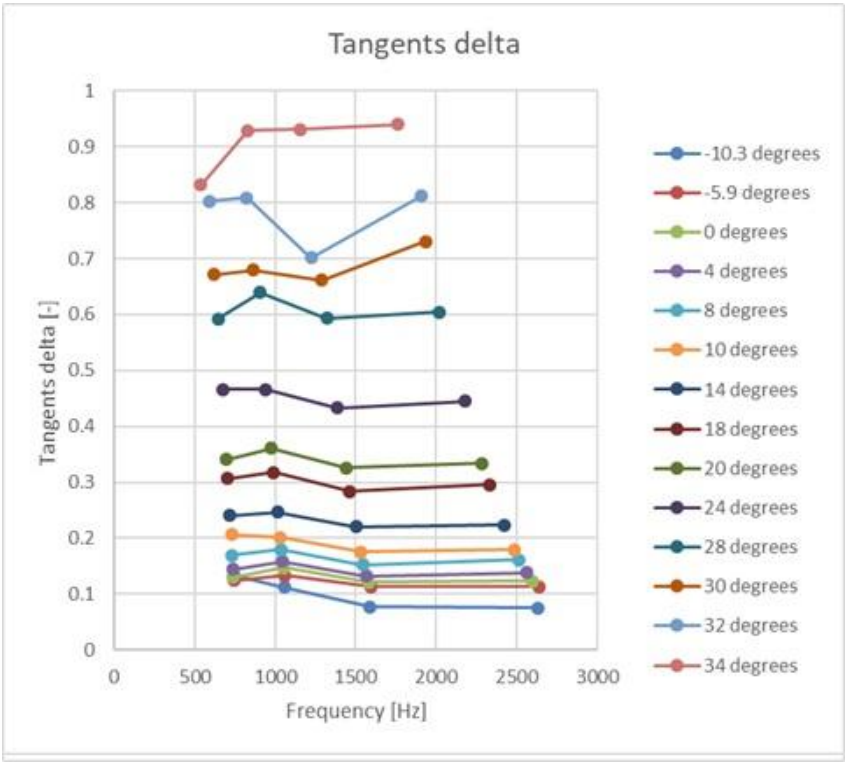

Figure 6.2.2.5. Tangents delta AL 2.28mm as function of frequency

It can be observed that for lower temperatures the storage modulus decreases as a function of frequency. It will be examined if this can be due to the influence of the interface layer between glass and PVB.

It can also be observed that the tangents delta values are irregular for higher temperatures. This can be explained by the fact that very high damping values are more difficult to estimate correctly, even with the 3DB law.

6.3 Test on sandwich beams with 1.52 mm PVB layer

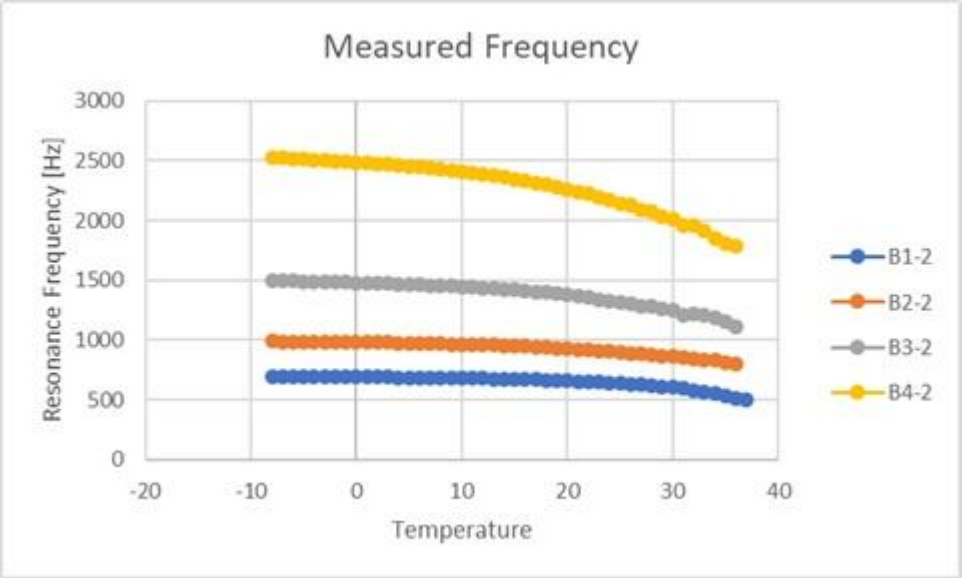

Figure 6.3.1. Measured resonance frequencies BL 1.52mm as function of temperature

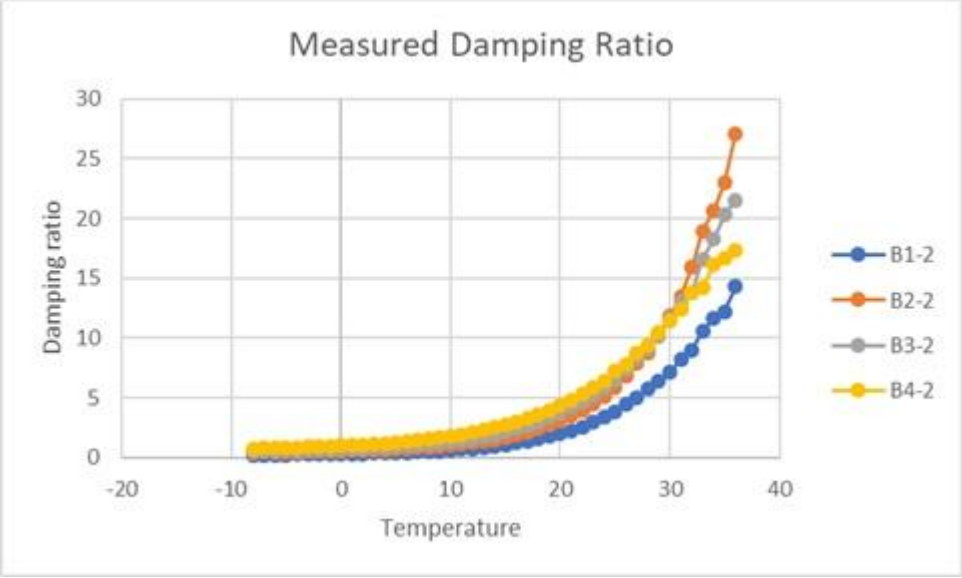

Figure 6.3.2. Measured damping ratios BL 1.52 mm as function of temperature

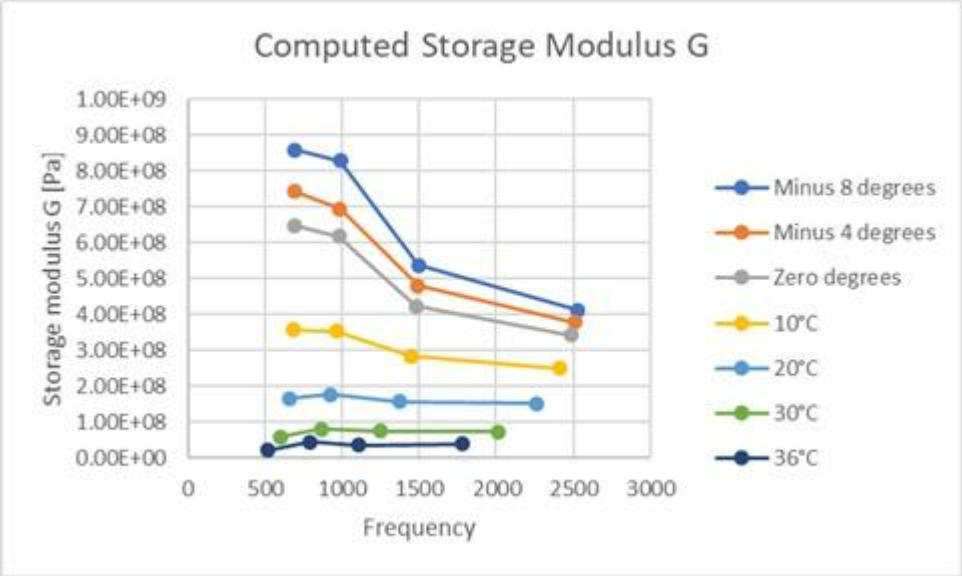

Figure 6.3.3. Computed storage modulus BL 1.52mm as function of frequency

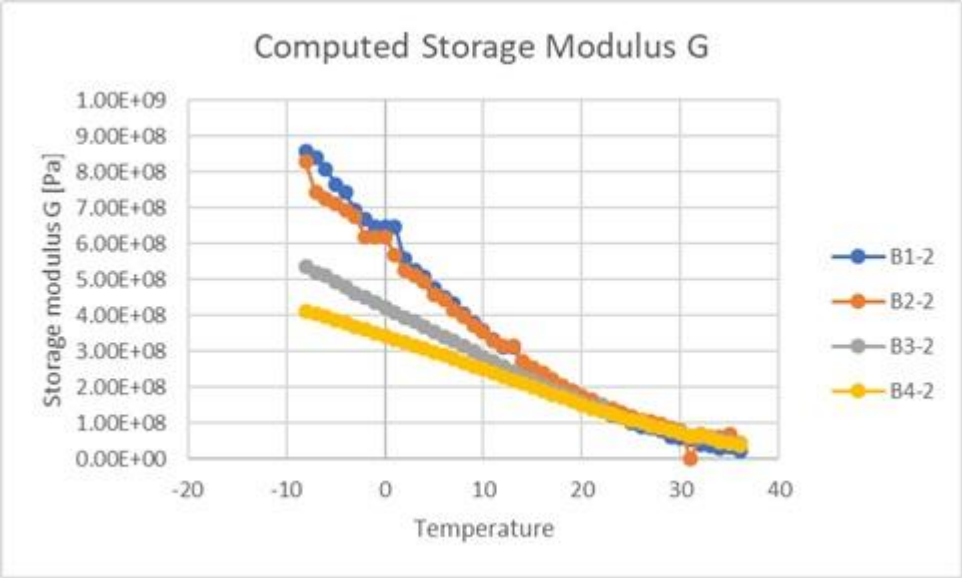

Figure 6.3.4. Computed storage modulus BL 1.52mm as function of temperature

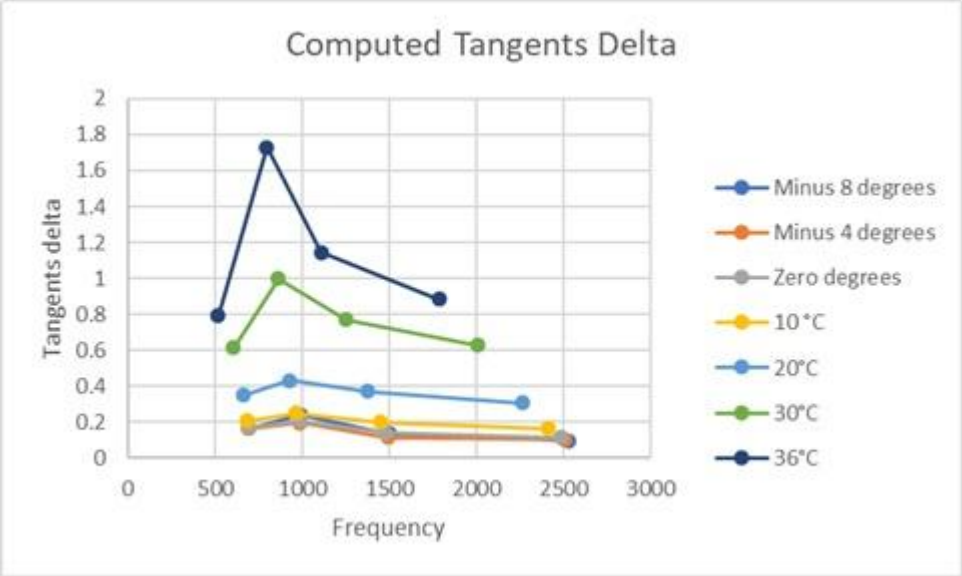

Figure 6.3.5. Computed tangents delta BL 1.52mm as function of frequency

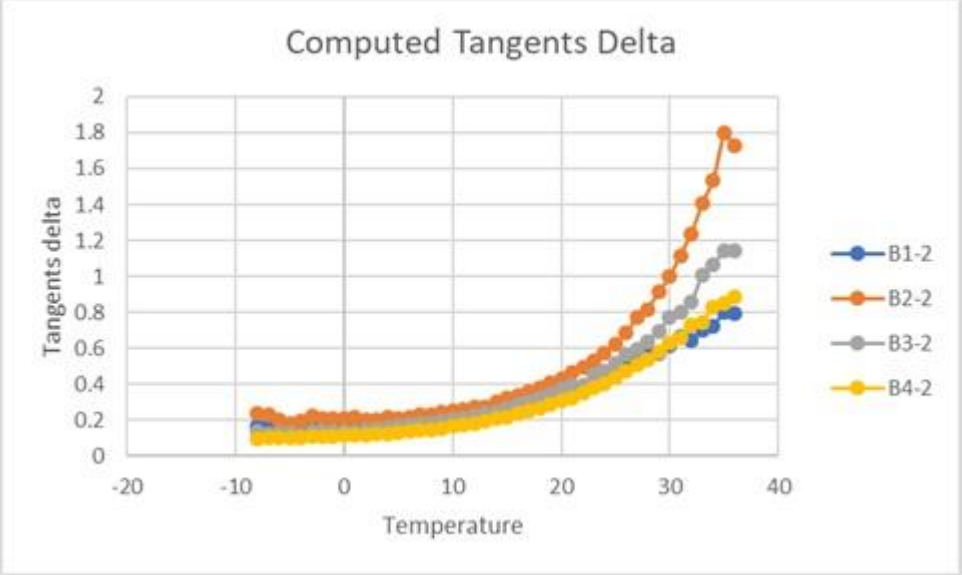

Figure 6.3.6. Computed tangents delta BL 1.52mm as function of temperature

On figure 6.3.2 it can be seen that the measurement of the value of the damping ratio at higher temperatures above 20°C is not stable, just as with the AL specimens.

The storage modulus at lower temperatures seems to decrease with increasing frequency (see figure 6.3.3). It must be investigated if the interface layer can be the cause of this decrease.

6.4 Test on sandwich beams with 0.76 mm PVB layer

The tests are cyclic from 22°C towards -10°C and backwards to study the stability of the identification routine.

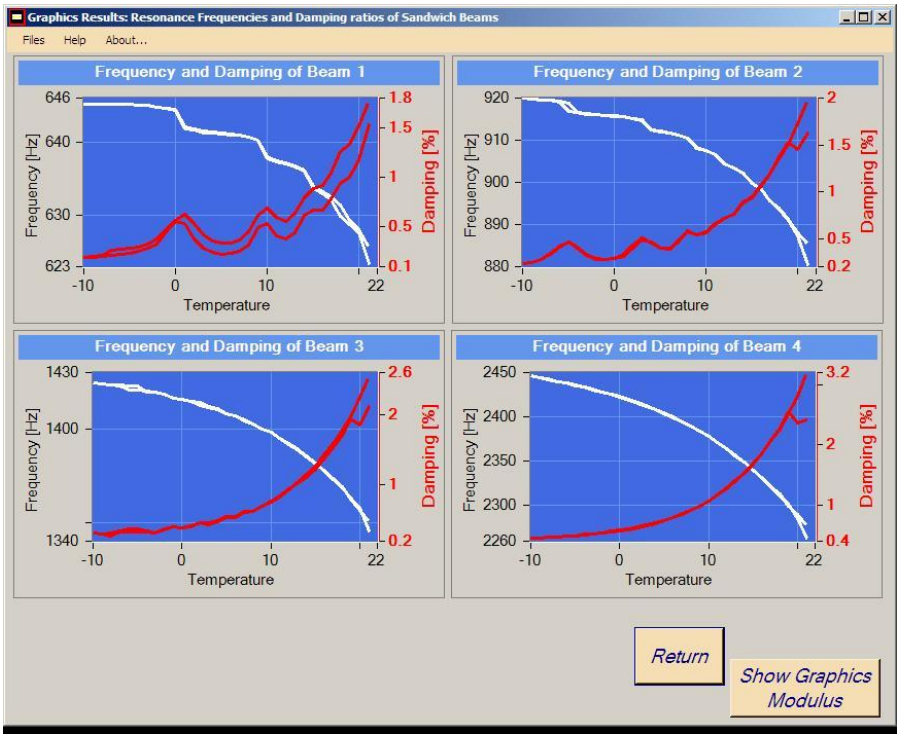

Figure 6.4.1. Frequencies and damping ratios as function of temperature (0.72mm)

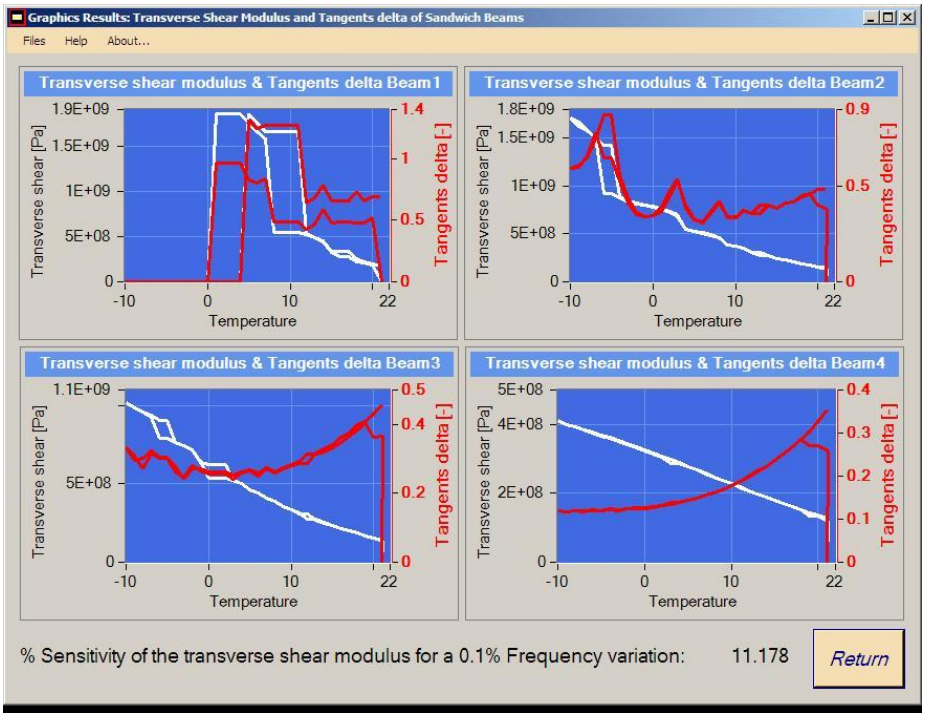

Figure 6.4.2. Identified storage modulus and tangents delta as function of temperature (0.72mm)

The thin 0.76 mm PVB layer makes identification of the storage modulus more cumbersome. The next graphs plot the situation for the separate beams.

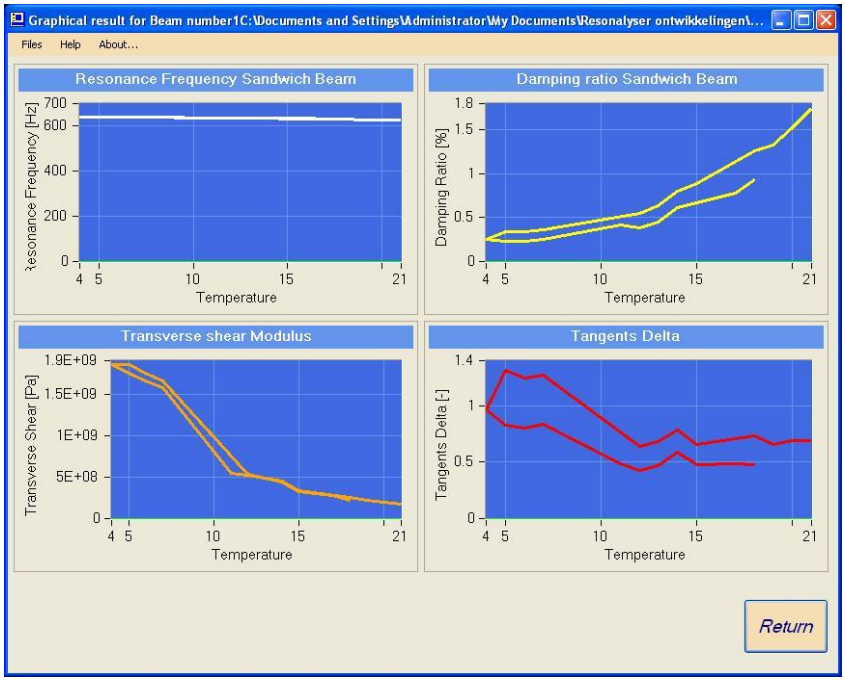

Figure 6.4.3. Resonance frequencies, damping ratios and identified storage modulus and tangents delta as function of temperature (0.72mm) for sandwich beam CL-1

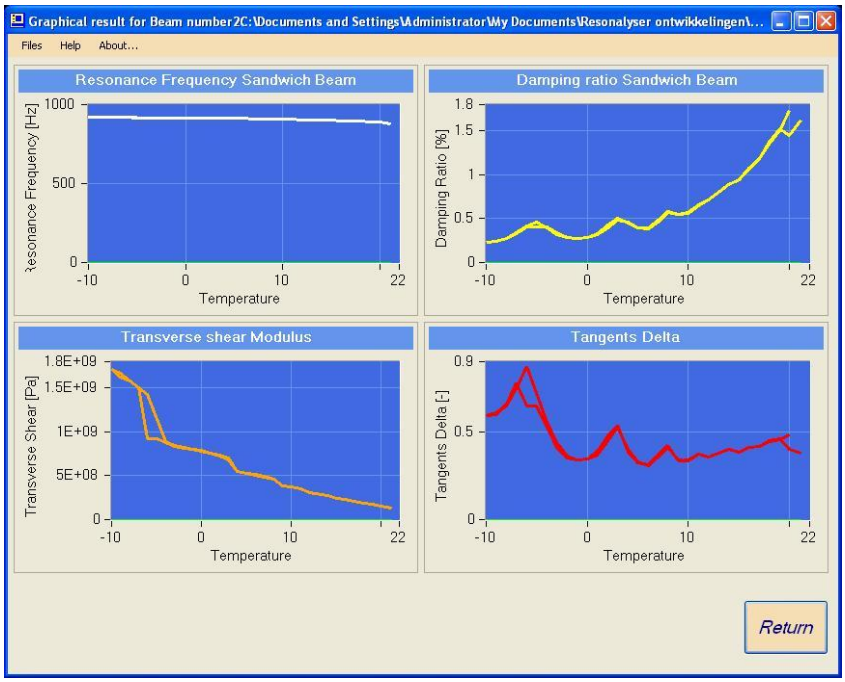

Figure 6.4.4. Resonance frequencies, damping ratios and identified storage modulus and tangents delta as function of temperature (0.72mm) for sandwich beam CL-2

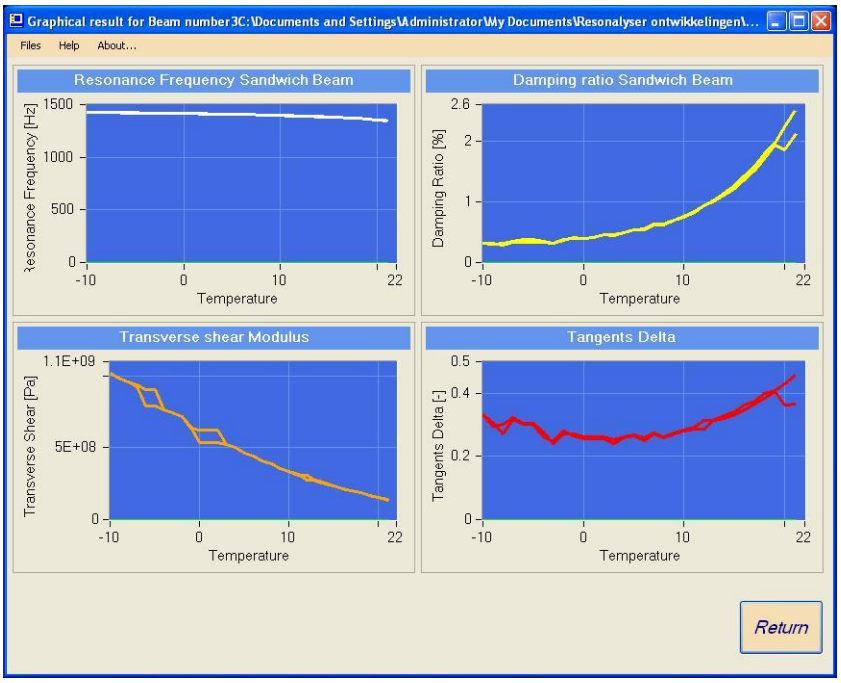

Figure 6.4.5. Resonance frequencies, damping ratios and identified storage modulus and tangents delta as function of temperature (0.72mm) for sandwich beam CL-3

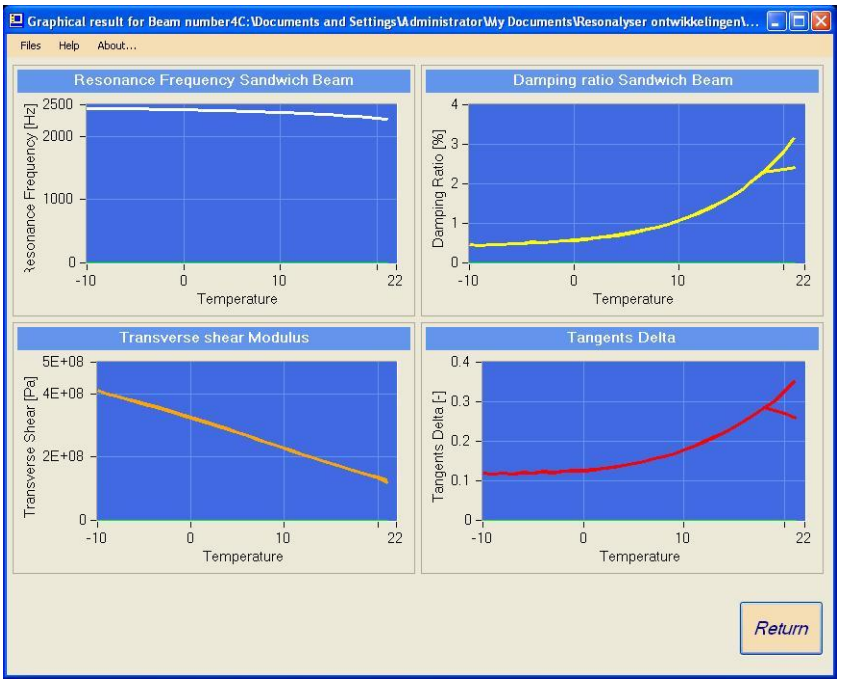

Figure 6.4.6. Resonance frequencies, damping ratios and identified storage modulus and tangents delta as function of temperature (0.72mm) for sandwich beam CL-4

Again it is noticed that the value of the storage modulus decreases with increasing frequency. In the next chapter, the influence of the interlayer between the glass and PVB layers will be examined.

7 Influence of the interlayer

It is investigated if an explicit algorithm in ABAQUS can identify the storage modulus in a model better than an eigenvalue algorithm. In this paragraph two models are created for sandwich beams: Sandwichbeam_150mm en sandwichbeam300mm. The models are excited with a sinusoidal varying pressure with a frequency equal to the resonance frequency of the model. A thin layer on top of the upper glass layer of 0.0001 mm is created as excitation surface.

The value of Poisson's ratio changes as follows:

-10°C Poisson ratio = 0.42

0°C Poisson ratio = 0.45

20°C Poisson ratio = 0.47

40°C Poisson ratio = 0.49

7.1 Tests at 20°C, sample BL (1.52mm)

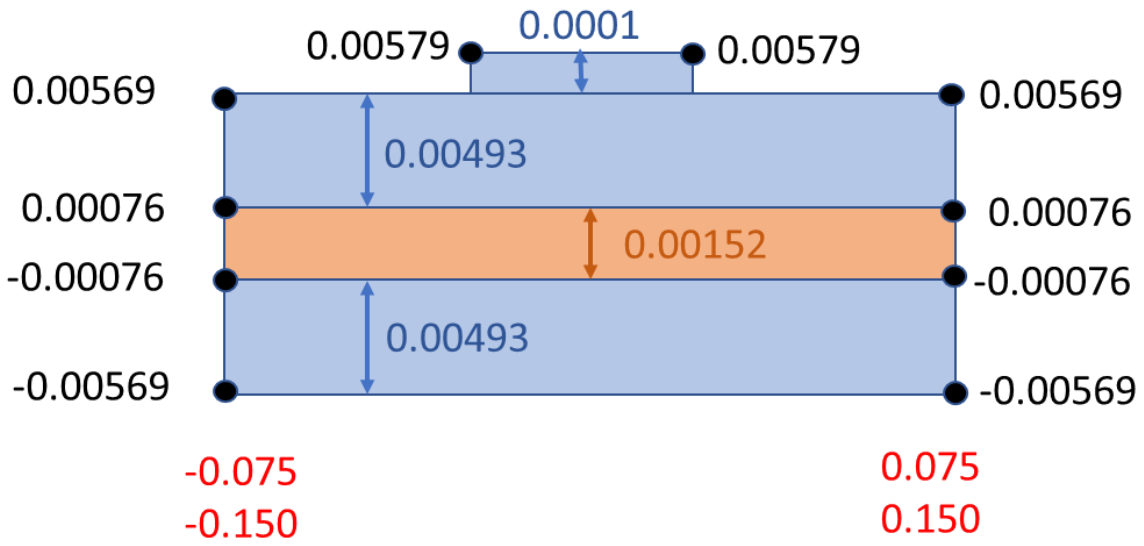

Figure 7.1. Geometry of the sandwich beam for the explicit algorithm (1.52mm)

7.1.1 Sample BL4

L = 0.150mm, Measured resonance freqeuncy 2263 Hz, Identification through Bytec model: G = 1.53 E8

Settings for the explicit model: circular frequency = **14219** rad/sec = 2263 x 2 x pi , pure sinus, load with pressure amplitude 1000, analysis duration: 0.02 sec, automatically calculated Step size: 2.13E-8 sec

Result: Resonance is reached with a Young's modulus of PVB = 4.8E+8 Pa, Storage G modulus 1.63E+08 and Poisson's ratio = 0.47 as can be seen in figure 7.2 and 7.3.

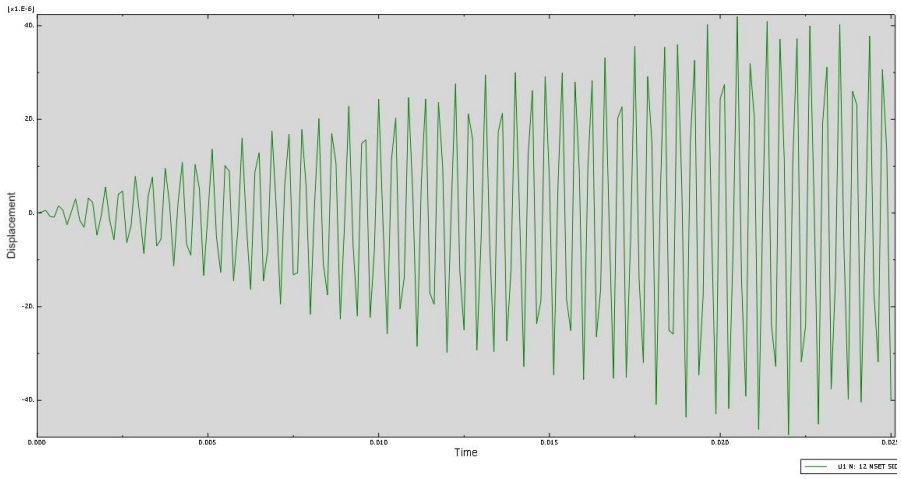

Figure 7.2. Displacement u in the x-direction (initiated by Poisson's ratio) 150mm

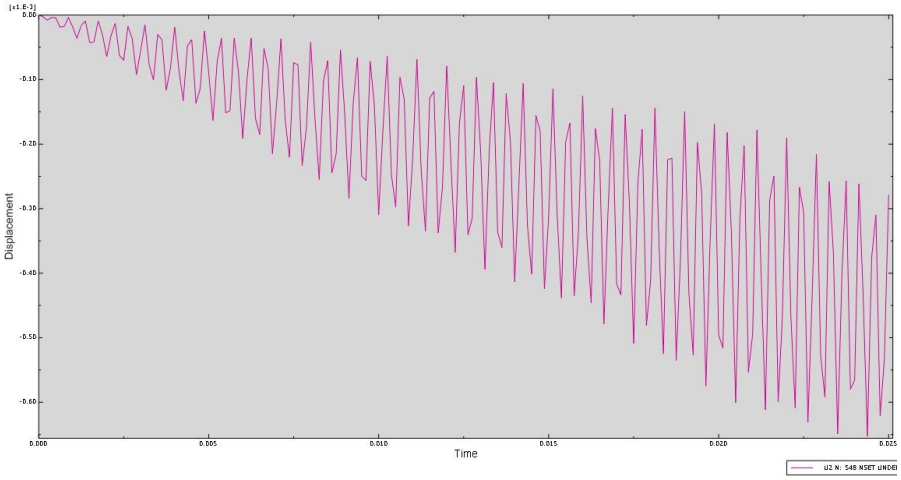

Figure 7.3. Displacement v in the y-direction (rigid body + vibrations) 150mm

At the start of the sine excitation, the response amplitude = 0

7.1.2 Sample BL1

L = 0.300mm, Measured resonance frequency 660.1 Hz, Identification via Bytec model G = 1.67 E8

Setting voor explicit model: amplitude = circular frequency = **4148** rad/sec = 660.1 x 2 x pi , pure sinus, load with pressure amplitude 1000, Analysis duration: 0.05 sec, Automatically calculated Step: 2.13E-8

Result: Resonance is reached with a Young's modulus of PVB = 6.25+8 Pa, Storage G modulus 2.13E+08 and Poisson's ratio = 0.47

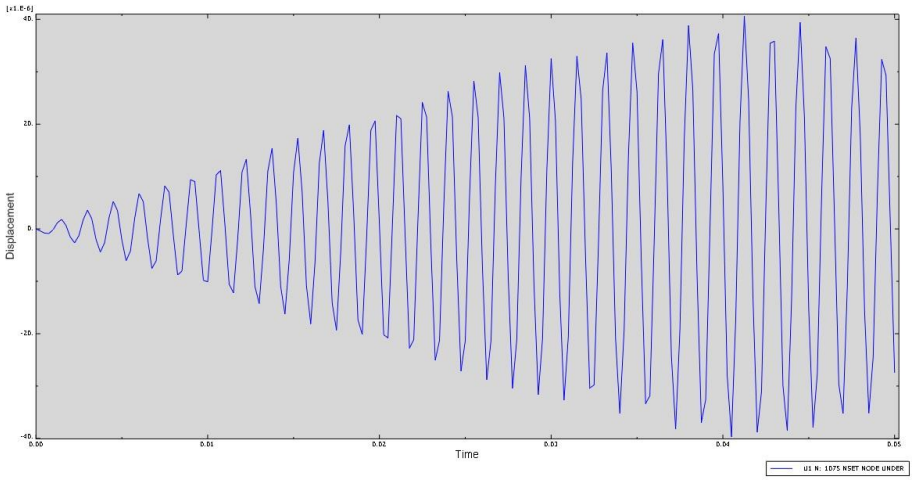

Fig.7.4. Displacment u in the x-direction (due to Poisson's ratio) 300mm

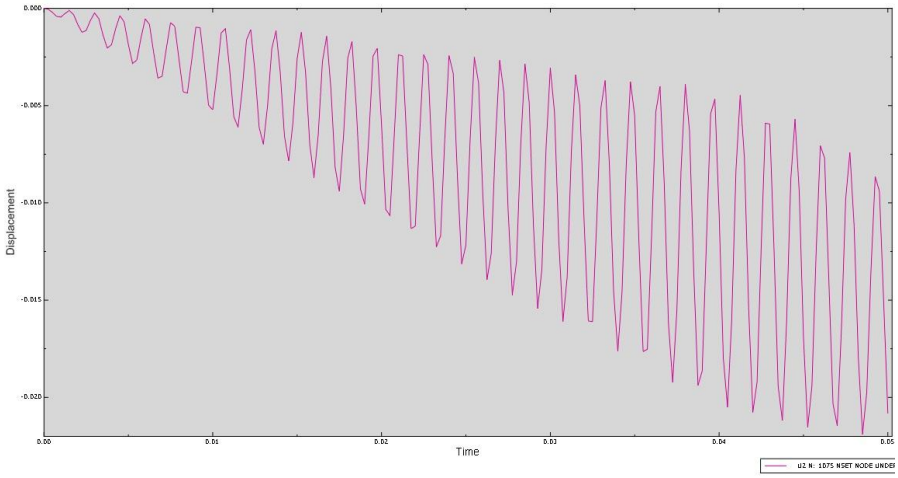

Fig. 7.5. Displacement v in the y-direction (rigid body + vibrations) 300mm

Further testing has shown that the ABAQUS model with length 300mm is not very sensitive for variations of the storage modulus G.

7.2 Tests at 20°C, sample AL (2.28mm)

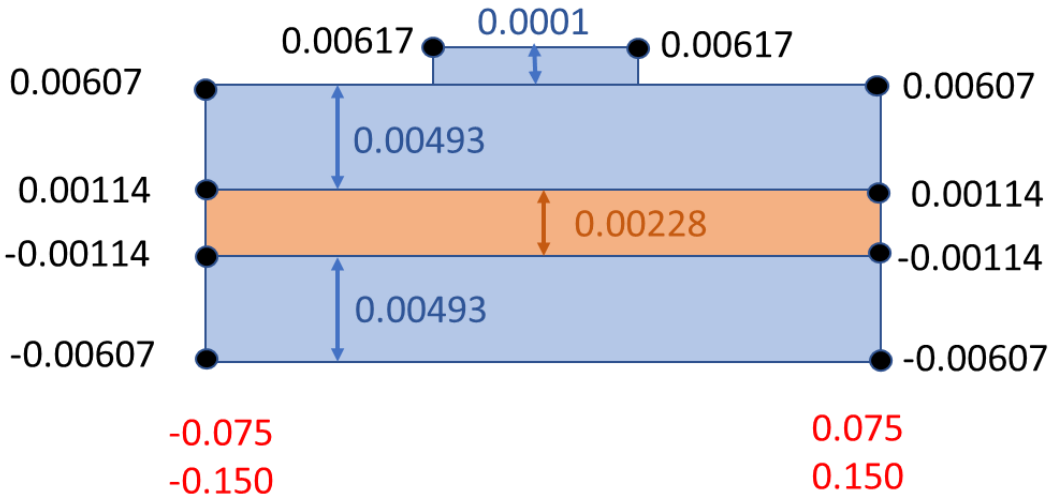

Figure 7.6. Geometry of the sandwich beam for the explicit algorithm (1.52mm)

7.2.1 Sample AL1

L = 0.300mm, Measured resonance **693.6 Hz**, Identification via Bytec model **G = 1.71 E8**

Extra computation via an Eigenvalue routine in ABAQUS yields:

Young's modulus 4.76E+8 Pa, Storage modulus transverse shear 1.62E+08 Pa, Poisson's ratio = 0.47, resonance frequency = 693.6 Hz

Setting for explicit model: circular frequency = **4358** = 693.6 x 2 x pi , load with pressure amplitude 1000, duration: 0.05 sec, automatically calculated Step: 2.13E-8

Result: Young's modulus 4.76E+8 Pa, Storage modulus transverse shear 1.62E+08 Pa, Poisson's ratio = 0.47, resonance frequency = 693.6 Hz

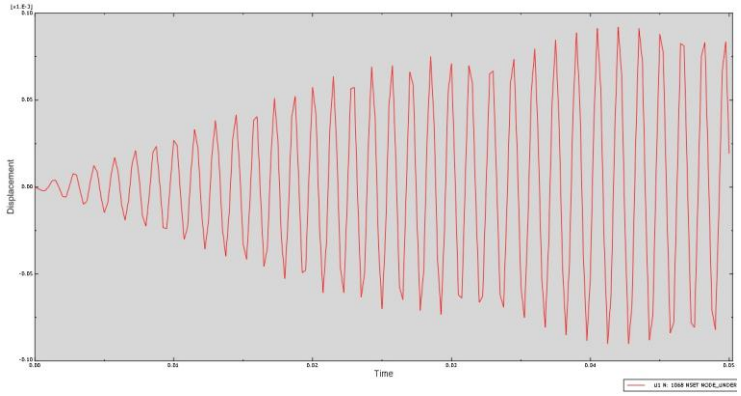

Fig. 7.7. Displacement u in the x-direction (rigid body + vibrations) 300mm

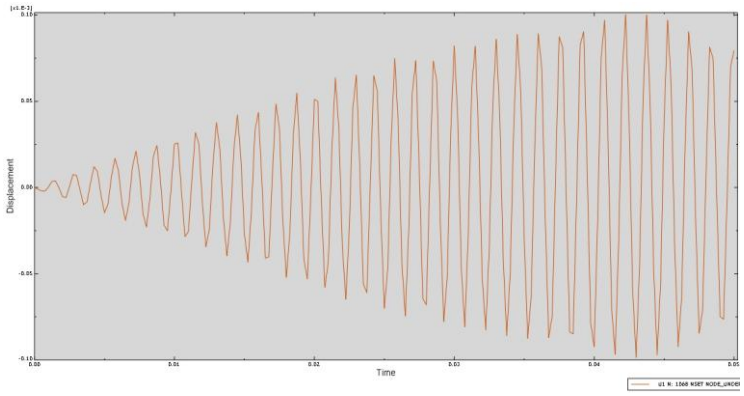

Fig. 7.8. Displacement v in the y-direction (rigid body + vibrations) 300mm

7.2.2 Sample AL4

L = 0.150mm, measured resonance **2293.2 Hz**, Identification via Bytec model **G = 1.76 E8**

Extra computation via an Eigenvalue routine in ABAQUS yields:

Young's modulus 5.20E+8 Pa, Storage modulus transverse shear 1.77E+08 Pa, Poisson's ratio = 0.47, resonance frequency = 2293.2 Hz

Setting for explicit model: circular frequency = **14409** = 2293.2 x 2 x pi , load with pressure amplitude 1000, duration: 0.05 sec, automatically calculated Step: 2.13E-8

Result: Young's modulus 5.20E+8 Pa, Storage modulus transverse shear 1.77E+08 Pa, Poisson's ratio = 0.47, resonance frequency = 2293.2 Hz

7.3 Tests at 0°C, sample AL (2.28mm)

7.3.1 Sample AL1

L = 0.300mm, Measured resonance frequency **741.4 Hz**, Identification via Bytec model **G = 5.09 E8**

Extra computation via an Eigenvalue routine in ABAQUS yields:

Young's modulus 12.4E+8 Pa, Storage modulus transverse shear 4.28E+08 Pa, Poisson's ratio = 0.45, resonance frequency 741.5 Hz

Setting voor explicit model: circular frequency = **4658** = 741.4 X 2 X pi , pure sinus, load with pressure amplitude 1000, duration: 0.05 sec, automatically calculated Step: 2.13E-8

Result: Young's modulus 12.4E+8 Pa, Storage modulus transverse shear 4.28E+08 Pa, Poisson's ratio = 0.45, resonance frequency = 741.4 Hz

7.3.2 Sample AL4

L = 0.150mm, Resonantie **2608.3 Hz**, Identificatie via Bytec model **G = 4.11 E8**

Extra computation via an Eigenvalue routine in ABAQUS yields:

Young's modulus 11.7E+8 Pa, Storage modulus transverse shear 4.03E+08 Pa, Poisson's ratio = 0.45, resonance frequency 2608.3 Hz

Setting voor explicit model: amplitude= circular frequency = **16388** = 2608.3 X 2 X pi , pure sine, load with pressure amplitude 1000, duration: 0.03 sec, automatically calculated Step: 2.13E-8

Result: Young's modulus 11.7E+8 Pa, Storage modulus transverse shear 4.03E+08 Pa, Poisson's ratio = 0.45, resonance frequency = 2608 Hz

7.4 Intermediate discussion

It can be concluded that the simulation with the ABAQUS explicit routine, the ABAQUS eigenvalue routine and the BYTEC numerical model all yield the same results. The only explanation left to explain the observed apparent decreasing transverse shear modulus with increasing frequency is that the interface between glass and PVB influences the sandwich beam stiffness and hence the identified storage transverse shear modulus.

7.5 Tests on sample AL (2.28mm) + Interface layer

Two interface layers of 0.0002 m are created in ABAQUS. The excitation layer above the upper glass layer is removed, since only eigenvalue problems will be considered.

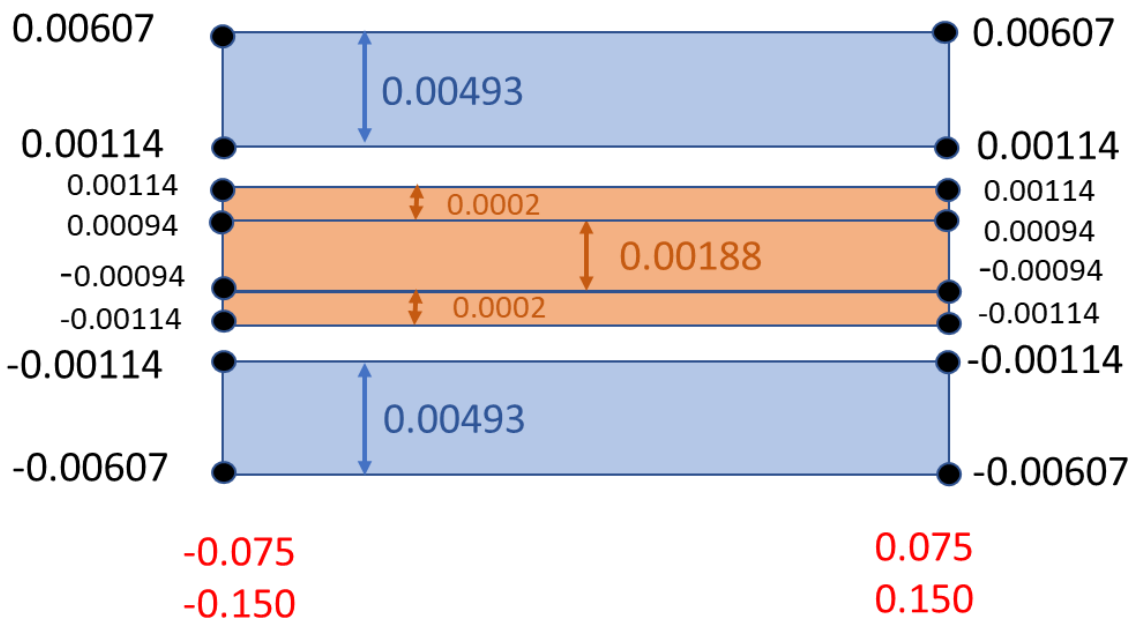

Figure 7.5.1 ABAQUS model with interface layers

The results with the Bytec model will be compared with results from the ABAQUS model with incorporated interface layers. The young'smodulus of the interface layers will be taken as about 1/3 of the Young's modulus of the PVB layer. The value of the storage modulus of PVB is iteratively adpated till the computed resonance frequency matches the measured value.

7.5.1 Tests at 0°C

AL1-2: L = 0.300mm, Resonance frequency **741.4 Hz**, Identification via Bytec model **G = 5.09 E8**

Eigenvalue ABAQUS: (Poisson's ratio = 0.45)

	Young's E Interface	Young's E PVB	Storage G PVB	Freq Hz
ABAQUS model	5.0E+8	16.0 E+8	5.52E+8	744
Linear FE	5.0E+8	15.0 E+8	5.17E+8	742.5
	5.00E+8	14.5E+8	5.00E+8	741.6

AL4-2: L = 0.150mm, Resonance frequency **2608.3 Hz**, Identification via Bytec model **G = 4.11 E8**

Eigenvalue ABAQUS: (Poisson's ratio = 0.45)

	Young's E Interface	Young's E PVB	Shear modulus G PVB	Freq Hz
ABAQUS model	6.0E+7	12.1E+8	4.17E+8	2025.1
Linear FE	10.E+8	16.0E+8	5.52E+8	2674
	8.0E+8	16.0E+8	5.52E+8	2656
	6.0E+8	16.0E+8	5.52E+8	2626
	5.0E+8	16.0E+8	5.52E+8	2604

7.5.2 Tests at 20°C

AL1-2: L = 0.300mm, Resonance frequency **693.6 Hz**, Identification via Bytec model **G = 1.71 E8**

Eigenvalue ABAQUS: (Poisson's ratio = 0.47)

	Young's Interface	Young's E PVB	Storage G PVB	Freq Hz
ABAQUS model	1.65E+8	4.96E+8	1.71E+8	686.2
Linear FE	1.65E+8	5.51E+8	1.90E+8	691.8
	1.65E+8	6.00E+8	2.10E+8	696.1
	1.65E+8	5.88E+8	2.00E+8	693.5

AL4-2: L = 0.150mm, Resonance frequency **2293.2 Hz**, Identification via Bytec model **G = 1.76 E8**

Eigenvalue ABAQUS: (Poisson's ratio = 0.47)

	Young's Interface	Young's E PVB	Shear modulus G PVB	Freq Hz
ABAQUS model	1.65E+8	5.07E+8	1.75E+8	2147.4
Linear FE	1.65E+8	6.17E+8	2.10E+8	2197.3
	1.65E+8	8.82E+8	3.00E+8	2276.3
	1.65E+8	9.11E+8	3.10E+8	2282.7
	1.65E+8	9.41E+8	3.20E+8	2289.0
	1.65E+8	9.70E+8	3.30E+8	2294.8
	1.65E+8	9.64E+8	3.28E+8	2293.6

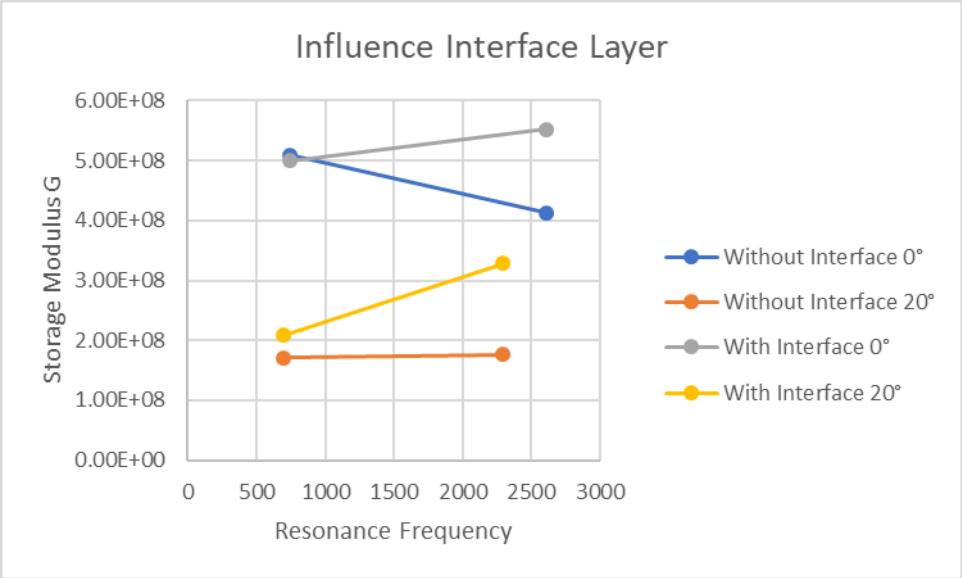

Figure 7.5.2 Results from ABAQUS model with interface layers

Figure 7.5.2 shows that in the model with interface layers, the transverse shear storage modulus increases with the frequency, while with the Bytec model without interface modeling, the modulus decreases with increasing frequency.

The value of the storage shear modulus in the interface layers and the thicknesses were arbitrary selected. The correct evaluation of the transverse shear modulus in the PVB layer can only be determined if the values in the interface layer are correctly evaluated in the model.

However, the above results show clearly that the presence of an interface layer can influence considerably the identification. It shows also that the influence on test samples with higher resonance frequency is bigger than for samples with lower frequencies.